

# Bifurcations and Chaos in Hořava-Lifshitz Cosmology

Juliette Hell\*, Phillipo Lappicy\*\* and Claes Uggla\*\*\*

\*

Institut für Mathematik, Freie Universität Berlin  
Arnimallee 3 - 14195 Berlin, Germany  
[blanca@math.fu-berlin.de](mailto:blanca@math.fu-berlin.de)

\*\*

Instituto Superior Técnico, Universidade de Lisboa  
Av. Rovisco Pais, 1049-001 Lisboa, Portugal

\*\*\*

ICMC, Universidade de São Paulo  
Av. trabalhador são-carlense, São Carlos, Brazil  
[lappicy@usp.br](mailto:lappicy@usp.br)

\*\*\*

Department of Physics, Karlstad University  
S-65188 Karlstad, Sweden  
[claes.uggla@kau.se](mailto:claes.uggla@kau.se)

## Abstract

The nature of generic spacelike singularities in general relativity is connected with first principles, notably Lorentzian causal structure, scale invariance and general covariance. To bring a new perspective on how these principles affect generic spacelike singularities, we consider the initial singularity in spatially homogeneous Bianchi type VIII and IX vacuum models in Hořava-Lifshitz gravity, where relativistic first principles are replaced with anisotropic scalings of Lifshitz type. Within this class of models, General Relativity is shown to be a bifurcation where chaos becomes generic. To describe the chaotic features of generic singularities in Hořava-Lifshitz cosmology, we introduce symbolic dynamics within Cantor sets and iterated function systems.

## 1 Introduction

The last couple of decades have seen considerable progress in our understanding of generic spacelike singularities in General Relativity (GR). In particular it has been shown that there are connections between the nature of such singularities and with three of the foundational first principles of GR: (i) Lorentzian causal structure, (ii) (conformal) scale invariance, and (iii) general covariance, i.e., spacetime diffeomorphism invariance, see e.g. the reviews [89, 90] and references therein.

Heuristic arguments by Belinskiĭ, Khalatnikov and Lifshitz (BKL) [53, 8, 9] suggest that generic spacelike singularities in GR are *vacuum dominated* for a broad range of matter sources, i.e., generically such sources asymptotically become test fields because gravity asymptotically generates more gravity than matter. For simplicity we will therefore only consider vacuum models.

The importance of *Lorentzian causal structure* for the nature of generic spacelike singularities in GR is connected with the locality conjecture of BKL [53, 8, 9]. This conjecture states that the asymptotic evolution toward a generic spacelike singularity in inhomogeneous cosmology is local, in the sense that each spatial point evolves toward the singularity independently of its neighbors as a spatially homogeneous model. By reformulating the Einstein field equations in GR, using the so-called conformally Hubble-normalized orthonormal frame dynamical systems approach, the BKL locality conjecture was made more precise in [89, 90, 91, 26, 2, 82, 55, 37]. In this formulation, there exists an invariant ‘local boundary set’ where the partial differential equations (PDEs) of inhomogeneous cosmology reduce to the ordinary differential equations (ODEs) of spatially homogeneous cosmology at each spatial point. Moreover, on the local boundary set, there exists an invariant subset identical to the attractor of the corresponding ODEs of spatially homogeneous cosmology, for each spatial point. In this approach, loosely speaking, the BKL locality conjecture amounts to that the invariant subset on the local boundary corresponding to the ODE attractor, for each spatial point, form a local PDE attractor, which describes the detailed nature of generic spacelike singularities in inhomogeneous cosmology. Presumably, a necessary condition for such asymptotic local evolution is asymptotic silence, i.e., that the extreme gravity in the vicinity of a generic spacelike singularity results

in particle horizons that shrink to zero size toward the singularity [89, 90, 91, 82, 55, 37].<sup>1</sup> If this is the case, the nature of generic spacelike singularities is connected with asymptotic Lorentzian causal structure induced by extreme gravity and certain *spatially homogeneous models*.

To describe generic spacelike singularities, it is therefore presumably essential to understand the properties of spatially homogeneous models, of which there are two categories: the Bianchi models and the spherically symmetric Kantowski-Sachs models, where the latter are too special to be of relevance for generic singularities. The Bianchi models are divided into class A and class B. In contrast to the general class B models, the class A models admit a Hamiltonian formulation and have a simpler hierarchical structure. We will therefore henceforth restrict considerations to the class A Bianchi models. Because of the BKL locality conjecture, this is further motivated by that the most general models within this class, the Bianchi type VIII and IX models, are believed to contain some of the key elements needed to describe generic spacelike singularities.

The class A Bianchi models have three-dimensional symmetry groups, which act simply transitively on the spatially homogeneous slices. These models thereby admit a symmetry-adapted spatial (left-invariant) co-frame  $\{\omega^1, \omega^2, \omega^3\}$ , such that

$$d\omega^1 = -n_1 \omega^2 \wedge \omega^3, \quad d\omega^2 = -n_2 \omega^3 \wedge \omega^1, \quad d\omega^3 = -n_3 \omega^1 \wedge \omega^2, \quad (1)$$

where the structure constants  $n_1, n_2, n_3$  determine the Lie algebras of the various class A Bianchi models, defined in Table 1, see also e.g. [95]:

Bianchi type	$n_\alpha$	$n_\beta$	$n_\gamma$
IX	+	+	+
VIII	-	+	+
VII <sub>0</sub>	0	+	+
VI <sub>0</sub>	0	-	+
II	0	0	+
I	0	0	0

**Table 1:** The class A Bianchi types are characterized by the zeroes and relative signs of the structure constants  $(n_\alpha, n_\beta, n_\gamma)$ , where  $(\alpha\beta\gamma)$  is a permutation of  $(123)$ . There are equivalent representations associated with an overall change of sign of the constants, e.g., another Bianchi type IX representation is  $(-, -, -)$ . It is also possible to scale the constants, e.g., in type IX we can set  $n_1 = n_2 = n_3 = 1$ .

The class A Bianchi models form a hierarchical structure, where more special models are obtained from more general ones by performing Lie contractions, i.e., by setting structure constants to zero, which results in the Lie contraction diagram given in Figure 1.

<sup>1</sup>Recent results indicate that this is not the whole story. There is also a connection between asymptotic silence, generic spacelike singularities, and infinitely recurring oscillating inhomogeneous spikes, described by certain inhomogeneous solutions [2, 56, 36, 35, 57].

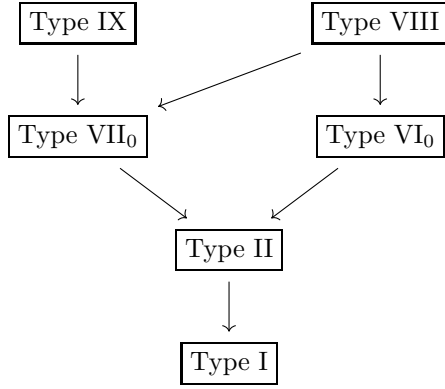


**Figure 1:** The class A Bianchi Lie contraction hierarchy.

The field equations of all vacuum GR models, and thus also the class A Bianchi models, are conformally *scale-invariant* and thereby admit a scale invariance symmetry. However, *general covariance* (i.e., diffeomorphism invariance), which also results in symmetries of the GR vacuum field equations, is broken by the preferred spatial homogeneous foliations in Bianchi cosmology. The symmetries of the Einstein vacuum field equations generated by the principle of general covariance reduce to those generated by the spatial diffeomorphisms that are compatible with the Bianchi symmetry groups, which are locally characterised by their Lie algebras defined in Table 1.<sup>2</sup> Furthermore, the symmetry generating spatial diffeomorphisms correspond to the automorphisms of the Lie algebras, i.e., the linear transformations of the symmetry adapted spatial frame that leave the associated structure constants unchanged [42, 43].

As discussed in Appendix A, the automorphism groups can be used to diagonalize the vacuum class A Bianchi models, which then leaves a diagonal automorphism group for each model. As described in Table 1 and Figure 1, the class A Bianchi types are grouped into a hierarchy defined by the number of non-zero structure constants: Bianchi type IX and VIII have three; type VII<sub>0</sub> and VI<sub>0</sub> have two; type II have one; Bianchi type I has none. Each structure constant that is zero results in a diagonal automorphism and an associated symmetry, see e.g., [43, 80, 81, 34], and references therein. Due to the increasing number of automorphisms as one goes down in the hierarchy by setting structure constants to zero (i.e., by performing Lie contractions), a new symmetry in the Einstein equations appears at each level of the hierarchy. At the levels below Bianchi type IX and VIII in the class A Bianchi symmetry hierarchy, the scale and automorphism groups combine into scale-automorphism groups, which yields a symmetry hierarchy of the class A Einstein vacuum field equations [80, 81, 34].

The above hierarchical features are naturally incorporated into the conformally Hubble-normalized orthonormal frame dynamical systems approach to Einstein's vacuum field equations. In this approach, each class A Bianchi model yields an invariant set of the ODEs, denoted by Bianchi type I, II, VI<sub>0</sub>, VII<sub>0</sub>, VIII and IX, respectively. Moreover, the class A Bianchi Lie contraction hierarchy results in that each model in the hierarchy form

---

<sup>2</sup>In the present paper, considerations are spatially local. For an investigation about the role of spatial topology in a Hamiltonian description of Bianchi models, see [5].

an invariant boundary set of the models at the next higher level according to Figure 1. Thus the invariant Bianchi type I set, which constitute a circle of fixed points, the Kasner circle, is the boundary of three physically equivalent invariant Bianchi type II sets, where each type II set forms a hemisphere filled with heteroclinic orbits (solution trajectories) between different points of said circle, see, e.g., [95]. At the higher levels of the Lie contraction hierarchy the scale and scale-automorphism symmetries generate monotone functions, which limit the asymptotic dynamics in a hierarchical manner: asymptotically the dynamics toward the initial singularity is pushed in the state space at the top of the hierarchy (the Bianchi type IX and VIII models) toward the bottom of the hierarchy, the Bianchi type II and I models, where the two latter are completely determined by the scale-automorphism symmetries [34].

The scale-automorphism symmetries are complemented by discrete symmetries. Together these symmetries limit but do not completely determine the asymptotic dynamics of Bianchi types VIII and IX. Nevertheless, the (past) attractor in these models is expected to reside on the union of the Bianchi type I and II boundary sets. Furthermore, the concatenation of heteroclinic type II orbits yields heteroclinic chains, which are expected to be generically asymptotically shadowed toward the initial singularity by the type VIII and IX orbits, see [14, 22] and references therein. The type II heteroclinic orbits induce a discrete map that acts on the fixed points of the Kasner circle, called the Mixmaster map. This map exhibits chaotic properties, and it is because of this feature GR is said to be chaotic [44]. Note that the above statements are partially supported by several theorems [78, 79, 31, 10, 51, 75, 52, 14, 22].

There thereby exist intricate connections in GR between the nature of generic spacelike singularities, asymptotic Lorentzian causal structure, spatial homogeneous models, and hierarchically induced scale and diffeomorphism symmetries. To bring a new perspective on GR, we therefore ask: *What happens if the first principles that lead to the structure of generic spacelike singularities in GR are gradually modified?*

To investigate this question we have to go beyond GR and it is natural to do so by considering Hořava-Lifshitz (HL) theories. These theories are based on a preferred foliation of spacetime that breaks full spacetime diffeomorphism invariance and introduce anisotropic Lifshitz type scalings between space and time, in analogy with condensed matter physics [39, 40, 70]. There are two classes of HL theories: ‘projectable’ theories for which the lapse only depends on time, which naturally encompasses spatially homogeneous cosmology, and ‘nonprojectable’ theories with a lapse depending on time and space, which was shown to result in dynamical inconsistencies in [38].

HL gravity is a gauge theory formulated in terms of a lapse  $N$  and a shift vector  $N^i$ , which serve as Lagrange multipliers for the constraints in a Hamiltonian context, and a three-dimensional Riemannian metric  $g_{ij}$  on the slices of the preferred foliation. In GR, these objects arise from a 3+1 decomposition of a 4-metric according to,

$$\mathbf{g} = -N^2 dt \otimes dt + g_{ij}(dx^i + N^i dt) \otimes (dx^j + N^j dt). \quad (2)$$

In suitable units and scalings, the dynamics of HL vacuum gravity is governed by the action

$$S = \int N \sqrt{\det g_{ij}} (\mathcal{T} - \mathcal{V}) dt d^3x, \quad (3a)$$

where  $\mathcal{T}$  and  $\mathcal{V}$  are given by

$$\mathcal{T} = K_{ij}K^{ij} - \lambda(K^k_k)^2, \quad (3b)$$

$$\mathcal{V} = k_1R + k_2R^2 + k_3R^i_jR^j_i + k_4R^i_jC^j_i + k_5C^i_jC^j_i + k_6R^3 + \dots. \quad (3c)$$

Here  $K_{ij}$  is the extrinsic curvature,  $R$  and  $R_{ij}$  are the scalar curvature and Ricci tensor (of the spatial metric  $g_{ij}$ ), respectively, while  $C_{ij}$  is the Cotton-York tensor [40, 38], while the constants  $\lambda, k_1, \dots, k_6$  are real parameters. Repeated indices are summed over according to Einstein's summation convention.<sup>3</sup>

Full spacetime diffeomorphism invariance in GR fixes  $\lambda = 1$  uniquely and set all parameters of  $\mathcal{V}$  in (3c) to zero, except  $k_1 = -1$  (i.e.,  $\mathcal{V} = -R$ ), see [39, 40]. Thus GR is a special case among the HL models. The introduction of  $\lambda$  changes the scaling properties of the field equations, as does the introduction of additional curvature terms. Since some of the curvature terms have different scaling properties, sums of such terms in  $\mathcal{V}$  result in that the field equations no longer are scale-invariant. Nevertheless, as heuristically argued in Appendix A, when there is a sum of curvature terms in the case of the HL class A Bianchi models, there is an ‘asymptotically dominant’ curvature term toward the initial singularity. Since each curvature term exhibits a certain scaling property, this implies that the corresponding field equations are asymptotically scale-invariant. Although their scaling properties differ, the HL and GR class A Bianchi models share the same Lie contraction hierarchy, see Table 1, and consequently the same automorphism structure. Combining the (asymptotic) scale and automorphism symmetry groups for the different levels of the HL hierarchy *continuously deforms* the corresponding scale-automorphism groups in GR. This in turn affects the nature of the generic initial Bianchi type VIII and IX singularity.

Although a significant part of the previous literature on the dynamics of cosmological HL models is about isotropic matter models, see e.g. [15, 46, 85, 49], the present work is by no means the first dealing with the anisotropic vacuum HL class A Bianchi models, see e.g. [6, 71, 72, 7, 68, 27]. The present paper, however, identifies and ties mathematical structures to physical first principles and introduces new mathematical tools, which yield rigorous results about discrete dynamics induced by heteroclinic chains.

We stress that we regard the HL class A Bianchi models as toy models. Here these models serve the purpose of contextualizing how first principles affect generic spacelike singularities in GR. Furthermore, this results in a new perspective, which generates new ideas and tools for how to study GR. This, however, only requires retaining the parameter  $\lambda$  in (3b) and the vacuum GR potential  $\mathcal{V} = -R$ , which yield the so-called  $\lambda$ - $R$  models [28, 11, 58]. For simplicity, we therefore restrict considerations in the main part of the paper to the vacuum  $\lambda$ - $R$  class A Bianchi models. Nevertheless, we perform a heuristic analysis of the HL models in Appendix A, which indicates that the generic asymptotic dynamics toward the singularity for a large class of vacuum HL class A Bianchi models formally coincide with that of the vacuum  $\lambda$ - $R$  class A Bianchi models. The results in the main part of the paper for the  $\lambda$ - $R$  models are thereby also relevant for a broad class of HL models.

---

<sup>3</sup>To study the differences that arise from imposing spacetime or only spatial diffeomorphism invariance on a theory, it is illuminating to even go beyond HL theories, as discussed in [16].

In Appendix A, the Hamiltonian formulation for the spatially homogenous vacuum  $\lambda$ - $R$  class A Bianchi models is used to obtain the following evolution equations,

$$\Sigma'_\alpha = 4v(1 - \Sigma^2)\Sigma_\alpha + \mathcal{S}_\alpha, \quad (4a)$$

$$N'_\alpha = -2(2v\Sigma^2 + \Sigma_\alpha)N_\alpha, \quad (4b)$$

for  $\alpha = 1, 2, 3$ , and the constraints,

$$0 = 1 - \Sigma^2 - \Omega_k, \quad (4c)$$

$$0 = \Sigma_1 + \Sigma_2 + \Sigma_3, \quad (4d)$$

where

$$\Sigma^2 := \frac{1}{6} (\Sigma_1^2 + \Sigma_2^2 + \Sigma_3^2), \quad (5a)$$

$$\Omega_k := N_1^2 + N_2^2 + N_3^2 - 2N_1N_2 - 2N_2N_3 - 2N_3N_1, \quad (5b)$$

$$\mathcal{S}_\alpha := -4[(N_\beta - N_\gamma)^2 - N_\alpha(2N_\alpha - N_\beta - N_\gamma)]. \quad (5c)$$

Here  $(\alpha\beta\gamma)$  is a permutation of  $(123)$ . A ' denotes the derivative with respect to the chosen time variable,  $\tau_-$ , defined in Appendix A, which is in the opposite direction of physical time. Since we are considering expanding models,  $\tau_- \rightarrow \infty$  describes the dynamics toward the initial singularity. Throughout,  $\alpha$ -limits ( $\tau_- \rightarrow -\infty$ ),  $\omega$ -limits ( $\tau_- \rightarrow \infty$ ), and stability issues refer to  $\tau_-$ . The parameter  $v$  is related to  $\lambda$  according to

$$v := \frac{1}{\sqrt{2(3\lambda - 1)}}. \quad (6)$$

The GR class A Bianchi models have  $\lambda = 1$  and hence  $v = 1/2$ . Since we are primarily interested in continuous deformations of GR with  $v = 1/2$ , we restrict  $v$  to  $v \in (0, 1)$ , although the bifurcation values  $v = 0$  and  $v = 1$  are briefly mentioned in the next section and in Appendix A.

The equations (4) are invariant under permutations of the axes, i.e., they are invariant under the transformation

$$(\Sigma_1, \Sigma_2, \Sigma_3, N_1, N_2, N_3) \mapsto (\Sigma_\alpha, \Sigma_\beta, \Sigma_\gamma, N_\alpha, N_\beta, N_\gamma), \quad (7)$$

where  $(\alpha\beta\gamma)$  is a permutation of  $(123)$ .

As defined in Appendix A, the variables  $N_\alpha$  are equal to the structure constants  $n_\alpha$  multiplied with positive time dependent functions. Thus there is a one-to-one correspondence between the zeroes and signs of  $n_\alpha$  and  $N_\alpha$ , as seen by a comparison of Tables 1 and 2.

Bianchi type	$N_\alpha$	$N_\beta$	$N_\gamma$	Dim	Scale-automorphism induced dynamics
IX	+	+	+	4	One monotone function
VIII	-	+	+	4	One monotone function
VII <sub>0</sub>	0	+	+	3	Two monotone functions
VI <sub>0</sub>	0	-	+	3	Two monotone functions
II	0	0	+	2	Hemispheres of heteroclinic orbits
I	0	0	0	1	Kasner circle of fixed points

**Table 2:** The invariant class A Bianchi sets of (4), characterized by different signs and zeroes of the variables  $(N_\alpha, N_\beta, N_\gamma)$ , where  $(\alpha\beta\gamma)$  is a permutation of (123). Dim denotes the dimension of the physical state space satisfying the constraints (4c) and (4d). The scale-automorphism group induces a dynamical structure for each Bianchi type, derived in Appendix B.

This in turn results in a correspondence between Bianchi types and invariant sets in (4). Thus  $N_1 = N_2 = N_3 = 0$  leads to the invariant Bianchi type I set, which yields a circle of fixed points, called the *Kasner circle*<sup>4</sup>, denoted by  $K^\circ$ . There are three invariant Bianchi type II sets, obtained by a single non-zero  $N_\alpha$  (and thus a non-zero  $n_\alpha$ ) while the other two variables  $N_\beta$  and  $N_\gamma$  are zero (which corresponds to  $n_\beta = n_\gamma = 0$ ), where  $(\alpha\beta\gamma)$  is a permutation of (123). On each Bianchi type II set, the solutions will be shown to be heteroclinic orbits connecting different fixed points on  $K^\circ$ . Bianchi type VI<sub>0</sub> has two non-zero variables  $N_\alpha$  with opposite signs, whereas type VII<sub>0</sub> has two non-zero variables  $N_\alpha$  with the same sign. The Bianchi type VIII models have three non-zero variables  $N_\alpha$  where two of them have an opposite signs compared to the third, while the Bianchi type IX models are described by three non-zero variables  $N_\alpha$  with the same sign, see Table 2.

Table 2 also indicates the dynamical structures induced by the scale-automorphism group, derived in Appendix B, which is what remains of the first principles of scale and spatial diffeomorphism invariance in the  $\lambda$ - $R$  class A Bianchi models. As will be seen, monotone functions push the dynamics as  $\tau_- \rightarrow \infty$  from the invariant sets at the top of the class A Bianchi hierarchy to those at the bottom, in a similar manner as in GR. Moreover, heuristic reasoning in Appendix A suggests that the asymptotic generic dynamics, as  $\tau_- \rightarrow \infty$ , of Bianchi type VIII and IX, described by (4), reside on the union of the invariant Bianchi type I and II sets, as in GR. The generic asymptotic dynamics is therefore expected to be described by heteroclinic chains obtained by concatenation of heteroclinic orbits of the three different type II sets, where the  $\omega$ -limit of one heteroclinic orbit in one type II set is the  $\alpha$ -limit of a subsequent heteroclinic orbit in another type II set. Note that recent asymptotic proofs in GR exploits the Bianchi type II heteroclinic chains. From this perspective, an analysis of the Bianchi type I and II heteroclinic structure is therefore a natural first step in the asymptotic analysis of the vacuum  $\lambda$ - $R$  class A Bianchi models.

To investigate the  $\lambda$ - $R$  Bianchi type I and II heteroclinic structure, note that the Bianchi type II sets give rise to the *Kasner circle map*  $\mathcal{K} : K^\circ \rightarrow K^\circ$ , which maps the  $\alpha$ -limit to the  $\omega$ -limit of each heteroclinic orbit of type II. The properties of  $\mathcal{K}$ , which depend on

<sup>4</sup>In [28, 11, 58] it was discussed if  $\lambda$ - $R$  gravity and GR were equivalent in the asymptotically spatially flat case with ultra-local dynamics, i.e., locally Bianchi type I. This is supported in the present work by the common description of the Bianchi type I set as the Kasner circle  $K^\circ$ . However, as we shall see, stability of  $K^\circ$  varies with  $v \in (0, 1)$ .

$v$ , give a discrete description of the properties of the  $\lambda$ - $R$  type II heteroclinic chains, and thus the expected generic asymptotic continuous dynamics.

The parameter  $v \in (0, 1)$  in equation (4) situates GR in a broader context. In particular, it will be shown that the GR value  $v = 1/2$  corresponds to a bifurcation. More precisely, the case  $v = 1/2$ , referred to as the ‘critical case’, corresponds to a transition from a situation without stable fixed points in  $K^\circ$  (the subcritical case,  $v \in (0, 1/2)$ ) to one with stable fixed points (the supercritical case,  $v \in (1/2, 1)$ ). The existence of stable fixed points in the supercritical case might tempt someone to conclude that all points in  $K^\circ$  end at one of them by the discrete dynamics of the Kasner circle map  $\mathcal{K}$ , yielding finite Bianchi type II heteroclinic chains, which would prevent asymptotic chaos. However, this is not the case: there remains a Cantor set associated with infinite Bianchi type II heteroclinic chains with chaotic dynamics. The critical GR case therefore represents a transition from non-generic to generic chaos, and may also exemplify an ‘attractor crisis’, an issue discussed in [30, 29]. More precisely, we will show:

**Theorem 1.1. General relativity ( $v = 1/2$ ) is a bifurcation point as follows:**

- (i)  $v \in (1/2, 1)$ : The set of points in  $K^\circ$  associated with infinite Bianchi type II heteroclinic chains is a Cantor set  $C$  of measure zero. Moreover, the Kasner circle map  $\mathcal{K}$  is chaotic in the invariant set  $C$ .
- (ii)  $v = 1/2$ : The set of points in  $K^\circ$  associated with infinite Bianchi type II heteroclinic chains has full measure. Moreover,  $\mathcal{K}$  is generically chaotic.
- (iii)  $v \in (0, 1/2)$ : All points in  $K^\circ$  are associated with infinite Bianchi type II heteroclinic chains.

Item (i) is proved in Theorems 4.1 and 4.2, which include bounds on the Hausdorff dimension of  $C$ . For an iterative construction of the set  $C$ , see Figure 13. Item (ii) was previously proved in [8, 44], see also [89, 90] and references therein. Item (iii) is shown in Lemma 5.1 and in this case, for which the Kasner circle map  $\mathcal{K}$  is multivalued, we conjecture that  $\mathcal{K}$  is chaotic on the whole circle  $K^\circ$ . To obtain our results, we use symbolic dynamics, not previously used in GR, which results in a new description of chaos for generic spacelike singularities.

The outline of the paper is as follows. Section 2 describes the building blocks for the heteroclinic structure, the Bianchi type I and II sets, which yield the Kasner circle  $K^\circ$  and the Kasner circle map  $\mathcal{K} : K^\circ \rightarrow K^\circ$ . We also identify the three dynamically distinct regimes, supercritical, critical, and subcritical. In the next three sections we focus on the concatenation of Bianchi type II orbits into heteroclinic chains through iterates of the Kasner circle map  $\mathcal{K}$ , and describe associated chaotic aspects. Section 3 sketches known results in the critical GR case. Section 4 treats the supercritical case using symbolic dynamics. Section 5 explores the subcritical case using iterated function systems. Then Section 6, primarily, contains proofs about the asymptotic dynamics for the  $\lambda$ - $R$  Bianchi type VI<sub>0</sub> and VII<sub>0</sub> models. The main part of the paper is concluded with Section 7 which contains dynamical asymptotic conjectures for the  $\lambda$ - $R$  Bianchi type VIII and IX models (and thereby implicitly also for more general HL models).

Appendix A contains a derivation of equation (4) and the associated HL equations. It also provides a heuristic analysis of both the  $\lambda$ -R and HL Bianchi models, which suggests that their generic asymptotic dynamics toward the singularity is associated with the Bianchi type I and II heteroclinic structure, described in the main part of the paper. In Appendix B, the scale-automorphism groups at each level of the class A Bianchi Lie contraction hierarchy of the  $\lambda$ -R and HL Bianchi models is used to derive monotone functions and conserved quantities, thereby tying the nature of generic singularities in GR,  $\lambda$ -R and HL gravity to physical first principles. Finally, Appendix C contains a unified symbolic treatment of the chaotic regime in the supercritical and critical cases.

## 2 Bianchi types I and II

In this section we describe the Bianchi type I set, i.e., the Kasner circle of fixed points,  $K^\circ$ , its stability features, and the three Bianchi type II sets, which consist of heteroclinic orbits between fixed points in the set  $K^\circ$ , thereby yielding the Kasner circle map  $\mathcal{K} : K^\circ \rightarrow K^\circ$ . The heteroclinic orbits of the different type II sets can subsequently be concatenated to heteroclinic chains on the Bianchi type I and II boundary sets of Bianchi type VIII and IX; for the GR case, see e.g. [95, 32, 89, 14, 22]. To illustrate concatenation, we explicitly construct heteroclinic cycles/chains with period 3 when  $v \in [0, 1]$ .

### 2.1 Bianchi type I

The Bianchi type I set is determined by  $N_1 = N_2 = N_3 = 0$ , which according to equation (4) results in the *Kasner circle* of fixed points:

$$K^\circ := \left\{ (\Sigma_1, \Sigma_2, \Sigma_3, 0, 0, 0) \in \mathbb{R}^6 \mid \begin{array}{l} 1 - \Sigma^2 = 0, \\ \Sigma_1 + \Sigma_2 + \Sigma_3 = 0 \end{array} \right\}. \quad (8)$$

There are three exceptional points in the set  $K^\circ$  called the *Taub points*, since they correspond to the Taub representation of Minkowski spacetime in GR, see [87]. They are characterized by  $(\Sigma_1, \Sigma_2, \Sigma_3)$  as follows:

$$T_1 := (2, -1, -1), \quad T_2 := (-1, 2, -1), \quad T_3 := (-1, -1, 2), \quad (9)$$

where  $T_\alpha$ ,  $\alpha = 1, 2, 3$ , is the point in the set  $K^\circ$  where  $\Sigma_\alpha$  attains its maximum value 2, see Figure 2.

The parameter  $v$  plays an important role in the dynamics of the variables  $N_\alpha$ ,  $\alpha = 1, 2, 3$ , where a bifurcation occurs at  $v = 1/2$ . This can be seen from the linearization at  $T_1$  in (4):

	$v < 1/2$	$v = 1/2$	$v > 1/2$	
$N'_1 = -(2v+2)N_1$ ;	$-(2v+2)$	$< 0$	$< 0$	$< 0$ , <span style="float: right;">(10a)</span>
$N'_2 = -(2v-1)N_2$ ;	$-(2v-1)$	$> 0$	$= 0$	$< 0$ , <span style="float: right;">(10b)</span>
$N'_3 = -(2v-1)N_3$ ;	$-(2v-1)$	$> 0$	$= 0$	$< 0$ . <span style="float: right;">(10c)</span>

The Taub point  $T_1$  thereby has one stable variable  $N_1$  while  $N_2$  and  $N_3$  are central when  $v = 1/2$ , whereas for  $v \neq 1/2$  the Taub point becomes hyperbolic:  $N_1$  is stable and both  $N_2$  and  $N_3$  are unstable when  $v < 1/2$ , while all  $N_\alpha$  are stable when  $v > 1/2$ . Using the permutation symmetry (7) leads to similar statements for  $T_2$  and  $T_3$ .

In general, linearization of equation (4b) at  $K^\circ$  results in

$$N'_\alpha = -(2v + \Sigma_\alpha|_{K^\circ})N_\alpha, \quad \alpha = 1, 2, 3. \quad (11)$$

For each  $\alpha = 1, 2, 3$ , the stability behaviour of  $N_\alpha$  changes when  $\Sigma_\alpha|_{K^\circ} = -2v$ . We define the *unstable Kasner arc*, denoted by  $\text{int}(A_\alpha)$ , to be the points in  $K^\circ$  that are unstable in the  $N_\alpha$  variable, i.e., when  $\Sigma_\alpha < -2v$ . The closure of  $\text{int}(A_\alpha)$  is denoted by  $A_\alpha$  and is given by

$$A_\alpha := \{(\Sigma_1, \Sigma_2, \Sigma_3, 0, 0, 0) \in K^\circ \mid \Sigma_\alpha \leq -2v\}. \quad (12)$$

Due to the axis permutation symmetry (7), the Kasner arcs  $A_\alpha$  are symmetric portions of  $K^\circ$  with points  $Q_\alpha = -T_\alpha$  in the middle, given by

$$Q_1 := (-2, 1, 1), \quad Q_2 := (1, -2, 1), \quad Q_3 := (1, 1, -2), \quad (13)$$

where  $Q_\alpha$  is the point where  $\Sigma_\alpha$  attains its minimum value  $-2$  in  $K^\circ$ .

The boundary set  $\partial A_\alpha$  consists of two fixed points, which we refer to as *tangential points*, for reasons explained below, see Figure 3. These tangential points are the Taub points when  $v = 1/2$ , but  $v \neq 1/2$  unfolds each Taub point into two non-hyperbolic tangential points, see Figure 2. The tangential points are determined by  $\Sigma_\alpha|_{K^\circ} = -2v$ , which taken together with the constraints in (8) yield

$$t_{\beta\gamma} := (\Sigma_\alpha, \Sigma_\beta, \Sigma_\gamma) = -vT_\alpha + (T_\beta - T_\gamma)\sqrt{(1-v^2)/3}, \quad (14)$$

where  $(\alpha\beta\gamma)$  is a permutation of (123), while the Taub points were given in (9). For example, the tangential points for the arcs  $A_2$  and  $A_3$  closest to  $T_1$  are given by

$$t_{12} = (v + \sqrt{3(1-v^2)}, v - \sqrt{3(1-v^2)}, -2v) \quad (15a)$$

$$t_{13} = (v + \sqrt{3(1-v^2)}, -2v, v - \sqrt{3(1-v^2)}). \quad (15b)$$

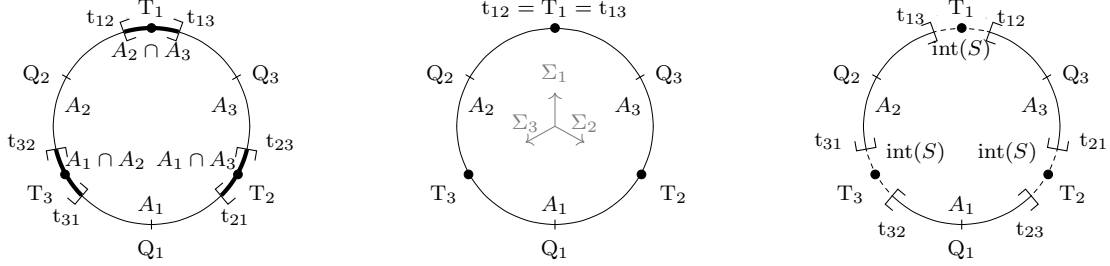
The bifurcation at  $v = 1/2$  induces the stability change of  $N_\alpha$  in equation (11), where equation (15) entails that the tangential points  $t_{12}$  and  $t_{13}$  pass through each other at  $T_1$  as  $v$  crosses the value  $1/2$ ; axis permutations result in similar statements for the other tangential points near the other Taub points, see Figure 2.

We are primarily interested in continuous deformations of GR,  $v = 1/2$ , and we therefore focus on the interval  $v \in (0, 1)$ . These models admit three cases, where  $(\alpha\beta\gamma)$  is a permutation of (123):

- (i) *The subcritical case*  $v \in (0, 1/2)$ : The union of the three arcs  $A_\alpha$  cover  $K^\circ$ , where both  $N_\beta$  and  $N_\gamma$  are unstable in the region  $\text{int}(A_\beta \cap A_\gamma)$  containing  $T_\alpha$ .
- (ii) *The critical case*  $v = 1/2$ : The three arcs  $A_\alpha$  cover  $K^\circ$  and each pair of arcs intersect only at a Taub point.

(iii) *The supercritical case*  $v \in (1/2, 1)$ : The union of the three arcs  $A_\alpha$  do not cover  $K^\circ$ . There is a *closed* region around the Taub points  $T_\alpha$  which is stable, defined by  $S := K^\circ \setminus \text{int}(A_1 \cup A_2 \cup A_3)$ .

Note that the fixed points in  $\text{int}(S)$  have negative eigenvalues associated with the  $N_\alpha$  variables, but, for future purposes, we also include the tangential boundary points in the definition of  $S$ , for which one of the negative eigenvalues is replaced by a zero eigenvalue.



(a): Subcritical:  $v \in (0, 1/2)$ . (b): Critical:  $v = 1/2$ . (c): Supercritical:  $v \in (1/2, 1)$ .

**Figure 2:** As  $v \in (0, 1)$  increases, the length of each closed arc  $A_1, A_2$  and  $A_3$  decreases. For  $v \in (0, 1/2)$  the union of all arcs cover  $K^\circ$ , where the length of their intersections (in bold) decreases when  $v$  increases. At  $v = 1/2$  the arcs only intersect at the Taub points  $T_1, T_2, T_3$ . For  $v \in (1/2, 1)$  the arcs do not intersect and their union therefore do not cover  $K^\circ$ , which results in the (dashed) set  $S$ , given by  $S := K^\circ \setminus \text{int}(A_1 \cup A_2 \cup A_3)$ .

## 2.2 Bianchi type II

There are three physically equivalent type II sets, due to (7), each characterized by a single non-zero variable  $N_\alpha$ ,  $\alpha = 1, 2, 3$ , where each set yields a two-dimensional hemisphere. The three hemispheres intersect only at their common  $K^\circ$  boundary. The Bianchi type II set with  $N_1 \neq 0$ , denoted by  $\text{II}_1$ , is given by

$$\text{II}_1 := \left\{ (\Sigma_1, \Sigma_2, \Sigma_3, N_1, 0, 0) \in \mathbb{R}^6 \mid \begin{array}{l} 1 - \Sigma^2 - N_1^2 = 0, \\ \Sigma_1 + \Sigma_2 + \Sigma_3 = 0, \\ N_1 \neq 0 \end{array} \right\}, \quad (16)$$

while the other two Bianchi type II sets  $\text{II}_2$  and  $\text{II}_3$  are obtained by permutation of the axes according to (7). Without loss of generality, we therefore explicitly only consider  $\text{II}_1$ .

As follows from (4), the evolution equations for  $\text{II}_1$  can be written as

$$(\Sigma_1, \Sigma_2, \Sigma_3)' = 4v \left[ (1 - \Sigma^2)(\Sigma_1, \Sigma_2, \Sigma_3) + \frac{T_1}{v} N_1^2 \right], \quad (17a)$$

$$N_1' = -2(2v\Sigma^2 + \Sigma_1)N_1. \quad (17b)$$

The constraints are given by  $\Sigma_1 + \Sigma_2 + \Sigma_3 = 0$  and  $N_1^2 = 1 - \Sigma^2$ , where  $\Sigma^2$  is defined in (5a).

Using  $N_1^2 = 1 - \Sigma^2$  to solve for  $N_1^2$  results in that (17a) can be written as

$$\left[ (\Sigma_1, \Sigma_2, \Sigma_3) + \frac{T_1}{v} \right]' = 4v(1 - \Sigma^2) \left[ (\Sigma_1, \Sigma_2, \Sigma_3) + \frac{T_1}{v} \right], \quad (18)$$

where  $\Sigma_1$  is monotonically increasing for any initial condition in the interior of  $\text{II}_1$ . The term  $4v(1 - \Sigma^2)$  is an Euler multiplier when  $\Sigma^2 \neq 1$ . This term is eliminated by an appropriate time rescaling,  $(.)' = 4v(1 - \Sigma^2)(.)$ , which leads to  $\dot{w} = w$  where  $w := (\Sigma_1, \Sigma_2, \Sigma_3) + \mathbf{T}_1/v$ .

Solutions of (18) are therefore straight lines in  $(\Sigma_1, \Sigma_2, \Sigma_3)$ -space, which we parametrize by introducing a variable  $\eta \in \mathbb{R}$ , defined by

$$\eta' = 4v(1 - \Sigma^2)\eta. \quad (19)$$

We thereby obtain

$$(\Sigma_1, \Sigma_2, \Sigma_3) = (\Sigma_1^i, \Sigma_2^i, \Sigma_3^i)\eta + \frac{\mathbf{T}_1}{v}(\eta - 1). \quad (20)$$

The straight lines pass through the auxiliary point  $Q_1/v$  outside the physical state space  $\text{II}_1$  when  $\eta = 0$ . A particular straight line solution then enters the physical state space at a point  $p = (\Sigma_1^i, \Sigma_2^i, \Sigma_3^i) \in A_1$  in the set  $K^\circ$  when  $\eta = 1$ . This point is the  $\alpha$ -limit of an associated heteroclinic orbit in  $\text{II}_1$ , with  $\Sigma^2 < 1$ , for which  $\eta > 1$  is monotonically increasing until the solution ends at its  $\omega$ -limit point  $p^f = (\Sigma_1^f, \Sigma_2^f, \Sigma_3^f)$  in  $K^\circ$ . The point  $p^f$  is determined by the constraints (4c) and (4d) when  $N_1 = N_2 = N_3 = 0$ , and equation (20). These conditions lead to two solutions for  $\eta$ :  $\eta = 1$  (for  $p$ ) and  $\eta = g$  (for  $p^f$ ), where

$$g := \frac{1 - v^2}{1 + v^2 + \Sigma_1^i v} \geq 1. \quad (21)$$

Using the constraints (4c) and (4d) for  $p$  to replace  $\Sigma_2^i$  and  $\Sigma_3^i$  with  $\Sigma_1^i$ , and the latter with  $g$  according to the above equation, give

$$N_1^2 = 1 - \Sigma^2 = \left( \frac{1 - v^2}{v^2} \right) (\eta - 1)(g - \eta)g^{-1}. \quad (22)$$

Similar results are obtained by axis permutation for  $\text{II}_2$  and  $\text{II}_3$ . Figure 3 gives an example of a Bianchi type  $\text{II}_1$  heteroclinic orbit, given by (20), (21), (22), and its projected straight line in  $(\Sigma_1, \Sigma_2, \Sigma_3)$ -space.

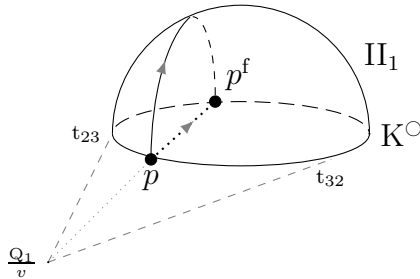


**Figure 3:** An example of a Bianchi type II solution; a heteroclinic orbit in the hemisphere  $\text{II}_1$ . Its projection is a (dotted) line parametrized by  $\eta$  in  $(\Sigma_1, \Sigma_2, \Sigma_3)$ -space given by (20). There are three special points on this line: the auxiliary point  $Q_1/v$  outside the physical state space  $\text{II}_1$  when  $\eta = 0$ ,  $p$  when  $\eta = 1$  and  $p^f$  when  $\eta = g$ . Furthermore, the nomenclature ‘tangential points’ is explained: they are the points where  $p = p^f$  and hence where the aforementioned lines are tangential to  $K^\circ$ .

Using equation (20) to eliminate  $\eta$  yields the unparametrized form of the heteroclinic orbits in  $\text{II}_1$ ,

$$\left(\Sigma_1^i + \frac{2}{v}\right)(\Sigma_2 - \Sigma_3) = \left(\Sigma_2^i - \Sigma_3^i\right)\left(\Sigma_1 + \frac{2}{v}\right), \quad (23)$$

where a cyclic permutation of (123) yields the orbits in  $\text{II}_2$  and  $\text{II}_3$ . Note that equation (23) is derived in Appendix B from the scale-automorphism group. In combination with axis permutations this establishes that the Bianchi type II heteroclinic chains arise from first principles, in GR,  $\lambda$ -R and HL gravity.

The type II heteroclinic orbits induce a map between different Kasner states on the Kasner circle, called *the Kasner circle map*  $\mathcal{K}: K^\circ \rightarrow K^\circ$ . It maps the  $\alpha$ -limits to the  $\omega$ -limits of heteroclinic orbits in each of the hemispheres  $\text{II}_1$ ,  $\text{II}_2$ ,  $\text{II}_3$ , see Figures 3 and 4.

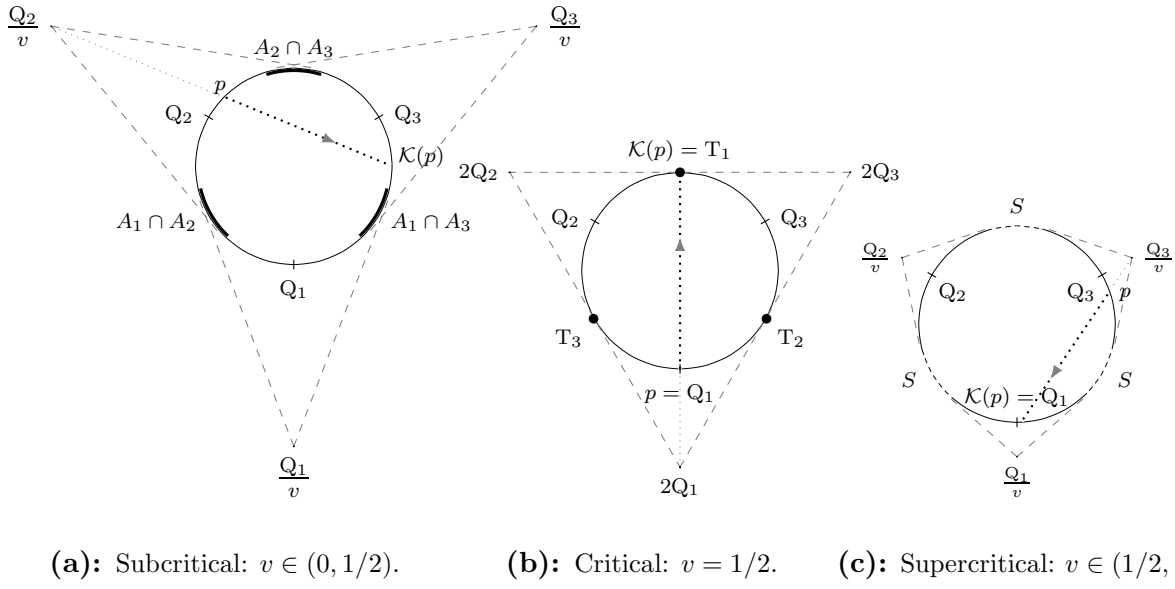


**Figure 4:** The Kasner circle map  $\mathcal{K}$  can be obtained from the straight lines that emanate from the three auxiliary points  $Q_\alpha/v$ , which intersect with two points in the set  $K^\circ$ :  $p$  and  $\mathcal{K}(p) := p^f$ . Each (bold dotted) line represents the projection onto  $(\Sigma_1, \Sigma_2, \Sigma_3)$ -space of a heteroclinic orbit from different hemispheres  $\text{II}_\alpha$ , originating from the auxiliary point  $Q_\alpha/v$ . Note that the points  $Q_\alpha/v$  approach  $Q_\alpha$  as  $v \rightarrow 1$ , whereas  $Q_\alpha/v$  goes to infinity as  $v \rightarrow 0$ .

Each point  $p = (\Sigma_\alpha^i, \Sigma_\beta^i, \Sigma_\gamma^i)$  in the set  $K^\circ$  is thereby mapped to  $p^f = (\Sigma_\alpha^f, \Sigma_\beta^f, \Sigma_\gamma^f)$  in  $K^\circ$ , where  $p^f$  is obtained from (20) and permutations thereof by setting  $\eta = g$ . Thus,

$$\mathcal{K}(p) := \begin{cases} g(p)p + (g(p) - 1)\frac{T_\alpha}{v} & \text{for } p \in A_\alpha \\ p & \text{for } p \notin A_1 \cup A_2 \cup A_3 \end{cases}, \quad (24)$$

where

$$g(p) := \frac{1 - v^2}{1 + v^2 + \Sigma_\alpha^i v} \geq 1, \quad \text{for } p = (\Sigma_1^i, \Sigma_2^i, \Sigma_3^i) \in A_\alpha, \quad (25)$$

and where the index  $\alpha$  in  $\Sigma_\alpha^i$  is the same index as for  $A_\alpha$ .

When  $v \in [1/2, 1)$  the Kasner circle map  $\mathcal{K}$  is well-defined and continuous, since the unstable arcs  $\text{int}(A_1)$ ,  $\text{int}(A_2)$  and  $\text{int}(A_3)$  are disjoint. Note that the set  $S$  consists of fixed points of the Kasner circle map  $\mathcal{K}$ . In the critical case,  $v = 1/2$ , the Kasner circle map  $\mathcal{K}$  is the Mixmaster map, discussed in Section 3, while the dynamics of  $\mathcal{K}$  in the supercritical case  $(1/2, 1)$  is discussed in Section 4.

For  $v \in [0, 1/2)$ , however,  $\mathcal{K}$  is not a well-defined map, since the unstable arcs  $\text{int}(A_\alpha)$  overlap and points in the overlapping regions  $\text{int}(A_\alpha \cap A_\beta)$  have two possible Bianchi type II heteroclinic orbits, making  $\mathcal{K}$  multivalued. Moreover, a discontinuity on at least one of the boundary points of  $A_\alpha \cap A_\beta$  is inevitable, since one must change the auxiliary vertex  $Q_\alpha/v$  for the map, see Figure 4. Nevertheless, we can still define iterates of  $\mathcal{K}$  through a family of piece-wise continuous maps to capture features of the dynamics, as explored in Section 5.

To describe the expansion properties of the Kasner circle map (24), it is convenient to first introduce Misner parametrized variables  $(\Sigma_+, \Sigma_-)$  adapted to the arc  $A_1$ , which, according to Appendix A, are given by

$$\Sigma_1 = -2\Sigma_+, \quad (26a)$$

$$\Sigma_2 = \Sigma_+ + \sqrt{3}\Sigma_-, \quad (26b)$$

$$\Sigma_3 = \Sigma_+ - \sqrt{3}\Sigma_-, \quad (26c)$$

which leads to  $\Sigma^2 = \Sigma_+^2 + \Sigma_-^2$  where  $\Sigma^2 = 1$  on  $K^\circlearrowright$ , due to the constraint (4c), thereby yielding a circle with unit radius. The variables  $(\Sigma_+, \Sigma_-)$  have the advantage of solving the constraint (4d), but the drawback of making the permutation symmetry (7) implicit, whereas it is explicit in  $(\Sigma_1, \Sigma_2, \Sigma_3)$ .

The variables  $\Sigma_\pm$  lead to the following form for the Kasner circle map (24):

$$\mathcal{K}_+(\Sigma_+^i, \Sigma_-^i) = g(-2\Sigma_+^i) \left[ \Sigma_+^i - \frac{1}{v} \right] + \frac{1}{v}, \quad (27a)$$

$$\mathcal{K}_-(\Sigma_+^i, \Sigma_-^i) = g(-2\Sigma_+^i) \Sigma_-^i, \quad (27b)$$

where  $g(-2\Sigma_+^i)$  is given by (25) in the Misner parametrization (26) of  $p \in A_1$ .

Next we introduce an angular variable  $\varphi$  adapted to  $A_1$ ,

$$\Sigma_+ = \cos(\varphi), \quad (28a)$$

$$\Sigma_- = \sin(\varphi), \quad (28b)$$

which solves the remaining constraint (4c), since  $\Sigma^2 = \Sigma_+^2 + \Sigma_-^2 = 1$  (similar variables  $\Sigma_\pm$  with associated angles  $\varphi$  can be introduced for  $A_2$  and  $A_3$ , by permutation of the axes). The map (27) can then be replaced by a map with the arc-length  $\varphi$  of the Kasner unit circle  $K^\circlearrowright$  as its domain,

$$\mathcal{K}(\varphi^i) = \int_{t_{23}}^{\varphi^i} \sqrt{(D\mathcal{K}_+(\varphi))^2 + (D\mathcal{K}_-(\varphi))^2} d\varphi, \quad (29)$$

where  $D = d/d\varphi$  on  $A_1$ , and similarly for  $A_2$  and  $A_3$ .

The derivative of  $\mathcal{K}(\varphi^i)$  with respect to  $\varphi^i$  is the tangent vector, with length

$$|D\mathcal{K}(\varphi^i)| = \sqrt{(D\mathcal{K}_+(\varphi^i))^2 + (D\mathcal{K}_-(\varphi^i))^2}. \quad (30)$$

Applying the chain rule to (27) at  $\varphi^i$  yields

$$|D\mathcal{K}(p)| = g(p) = \frac{1 - v^2}{1 + v^2 - 2 \cos(\varphi^i)v}, \quad (31)$$

where  $g$  in (25) is expressed in  $\varphi^i$  by means of (28), which yields  $\Sigma_1^i = -2\Sigma_+^i = -2 \cos(\varphi^i)$ . Using the symmetry under axes permutations (7) proves the following Lemma:

**Lemma 2.1.** *The derivative of the Kasner circle map  $\mathcal{K}$  with respect to the arc-length of the Kasner unit circle  $K^\circ$ ,  $\varphi \in A_\alpha$ , is given by*

$$|D\mathcal{K}(p)| = \begin{cases} g(p) & \text{for } p \in A_\alpha \\ 1 & \text{for } p \notin A_1 \cup A_2 \cup A_3. \end{cases} \quad (32)$$

In other words, the Kasner circle map  $\mathcal{K}$  is expanding on the interior of each  $A_\alpha$ , but not uniformly<sup>5</sup> since  $g$  is a varying function that attains 1 at  $\partial A_\alpha$ . In the arc  $A_1$ , the map  $\mathcal{K}$  is symmetric with respect to  $Q_1$ , which is due to the permutation of  $\Sigma_2$  and  $\Sigma_3$  according to (7), and it is monotonically increasing on each side of  $Q_1$  starting from the tangential points  $t_{32}$  and  $t_{23}$ , where  $g = 1$ , until  $g$  reaches its maximum  $g = (1 + v)/(1 - v)$  at  $Q_1$ , where  $\Sigma_1^i = -2$ , see Figure 5. Similar statements hold for  $A_2$  and  $A_3$  by permuting the axes, as in (7).

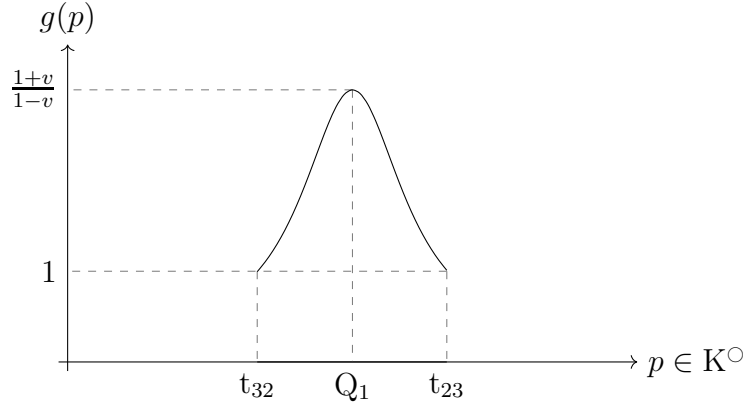


**Figure 5:** The function  $g(p)$  for  $p \in A_1$  between the tangential points  $t_{32}$  and  $t_{23}$ .

In Bianchi type VIII and IX, it is possible to concatenate type II heteroclinic orbits on the type I and II boundaries to form heteroclinic chains. This heteroclinic structure is expected to play a key role for type VIII and IX when  $\tau_- \rightarrow \infty$ , and is the focus of the next three sections. However, before proceeding, we describe the bifurcations at  $v = 0$  and  $v = 1$ . We then construct heteroclinic chains with period 3 when  $v \in [0, 1]$ , as an example of concatenation of heteroclinic Bianchi type II orbits.

<sup>5</sup>Hence  $\mathcal{K}$  is an example of a non-uniformly hyperbolic circle map, and it would be interesting to investigate its dynamical properties with recent mathematical methods developed in [45, 12, 54, 22] and references therein.

### The cases $v = 0$ and $v = 1$

Even though the cases  $v = 0$  and  $v = 1$  are not our main focus, they are useful in order to obtain results for  $v \in (0, 1)$ , as illustrated by the construction of the heteroclinic cycles/chains with period 3 below. In contrast to when  $v \in (0, 1)$ , the Kasner circle map  $\mathcal{K}$  is not chaotic for  $v = 0$  and  $v = 1$ , and thus bifurcations occur at these parameter values, see Figure 6.

As  $v \rightarrow 0$ , the heteroclinic orbits become parallel lines<sup>6</sup>, see Figure 6. The derivative of the Kasner circle map  $\mathcal{K}$ , given by (32), thereby equals 1 at any point on  $K^\circ$ , as is seen from the limit  $v \rightarrow 0$  in equation (25). Since there is no expansion, the case  $v = 0$  has a network of heteroclinic orbits that is not associated with chaos, but see Appendix A.2 for further discussions on HL models and their relation to the case  $v = 0$ . Note the connection with ‘frame transitions’ in, e.g., Bianchi type VI<sub>-1/9</sub> vacuum models, and when using an Iwasawa frame in GR [89, 90, 37, 18], since these also consist of parallel heteroclinic orbits. In contrast to these situations in GR, however, there are three (instead of two) families of non-expanding orbits when  $v = 0$ , and no family of expanding type II orbits.

As  $v \rightarrow 1$ , the Kasner circle map  $\mathcal{K}$  is not continuous anymore: it becomes the identity on  $K^\circ$ , except at each of the three points  $Q_\alpha$ , which are mapped to the entire set  $K^\circ$ . In particular, the points  $Q_\alpha$  are mapped to each other, thereby yielding a network of heteroclinic chains: chains of period 2 between each two points  $Q_\alpha$  and  $Q_\beta$ , and chains with period 3 between the three points  $Q_\alpha$ . The situation for  $v = 1$  is somewhat reminiscent to that of the Bianchi type I Einstein-Vlasov models, where there is a heteroclinic network associated with the Taub points  $T_\alpha$ , see [33]; for a recent paper on the future dynamics of these Einstein-Vlasov models, see [48].



**(a):** For  $v \rightarrow 0$ , the points  $Q_\alpha/v \rightarrow \infty$ . Hence the type II heteroclinic orbits are parallel lines that emanate from infinity. The overlapping arcs (in bold) have two unstable directions. Moreover,  $|A_\alpha| = \pi$  and  $|A_\alpha \cap A_\beta| = \pi/3$ .

**(b):** For  $v \rightarrow 1$ , the points  $Q_\alpha/v \rightarrow Q_\alpha$  on  $K^\circ$ , where  $A_\alpha$  consists of a single point  $Q_\alpha$ . Hence any point on  $K^\circ$  can be reached by a type II heteroclinic orbit from  $Q_\alpha$ . The dashed arcs have three stable directions.

**Figure 6:** Heteroclinic type II orbits for  $v = 0$  and  $v = 1$  projected onto  $(\Sigma_1, \Sigma_2, \Sigma_3)$ -space.

<sup>6</sup>Multiplying (23) by  $v$  and setting  $v = 0$  results in  $\Sigma_2 - \Sigma_2^i = \Sigma_3 - \Sigma_3^i$  for the  $v = 0$  type II<sub>1</sub> models, in agreement with Figure 6 when  $v = 0$ . In [27], the authors considered Bianchi type II models with  $\lambda = 1$  and a quadratic curvature term, which is mathematically equivalent to  $v = 1/8$  in the  $\lambda$ - $R$  case, and a cubic curvature term, which corresponds to  $v = 0$ , as seen in Appendix A.2. In the latter case, it was pointed out that the Kasner parameter  $u = u^i = \sqrt{3} + 1$  results in  $u^i = u^f$ , which yields the period 3 heteroclinic cycles in the present formulation.

## Example of Bianchi type II concatenation: Period 3 chains

We will now construct heteroclinic chains with period 3 (i.e., period 3 heteroclinic cycles), and describe how these chains change as the parameter  $v \in [0, 1]$  varies. For the GR case  $v = 1/2$ , these chains/cycles have been previously found, see e.g. [32]. First, note that chains with period 3 consist of equilateral triangles in the plane of the Kasner circle in the projected  $(\Sigma_1, \Sigma_2, \Sigma_3)$ -space, which follows from the permutation symmetry described in (7), where the corners of the triangles on  $K^\circlearrowright$  correspond to physically equivalent Kasner states, again related by axis permutations. Second, there are two equilateral triangles for each value of  $v \in [0, 1]$ , which due to (7) are symmetric with respect to reflections with respect to the coordinate lines  $\Sigma_\alpha$ , while the two triangles coalesce to a single one with corners at the points  $Q_\alpha$  when  $v = 1$ . Third, the triangles depict  $(\Sigma_1, \Sigma_2, \Sigma_3)$ -space projections of two different heteroclinic chains on the Bianchi type II boundary of the Bianchi type VIII and IX state spaces, with clockwise and anti-clockwise orientation of the projected heteroclinic chains in  $(\Sigma_1, \Sigma_2, \Sigma_3)$ -space, see Figure 7.

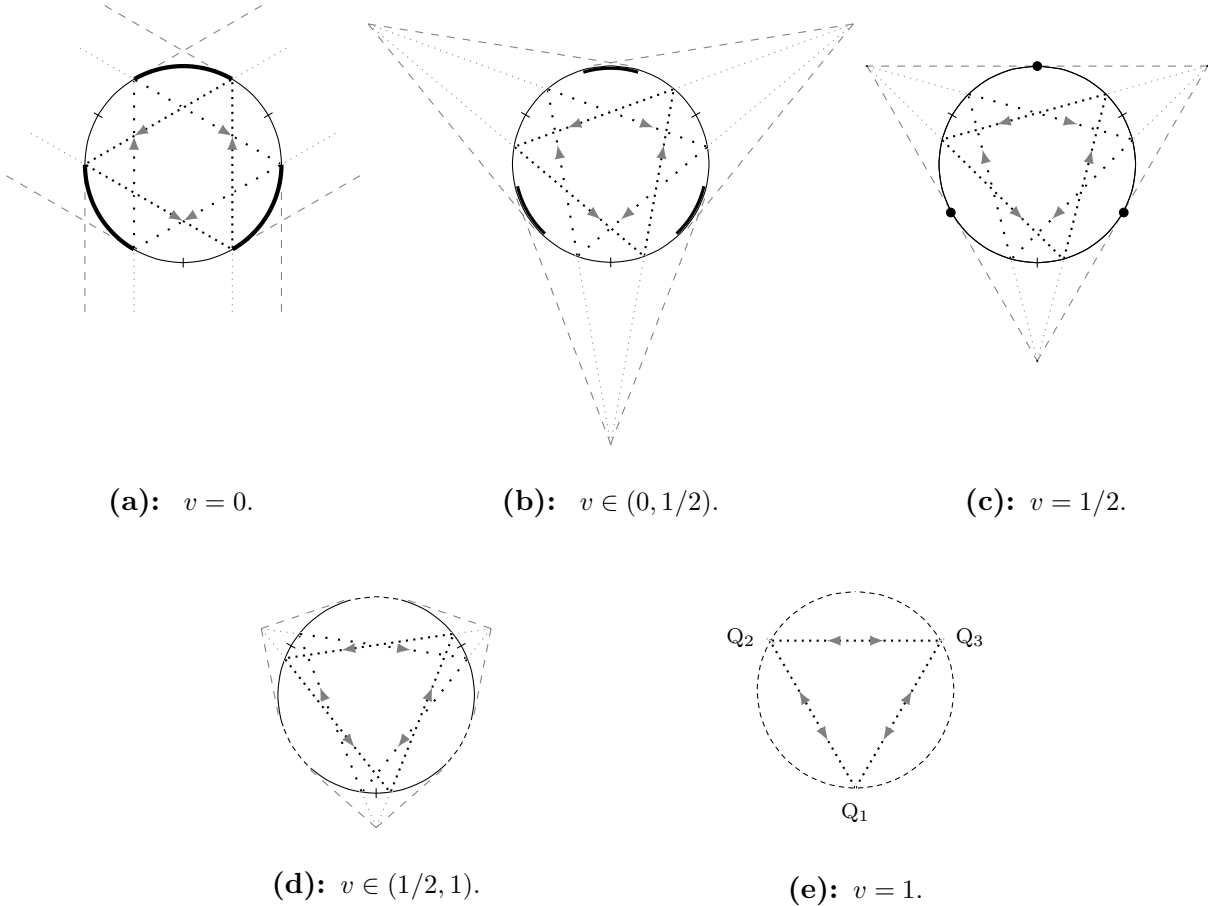
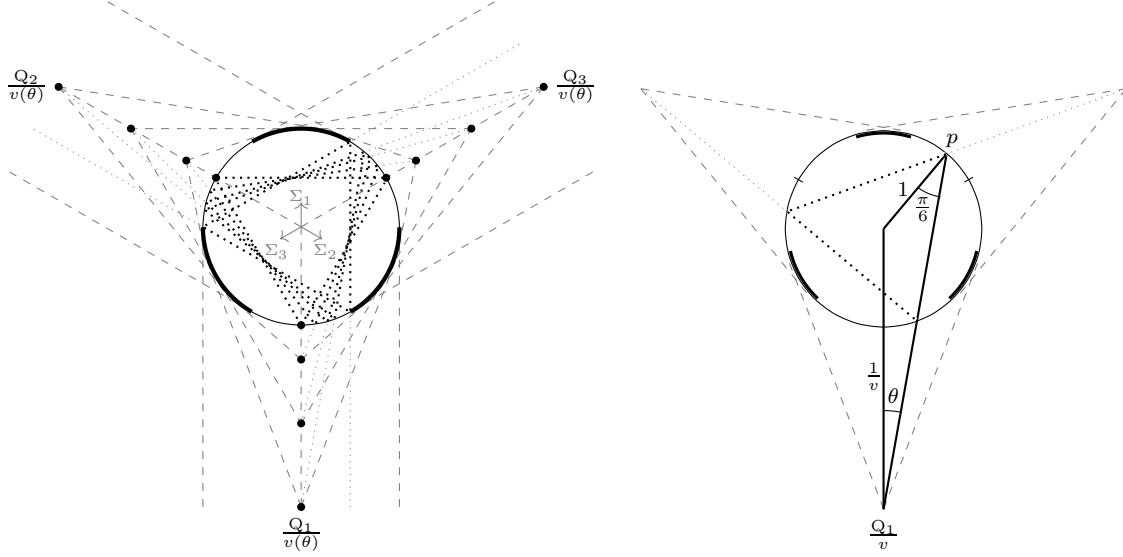


**Figure 7:** The two triangles in each figure depict the two periodic heteroclinic chains with period 3 projected onto  $(\Sigma_1, \Sigma_2, \Sigma_3)$ -space. As  $v \in [0, 1]$  increases, these triangles rotate: the densely (sparsely) dotted one rotates clockwise (counter-clockwise).

The heteroclinic chains with period 3 can be constructed as follows from the  $v = 0$  case, for which the period 3 chains are easily obtained due to the simple heteroclinic

structure. Without loss of generality, consider the densely dotted triangle in Figure 7 for  $v = 0$  and rotate it clockwise by an angle  $\theta \in (0, \pi/6]$ . The three prolonged sides of the rotated triangle intersect each projected  $\Sigma_\alpha$  axis (projected onto the plane that contains the Kasner circle) at the same distance from  $K^\circ$  due to the axis permutation symmetry. Since the prolonged lines correspond to Bianchi type II orbits in the physical state space, the points of intersection are given by  $Q_\alpha/v$  for some  $v = v(\theta)$ . Continuity of the rotation and the parametrization  $v(\theta)$  yields the period 3 chains for all  $\theta \in [0, \pi/6]$ , i.e., all  $v = v(\theta) \in [0, 1]$ . The boundary cases  $v = 0$  and  $v = 1$  yield  $\lim_{\theta \rightarrow 0} Q_\alpha/v(\theta) \rightarrow \infty$  and  $\lim_{\theta \rightarrow \pi/6} Q_\alpha/v(\theta) \rightarrow Q_\alpha$ , respectively, see Figure 8.



**(a):** Superposition of the densely dotted heteroclinic chains with period 3 for different  $v \in [0, 1]$ . The prolonged sides of each triangle intersect the projected  $\Sigma_\alpha$  axis at some  $Q_\alpha/v(\theta)$  and describe type II orbits.

**(b):** The angle of rotation  $\theta = \theta(v)$  is obtained by the law of sines using the triangle in the plane of  $K^\circ$  between the center of  $K^\circ$ , the point  $Q_1/v$  and the vertex  $p \in A_3$  of the triangle that describes a period 3 chain.

**Figure 8:** As  $v$  increases, the triangles rotate clockwise by the angle  $\theta \in [0, \pi/6]$  in (33).

Moreover,  $v(\theta) = 2 \sin \theta$ , or alternatively,

$$\theta(v) = \arcsin\left(\frac{v}{2}\right). \quad (33)$$

This equation yields the clockwise (counter-clockwise) rotation of the densely (sparsely) dotted triangle and can be derived as follows. The rotation angle  $\theta$  for the densely dotted triangle is given by the angle between the line from  $Q_1/v$  to the center of  $K^\circ$  and the Bianchi type II trajectory originating from  $Q_1/v$  and ending at the vertex of the triangle in the arc  $A_3$ , which we denote by  $p$ , see Figure 8. Consider the triangle that connects the center of  $K^\circ$ ,  $Q_1/v$ , and the vertex  $p$  in the plane of  $K^\circ$ , which has unit radius in the  $(\Sigma_+, \Sigma_-)$  coordinates. In these coordinates, the line from the origin  $(0, 0)$  to  $Q_1/v$  has length  $1/v$ , while the unit radius from  $(0, 0)$  to the vertex  $p$  bisects the angle of the equilateral triangle, due to the permutation symmetry (7), which yields an angle of  $\pi/6$ ,

see Figure 8. The law of sines then implies that  $\sin \theta = v \sin(\pi/6) = v/2$ , and thereby the above formula. Combining the result in equation (33) with the geometry in Figure 8 yields

$$\Sigma_1 = \sqrt{3 \left( 1 - \left( \frac{v}{2} \right)^2 \right)} - \frac{v}{2} \quad (34)$$

for the upper vertices (and thus with maximum  $\Sigma_1$ ) of the densely and sparsely dotted period 3 triangles in Figures 7 and 8.

We have thereby proved the following result:

**Proposition 2.2.** *There are two heteroclinic chains with period 3 for all  $v \in [0, 1]$ . When projected onto the plane of the Kasner circle  $K^\circ$ , these chains/cycles are given by two equilateral triangles within  $K^\circ$ . As  $v \in [0, 1)$  increases, the two triangles rotate in different directions and coalesce into one when  $v = 1$ .*

### 3 Critical case

GR belongs to the critical case  $v = 1/2$  where the concatenated Bianchi type II orbits describe the heteroclinic chains that are expected to be asymptotically shadowed by solutions when  $\tau_- \rightarrow \infty$  in the Bianchi type VIII and IX models. An example of part of a heteroclinic chain is given in Figure 9.

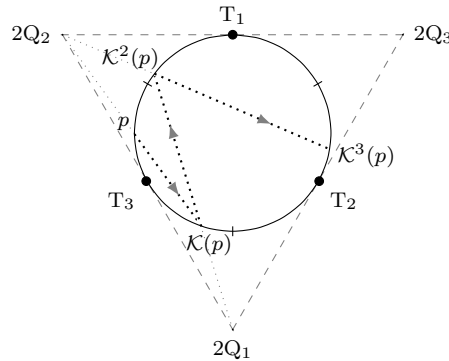


**Figure 9:** The concatenation of three projected heteroclinic orbits onto  $(\Sigma_1, \Sigma_2, \Sigma_3)$ -space, which form part of a heteroclinic chain described by iterates of the Kasner circle map  $\mathcal{K}$ .

In GR it is useful to define the *Kasner parameters*  $(p_1, p_2, p_3)$  on the Kasner circle  $K^\circ$  according to

$$\Sigma_\alpha = 3p_\alpha - 1, \quad \text{for } \alpha = 1, 2, 3, \quad (35)$$

where  $p_1 + p_2 + p_3 = 1 = p_1^2 + p_2^2 + p_3^2$ , due to the constraints (8) on  $K^\circ$ .

The Kasner circle  $K^\circ$  is described by six sectors characterized by  $p_\alpha < p_\beta < p_\gamma$ , where  $(\alpha\beta\gamma)$  is a permutation of  $(123)$ . All sectors are related by axis permutations given by (7), see Figure 2. Each sector is half of an arc  $\text{int}(A_\alpha)$  when  $v = 1/2$ , excluding the boundary, which consists of the points  $Q_\alpha$  and  $T_\beta$  or  $T_\gamma$ .

The Kasner parameters  $(p_1, p_2, p_3)$  can be described by a single parameter  $u$  such that

$$p_\alpha = \frac{-u}{1+u+u^2}, \quad p_\beta = \frac{1+u}{1+u+u^2}, \quad p_\gamma = \frac{u(1+u)}{1+u+u^2}, \quad (36)$$

where  $u \in (1, \infty)$  when  $p_\alpha < p_\beta < p_\gamma$ , while  $u = 1$  and  $u = \infty$  at the boundary points of the sectors,  $Q_\alpha$  and  $T_\gamma$ , respectively.

Invariance of  $u$  under axis permutations follows from  $\Sigma_1 \Sigma_2 \Sigma_3 = 2 + 27p_1 p_2 p_3$  where

$$p_1 p_2 p_3 = \frac{-u^2(1+u)^2}{(1+u+u^2)^3}, \quad \text{where } u \in [1, \infty], \quad (37)$$

which is monotone in  $u$ . In principle  $u$  can be replaced by  $\Sigma_1 \Sigma_2 \Sigma_3$  or  $p_1 p_2 p_3$  on  $K^\circ$ .

The following theorem was shown in [8, 44], see also [89, 90] and references therein.

**Theorem 3.1.** *There is only a countable set of points in the set  $K^\circ$  associated with finite heteroclinic chains ending at a Taub point. The set of points associated with periodic or infinite heteroclinic chains is thereby topologically generic and has full measure.*

There are different points of view regarding the genericity property. A set is *measure theoretical generic* if it has full measure. On the other hand, a set is *topologically generic* if it is a countable intersection of dense open sets. Those definitions are not equivalent. In physical empirical contexts measure theoretical genericity makes more sense, since it is a property that is potentially observable.

The proof of Theorem 3.1 follows from describing the Bianchi type II orbits in the GR case using the *Kasner map* (obtained from the Kasner circle/Mixmaster map  $\mathcal{K}$  in (24) when  $v = 1/2$  by quoting out axis permutations) for the Kasner parameter  $u$  in (36):

$$u \mapsto \begin{cases} u-1 & \text{if } u \geq 2 \\ \frac{1}{u-1} & \text{if } u < 2 \end{cases}, \quad u \in (1, +\infty). \quad (38)$$

The properties of the Kasner map (38) are intimately connected with the properties of continued fraction expansions of  $u$ , see [44, 32, 83, 69]. Using the parameter  $u$  and number theory, we obtain additional facts about heteroclinic chains:

- Points in the set  $K^\circ$  associated with finite heteroclinic chains correspond to  $u \in \mathbb{Q}$ , whereas  $u \notin \mathbb{Q}$  yields periodic or infinite heteroclinic chains.
- Points in the set  $K^\circ$  associated with periodic heteroclinic chains are dense. They correspond to Kasner parameters  $u$  with periodic continued fraction expansions.
- Heteroclinic chains with points that are a finite distance away from the Taub points are non-generic, whereas chains with points that come arbitrarily close to the Taub points are generic.

The usefulness of the Kasner parameter  $u$  in the GR case is due to the simplicity of the map induced by the Bianchi type II solutions, described in (38). This simplicity and its

relationship to continued fraction expansions and number theory is lost when  $v \neq 1/2$ . Nevertheless, for different values of  $v$  we will establish some common elements using symbolic dynamics, such as the chaoticity of the Kasner circle map  $\mathcal{K}$ .

Recall that the map  $\mathcal{K}$  is *chaotic* if it is topologically mixing and periodic orbits are dense. Mathematically the former means that given any open sets  $A, B \subseteq K^\circ$ , the  $n$ -th iteration  $\mathcal{K}^n(A)$  intersects  $B$  for sufficiently large  $n$ ; the latter means that given  $p \in K^\circ$ , there is a periodic heteroclinic chain  $q \in U$  for every neighborhood  $U \subseteq K^\circ$  of  $p$ . A popular description of chaos includes sensitivity of initial conditions, but we omit this requirement since it is a consequence of topological mixing and density of periodic orbits.

In order to prove that the discrete dynamical system generated by iterates of the Kasner map (38) is chaotic, we follow [61] and introduce the inverse of the Kasner parameter  $x = 1/u$ , which leads to the *Farey map* on the unit interval,

$$x \mapsto \begin{cases} \frac{x}{1-x} & \text{if } 0 \leq x \leq \frac{1}{2}, \\ \frac{1-x}{x} & \text{if } \frac{1}{2} \leq x \leq 1. \end{cases} \quad (39)$$

Then note that  $x = (\sqrt{13} - 1)/6$  is a periodic point with minimal period 3, see [60] and also [95, 83]. Therefore the ‘period 3 implies chaos theorem’ applies, proved independently by Sharkovsky [84] and Li and Yorke [50]. Thus the iterates of the Farey map (39) generate a chaotic discrete dynamical system on  $[0, 1]$ . This leads to the following theorem:

**Theorem 3.2.** *The Kasner map (38) is generically chaotic.*

It is also possible to prove chaoticity of the Kasner circle map  $\mathcal{K}$  in the critical case by using symbolic dynamics, although there is a technicality arising in the encoding of the Taub points into symbolic sequences. We provide such a new proof in Appendix C, which modifies the proof in Section 4 for the supercritical case  $v \in (1/2, 1)$ , and shows how chaoticity is carried from the supercritical case to the critical case  $v = 1/2$ .

## 4 Supercritical case

In the supercritical case,  $v \in (1/2, 1)$ , the Kasner circle map  $\mathcal{K}$  admits a *closed* set of fixed points called the *stable set*  $S$ , defined by  $S := K^\circ \setminus \text{int}(A_1 \cup A_2 \cup A_3)$ , where the interior of  $S$  contains fixed points of the dynamical system (4) with only negative eigenvalues in the eigendirections normal to the Kasner circle  $K^\circ$ , see Figures 2 and 4. The set  $S$  represents the end of heteroclinic chains. Accordingly, periodic and infinite heteroclinic chains are trajectories under the map  $\mathcal{K}$  never ending at the set  $S$ .

The set  $C$  of initial conditions leading to periodic and infinite heteroclinic chains is thereby defined by

$$C := \{p \in K^\circ \mid \mathcal{K}^n(p) \notin S \text{ for all } n \in \mathbb{N}_0\}. \quad (40)$$

For example, the two chains with period 3 obtained in Lemma 2.2, depicted in Figure 7, and the three chains with period 2, see Figure 14, are contained in  $C$ .

The complement of the set  $C$  in  $\mathcal{K}^\circlearrowleft$  is defined by

$$F := \mathcal{K}^\circlearrowleft \setminus C = \{p \in \mathcal{K}^\circlearrowleft \mid \mathcal{K}^n(p) \in S \text{ for some } n \in \mathbb{N}_0\}. \quad (41)$$

Two of our main results describe properties of the set  $C$ , and the associated dynamics of the Kasner map  $\mathcal{K}$ :

**Theorem 4.1.** *The set  $C$  is a nonempty Cantor set of Lebesgue measure zero and a Hausdorff dimension  $d_H(C)$  satisfying*

$$d_H(C) \in \left[ \frac{\log(2)}{\log\left(\frac{2+v^2}{1-v^2}\right)}, \min \left\{ 1, \frac{\log(2)}{\log\left(\frac{2(1-v^2)}{1+2v^2-\sqrt{12v^2-3}}\right)} \right\} \right]. \quad (42)$$

The bounds in (42) are positive and well-defined when  $v \in (1/2, 1)$ , see Figure 10. In particular,  $12v^2 - 3 > 0$ , where the  $v$ -dependent arguments, both larger than 1, are the minimum and maximum expansion rates of the Kasner circle map  $\mathcal{K}$  restricted to the Cantor set  $C$ , as will be shown in Lemma 4.4.

As a consequence of Theorem 4.1, the Cantor set  $C$  is non-generic both in a measure theoretical and a topological sense. The former is not always true, since there are some Cantor sets with positive measure, such as the Smith—Volterra—Cantor set; the latter follows since Cantor sets by definition are closed and nowhere dense.

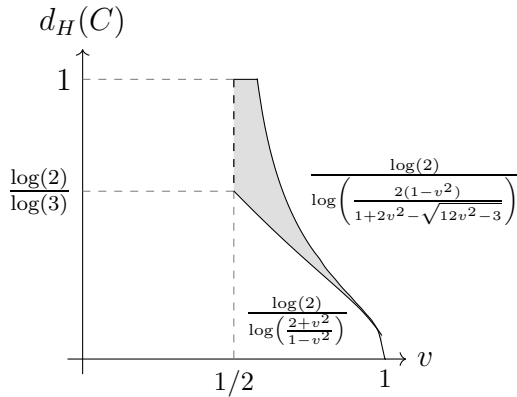


**Figure 10:** The Hausdorff dimension  $d_H(C)$  in (42) resides in the shaded region.

**Theorem 4.2.** *The Kasner circle map  $\mathcal{K}$  restricted to the Cantor set  $C$  generates a chaotic discrete dynamical system.*

Outside the Cantor set  $C$  the map  $\mathcal{K}$  is not chaotic, since heteroclinic chains end in the stable set  $S$  after finitely many iterations.

Let us now compare the GR critical case  $v = 1/2$  with the supercritical case  $v \in (1/2, 1)$ , in view of Theorems 4.1 and 4.2. For GR, the set  $S$  is the union of the three Taub points, while the analog of  $C$  is the set of points never reaching the Taub points under some iteration of  $\mathcal{K}$ , i.e., the set associated with periodic or infinite heteroclinic chains. This set, however, is not a Cantor set since it is not closed — its closure is the whole Kasner

circle  $K^\circ$ , which is different than itself. Furthermore, this set is generic in both a measure theoretical and a topological sense, while its complement is countable, see Theorem 3.1. In conclusion, the generic chaos for  $v = 1/2$  is carried by the non-generic set  $C$  when  $v \in (1/2, 1)$ .

The remaining section is divided into four parts. First, a background on Cantor sets and their dimensionality. Second, we describe how  $C$  is iteratively constructed, which is the basis for Theorems 4.1 and 4.2. Third, we characterize the connected components in each iterative step by means of symbolic dynamics. Lastly, we prove Theorems 4.1 and 4.2.

## 4.1 Background: Cantor sets and Hausdorff dimension

A non-empty set  $C$  in a complete metric space is a *Cantor set* if it is perfect, i.e., it is closed, without isolated points, and nowhere dense, i.e., its closure has an empty interior.

As an illustration, consider the iteratively constructed ternary Cantor set. Let  $T_0$  be the unit interval. The set  $T_{n+1}$  is obtained from  $T_n$  by removing the open middle third of each connected component of  $T_n$ , see Figure 11. Then define  $T$  as

$$T := \bigcap_{n \in \mathbb{N}_0} T_n. \quad (43)$$

In all steps  $n \geq 1$  of the construction, we can encode each closed connected component of  $T_n$  by a sequence of symbols  $L$  or  $R$ , which respectively denotes the left or right connected component from the previous iterations, see Figure 11. From this it follows that  $T$  fulfills the abstract definition of a Cantor set and has measure zero. A similar procedure will be adapted in order to construct the connected components of the set  $C$  in (40), and prove that it is also a Cantor set of measure zero.

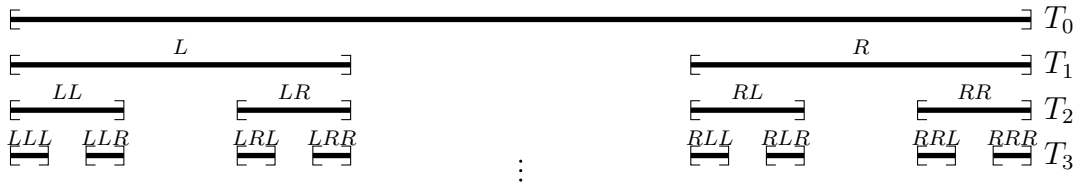


**Figure 11:** The iterations  $T_n$  for  $n = 0, 1, 2, 3$  in the construction of the ternary Cantor set. Note that  $T_1$  has two closed connected components, a left and right, denoted by  $L$  and  $R$ . In the next step, each of those two components  $L$  and  $R$  have two further left and right closed connected components in  $T_2$ , denoted by  $LL, LR, RL, RR$ . Similarly for  $T_3$ , and onwards.

A natural question regarding Cantor sets is their dimensionality. There are several notions of dimension, each with its advantages and disadvantages, see [24]. By introducing the Hausdorff dimension a set within the Kasner circle  $K^\circ$  can have any real dimension between 0 and 1: more than a discrete set of points, less than the circle itself.

Given  $d \in [0, \infty)$ , for any  $\epsilon > 0$  the  $d$ -Hausdorff measure of  $C$  is

$$\mu^d(C) := \liminf_{\epsilon \rightarrow 0} \left\{ \sum_{i \in \mathbb{N}} [\text{diam}(U_i)]^d \mid C \subseteq \bigcup_{i \in \mathbb{N}} U_i \text{ with } \text{diam}(U_i) \leq \epsilon \right\}. \quad (44)$$

That is, consider all coverings  $\cup_{i \in \mathbb{N}} U_i$  of  $C$  such that each  $U_i$  has a diameter<sup>7</sup> at most  $\epsilon$  minimizing the sum of the  $d^{\text{th}}$  powers of the diameters. As  $\epsilon$  decreases the number of possible covers is reduced, which accounts for the roughness of  $C$ : the more detailed a shape is, the more impact decreasing  $\epsilon$  has. The value of  $d$  incorporates the behavior of shapes under rescaling in a  $d$ -dimensional space: scaling a set  $C$  with a factor  $r$  will scale its  $d$ -Hausdorff measure with a factor  $r^d$ .

The *Hausdorff dimension* of  $C$  is defined as

$$d_H(C) := \inf_{d \geq 0} \{\mu^d(C) = 0\} = \sup_{d \geq 0} \{\mu^d(C) = \infty\}. \quad (45)$$

The measure  $\mu^d(C)$  is therefore 0 when  $d > d_H(C)$  and  $\infty$  for  $d < d_H(C)$  so that  $d_H(C)$  is a value such that the measure  $\mu^d(C)$  jumps from  $\infty$  to 0. This means that if  $\mu^d(C)$  is positive and bounded for some  $d$ , then this value of  $d$  is the Hausdorff dimension  $d_H(C)$ . Intuitively, we compare the  $d$ -dimensional scaling of the surrounding space with the set  $C$ : for too large  $d$  the set  $C$  will be of negligible size (of measure zero), whereas if  $d$  is too small then this leads to an over-sized  $C$  (infinite measure).

For example, the ternary Cantor set  $T$  in equation (43) has a Hausdorff dimension given by  $d_H(T) = \log(2)/\log(3) \approx 0.631$ , as can be seen as follows: Divide the Cantor set  $T$  into its left  $T_L := T \cap [0, 1/2]$  and right  $T_R := T \cap [1/2, 1]$  disjoint parts. Then  $\mu^d(T) = \mu^d(T_L) + \mu^d(T_R)$ . Moreover, since  $T_L$  and  $T_R$  have the same measure and are scalings of  $T$  by a factor  $3^{-1}$ , which scales the measure by  $3^{-d}$ , it follows that

$$\mu^d(T) = 2 \cdot 3^{-d} \mu^d(T). \quad (46)$$

If  $\mu^d(T) \neq 0, \infty$  for some  $d \geq 0$ , then it can be divided out yielding  $1 = 2 \cdot 3^{-d}$ , and its logarithm provides the desired dimension.

## 4.2 Characterization of $C$ through iterations

Analogously to the ternary Cantor set in equation (43), which is obtained by iteratively removing an open middle third from an interval, the set  $C$  in equation (40) can be iteratively constructed by removing arcs given by pre-images of  $S$  via  $\mathcal{K}$  from  $\mathcal{K}^\circ$ .

For each  $n \in \mathbb{N}_0$ , consider the removal process iteratively defined by

$$C_0 := \mathcal{K}^\circ, \quad (47a)$$

$$F_n := \text{int}_{C_n}(\mathcal{K}^{-n}(S)), \quad (47b)$$

$$C_{n+1} := C_n \setminus F_n, \quad (47c)$$

where  $\text{int}_{C_n}(B) := \text{int}(B \cap C_n) \cup (B \cap \partial C_n)$  denotes the interior of the set  $B = \mathcal{K}^{-n}(S)$  relative to  $C_n$ . See Figures 12 and 13 for a visualization of the process defined in equation (47), which we now describe in more detail.

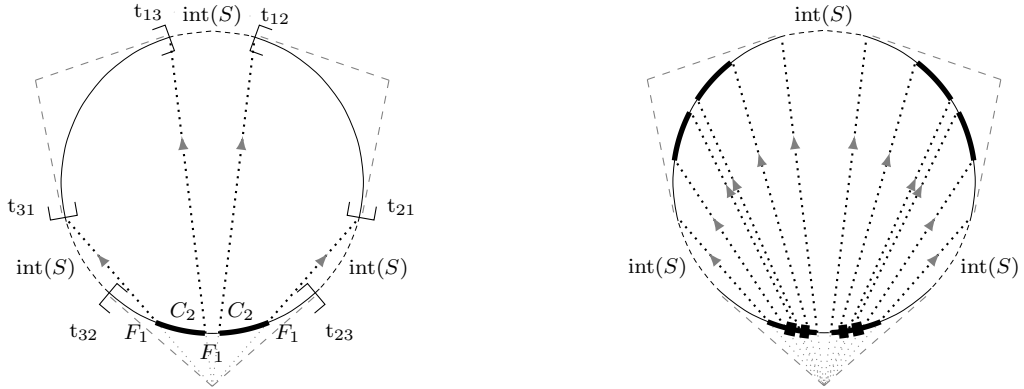
The *removed set*  $F_n$  consists of two different types of points within  $C_n$ ,  $\text{int}(\mathcal{K}^{-n}(S))$  and  $\partial C_n$ , since we can write  $F_n$  as  $F_n = \text{int}(\mathcal{K}^{-n}(S)) \cup \partial C_n$ . This is due to that the points

---

<sup>7</sup>Recall that the diameter is defined as  $\text{diam}(U_i) := \sup\{\rho(x, y) : x, y \in U_i\}$ , where  $\rho(x, y)$  is the metric between  $x$  and  $y$  in the metric space  $(X, \rho)$ .

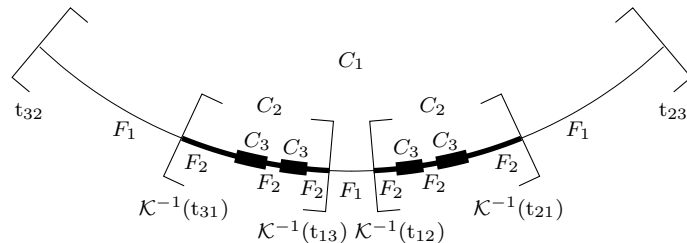
in  $F_n$  either have an  $n^{th}$  iteration  $\mathcal{K}^n(p)$  that falls in the interior of the stable set,  $\text{int}(S)$ , or points whose  $(n-1)^{th}$  iteration  $\mathcal{K}^{n-1}(p)$  ends at one of the tangential points, which are the boundary points of  $C_n$ . Thus the tangential points and their pre-images are all eventually removed. As a consequence,  $C_{n+1}$  is the *closed* set of points that remains after removing  $F_n$  from  $C_n$ . The removal procedure, which is analogous to the removal process of the ternary Cantor set depicted in Figure 11, is illustrated in Figures 12 and 13. .

The set  $C$  is obtained as the intersection of the sets  $(C_n)_{n \in \mathbb{N}_0}$  according to Lemma 4.3 below, which is proved to be a nested sequence of closed sets in Lemmata 4.5 and 4.6.



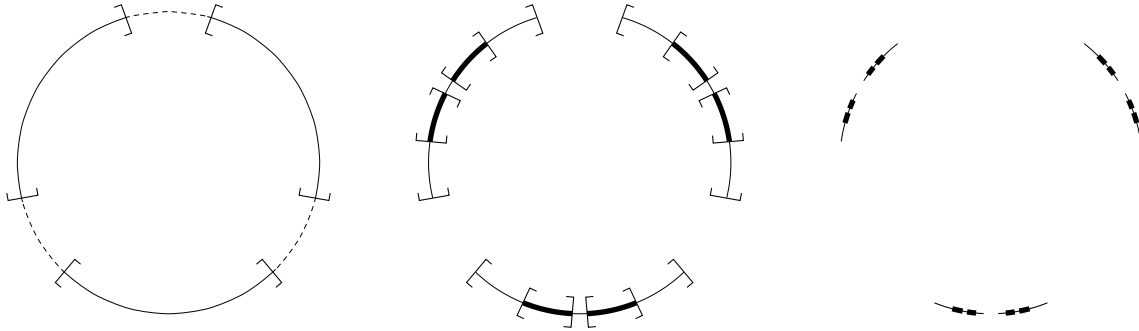
**(a):** The set  $F_1$  in  $A_1$  is obtained as follows: It is the interior (in the arc  $A_1$ ) of the pre-image  $\mathcal{K}^{-1}(S)$ , and hence contains the tangential points  $t_{32}$  and  $t_{23}$ , but not the pre-image of the other four tangential points. The set  $F_1$  has three connected components in  $A_1$ . Removing  $F_1$  from  $C_1$  yields the (thicker bold) closed set  $C_2$  with two connected components in  $A_1$ . Repeating this argument for the other arcs provides the full set  $C_2$ .

**(b):** Repeating the argument in (a) for the arcs  $A_2, A_3$  yields the (bold) closed set  $C_2$  with six connected components. The set  $F_2$  in  $A_1$  is obtained by the pre-images of the (thin) sets, since those are the points reaching  $\text{int}(S)$  in two iterations of  $\mathcal{K}$ . The set  $F_2$  has six connected components in  $A_1$ , which when removed yields the (thicker bold) closed set  $C_3$  in  $A_1$ . Figure (c) reveals more details for the bottom arc  $A_1$ .



**(c):** In  $A_1$  the (thin) set  $F_1$  has three connected components, which includes the tangential points  $t_{32}$  and  $t_{23}$ , but not the pre-images of the other four tangential points. The (bold) closed set  $C_2$  has two connected components, and the (bold) set  $F_2$  has six — both sets contain the pre-images of the four tangential points which are not in  $F_1$ . The (thicker bold) closed set  $C_3$  has four connected components.

**Figure 12:** The removal process of the open sets  $F_n$  from the Kasner circle  $K^O$  in equation (47). The open set  $F_0 = \text{int}(S)$  has three connected components. The closed set  $C_1$  consists of the three arcs  $A_1, A_2, A_3$ . Due to the axis permutation (7), we only describe the sets  $F_1, C_2$  in (a) and  $F_2, C_3$  in (b) in the bottom arc  $A_1$ .



(a): Deleting the three (dashed) connected components of  $F_0$  from the Kasner circle  $K^O = C_0$  yields the closed set  $C_1$ .

(b): Removing the nine (thin) connected components of  $F_1$  from the three arcs of  $C_1$  leads to the (bold) closed set  $C_2$ .

(c): Erasing the eighteen (thin) connected components of  $F_2$  from the six components of  $C_2$  yields the (bold) closed set  $C_3$ .

**Figure 13:** The iterative construction of the Cantor set  $C$ : Start (at the left) with the Kasner circle  $K^O$  and remove (when going to the right) the (thin) arcs  $F_n$  keeping the closed (bold) arcs  $C_{n+1}$ . Note that  $C_n$  has  $3 \cdot 2^{n-1}$  connected components for  $n \geq 1$ , in accordance with Lemma 4.5. To avoid clutter, we refrain from drawing the boundaries of the arcs in (c).

**Lemma 4.3.** *The sets  $C$  and  $F$  defined respectively in (40) and (41) can be written as*

$$C = \bigcap_{n \in \mathbb{N}_0} C_n \quad \text{and} \quad F = \bigcup_{n \in \mathbb{N}_0} F_n, \quad (48)$$

where  $C_n$  and  $F_n$  are defined by (47).

*Proof.* First, we prove the equality for  $F$ . The inclusion  $\bigcup_{n \in \mathbb{N}_0} F_n \subseteq F$  follows from the definition of  $F_n$  in (47b) and  $F$  in equation (41). The reverse,  $F \subseteq \bigcup_{n \in \mathbb{N}_0} F_n$ , is proved next, where we show that any point  $p \in F$  is also in  $F_n$  for some  $n \in \mathbb{N}_0$ . For any  $p \in F$ , there is a minimal  $n_0 \in \mathbb{N}_0$ ,  $p \notin \mathcal{K}^{-k}(S)$  for all  $k \in \mathbb{N}_0$  such that  $k < n_0$ , whereas  $p \in \mathcal{K}^{-k}(S)$  for all  $k \geq n_0$ . In other words,  $p \in C_{n_0}$  and  $p \notin F_k$  for all  $k < n_0$ . Consequently,  $p$  is not removed in the  $n_0 - 1$  iteration and  $p$  therefore lies in  $C_{n_0} = C_{n_0-1} \setminus F_{n_0-1}$ . There are two possibilities: Either  $p \in F_{n_0}$  or  $p \notin F_{n_0}$ . Since the former completes the proof, we consider the latter and conclude that  $p \in F_{n_0+1}$ . On the one hand,  $p \notin F_{n_0} = \text{int}_{C_{n_0}}(\mathcal{K}^{-n_0}(S))$ , and on the other hand  $p \in \mathcal{K}^{-n_0}(S)$ . The point  $p$  must therefore lie in the boundary of  $F_{n_0}$ , which is contained in  $F_{n_0+1}$ , see Figure 12.

Second, we prove the equality for  $C$ . The inclusion  $C \subseteq \bigcap_{n \in \mathbb{N}_0} C_n$  follows from the claim  $C \subseteq C_n$  for all  $n \in \mathbb{N}_0$ , which is proved by induction. For the basis, obviously  $C \subseteq C_0 = K^O$ . For the induction step, assume  $C \subseteq C_n$  for all  $n \leq N$  and show that  $C \subseteq C_{N+1}$ . Note that  $C$  in (40) and  $F_N$  in (47b) are disjoint. The induction hypothesis and (47c) yield  $C \subseteq C_{N+1}$ . The reverse inclusion  $\bigcap_{n \in \mathbb{N}_0} C_n \subseteq C$  follows from the characterization of  $F$  since points  $p \in \bigcap_{n \in \mathbb{N}_0} C_n$  are never removed in the iterative construction (47), that is,  $p \notin \bigcup_{n \in \mathbb{N}_0} F_n = F$ . Hence,  $p \in K^O \setminus F = C$ .  $\square$

The next Lemma describes the maximum and minimum expansion rates of  $\mathcal{K}$  within the set  $C$ , which are used later to bound the Hausdorff dimension of  $C$ .

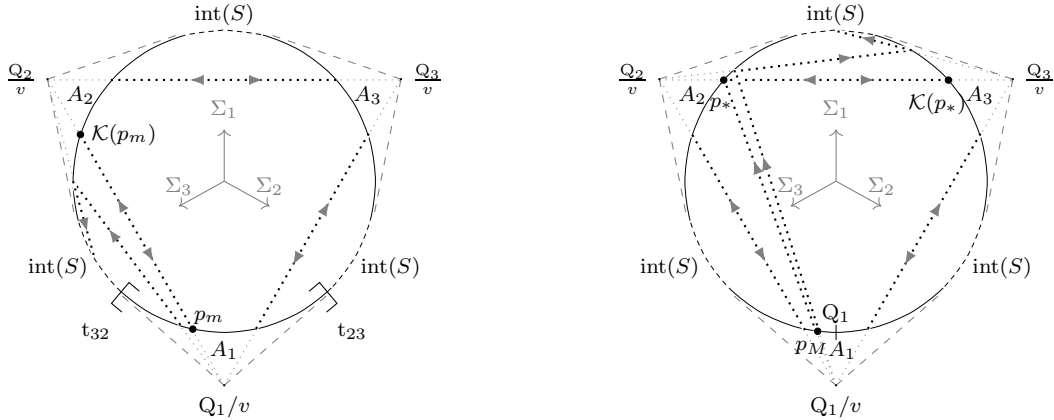
**Lemma 4.4.** *The extrema of the derivative of the Kasner map within  $C$  are*

$$m := \min_{p \in C} |D\mathcal{K}(p)| = \frac{2(1-v^2)}{1+2v^2 - \sqrt{12v^2-3}} \quad (49a)$$

$$M := \max_{p \in C} |D\mathcal{K}(p)| = \frac{2+v^2}{1-v^2}. \quad (49b)$$

The proof is based on two main features. First, the three lines in  $(\Sigma_1, \Sigma_2, \Sigma_3)$ -space that connect each pair of auxiliary points  $Q_1/v$ ,  $Q_2/v$  and  $Q_3/v$  describe physically equivalent heteroclinic chains with period 2 in  $K^\circ$ <sup>8</sup> constructed by concatenation of two heteroclinic Bianchi type II orbits related by axis permutations, see Figure 14. In particular, the line between  $Q_\alpha/v$  and  $Q_\beta/v$  is characterized by  $\Sigma_\gamma = 1/v$ , which yields a heteroclinic chain of period 2 under iterates of  $\mathcal{K}$  that maps two physically identical Kasner states (related by interchanging the axes  $\Sigma_\alpha$  and  $\Sigma_\beta$ ) at  $A_\alpha$  and  $A_\beta$  to each other, where  $(\alpha, \beta, \gamma) = (1, 2, 3)$  or a permutation thereof.

Second, due to symmetry under axis permutations (7), we can without loss of generality restrict attention to the left half of the arc  $A_1$  when considering  $|D\mathcal{K}(p)| = g(p)$  (recall Lemma 2.1), where  $g(p)$  monotonically increases between  $t_{32}$  and  $Q_1$ , see Figure 5. As a consequence the minimum  $m$  (maximum  $M$ ) is determined by the left-most (right-most) point  $p_m \in C$  ( $p_M \in C$ ) in this half arc. Moreover, according to (25), the coordinate  $\Sigma_1$  of  $p_m$  and  $p_M$  determines  $g(p_m)$  and  $g(p_M)$ , respectively.



**(a):** The minimum of  $g$  on  $C$  occurs at  $p_m$  where  $\Sigma_3 = 1/v$ . Any point in  $A_1$  between  $t_{32}$  and  $p_m$  eventually ends up in  $S$ , since  $\Sigma_3 > 1/v$  monotonically increases on the type II<sub>1</sub> and II<sub>2</sub> subsets.

**(b):** The maximum of  $g$  on  $C$  is at  $p_M := \mathcal{K}^{-1}(p_*)$ , where  $p_*$  has  $\Sigma_1 = 1/v$ . Points between  $p_M$  and  $Q_1$  eventually end up in  $S$ , since  $\Sigma_1 > 1/v$  monotonically increases on the type II<sub>2</sub> and II<sub>3</sub> subsets.

**Figure 14:** Depiction of the lines connecting each pair of points  $Q_1/v$ ,  $Q_2/v$  and  $Q_3/v$ , which determine the periodic heteroclinic chains with period 2; the points  $p_m$  and  $p_M$  for the extrema of  $|D\mathcal{K}| = g$  on  $C$ ; examples of points with finite heteroclinic chains ending in  $S$ .

<sup>8</sup>Note that these heteroclinic chains with period 2 are the full unfolding of the Taub points, as seen in Figure 14. These orbits collapse at the Taub points when  $v \rightarrow 1/2$ , and disappear when  $v \in (0, 1/2]$ . The role of the collapse of these objects toward the Taub points when  $v \rightarrow 1/2$  in Bianchi type VIII and IX is unclear, particularly the (two-dimensional) center manifold of the tangential points, and the stable manifold of the chain with period 2, see also Appendix C.

*Proof.* The point  $p_m$  is determined by the periodic heteroclinic chain characterized by the line between  $Q_1/v$  and  $Q_2/v$  for which  $\Sigma_3 = 1/v$ . This follows since  $p_m$  thereby belongs to  $C$ , and since any point  $p$  in the half arc between  $t_{32}$  and  $p_m$  with  $g(p) < g(p_m)$  is not in  $C$ . This is due to that  $p$  eventually ends up in  $S$ , either directly via a heteroclinic orbit or by a finite heteroclinic chain, since  $\Sigma_3$  monotonically increases when  $\Sigma_3 > 1/v$  along such heteroclinic orbits and chains, see Figure 14.

To find the coordinate  $\Sigma_1$  of  $p_m$  we insert  $\Sigma_3 = 1/v$  into the constraint (4d), which yields  $\Sigma_2 = -(\Sigma_1 + 1/v)$ . Inserting the values for  $\Sigma_2$  and  $\Sigma_3$  into the constraint (4c),  $\Sigma^2 = 1$ , results in

$$\Sigma_1^2 + \frac{\Sigma_1}{v} + \frac{1 - 3v^2}{v^2} = 0. \quad (50)$$

This equation has two solutions (which coincide with  $T_3$  for  $v = 1/2$ ), where the one with the smaller  $\Sigma_1$  yields a point that resides in the left arc of  $A_1$ , while the other solution gives the image of this point, which is in  $A_2$ , see Figure 14. The relevant solution is therefore the one with the smaller value

$$\Sigma_1 = \frac{-1 - \sqrt{12v^2 - 3}}{2v}. \quad (51)$$

Inserting this into  $g(p_m)$  in (25) results in (49a),  $m = |D\mathcal{K}(p_m)| = g(p_m)$ , as desired.

Next, we show that the point  $p_M$  is the pre-image  $\mathcal{K}^{-1}(p_*) \in A_1$ , where  $p_*$  is the point in  $A_2$  determined by the line between  $Q_2/v$  and  $Q_3/v$  characterized by  $\Sigma_1 = 1/v$ , see Figure 14. Note that  $p_M \in C$ , since  $\mathcal{K}(p_M) = p_*$  resides on a heteroclinic cycle forming a heteroclinic chain with period 2. Moreover, the point  $p_M$  yields  $M$ , since any point  $p$  in the half arc between  $p_M$  and  $Q_1$  with  $g(p) > g(p_M)$  is not in  $C$ . This follows since  $p$  yields an orbit such that  $\mathcal{K}(p)$  ends above  $p_*$  in Figure 13(b) with  $\Sigma_1 > 1/v$ , either in  $S$  or in  $A_2$ . In the latter case the orbit is concatenated with other heteroclinic orbits for which  $\Sigma_1 > 1/v$  monotonically increases, which thereby yields a finite heteroclinic chain that ends at  $S$ .

The point  $\mathcal{K}(p_M) = p_*$  is the  $\omega$ -limit of the heteroclinic orbit with  $p_M$  as its  $\alpha$ -limit. Inserting  $\eta = g(p_M)$  into (20) yields

$$\Sigma_1^f = \Sigma_1^i g(p_M) + \frac{2}{v} (g(p_M) - 1), \quad (52)$$

where  $\Sigma_1^f$  is the value of  $\Sigma_1$  at  $p_*$  and  $g(p_M)$  is given in (25). Moreover,  $\Sigma_1^f = 1/v$ , since  $p_*$  lies on the line between  $Q_2/v$  and  $Q_3/v$ , which, when inserted into (52), gives

$$\Sigma_1^i = -\frac{1 + 5v^2}{v(2 + v^2)}. \quad (53)$$

Inserting this result into (25) yields  $M = |D\mathcal{K}(p_M)| = g(p_M)$  and thereby (49b).  $\square$

### 4.3 Characterization of $C$ by symbolic dynamics

To know more about the connected components of  $C_n$  with  $n \geq 1$ , i.e., the bold sets in Figure 13, we introduce symbolic dynamics in a manner similar to that of the ternary

Cantor set in Figure 11, where each connected component was encoded by a sequence of two symbols  $L$  and  $R$ . The starting point  $n = 0$  consists of the removal of the set  $F_0 = \text{int}(S)$  from the Kasner circle  $C_0 = K^\circ$ , which yields  $C_1 = A_1 \cup A_2 \cup A_3$ .

Consider any  $p \in C_n$  with  $n \geq 1$ . By the definitions in equation (47), there is a unique symbol  $a_n \in \{1, 2, 3\}$  such that  $\mathcal{K}^n(p) \in \text{int}(A_{a_n})$  for each  $n \in \mathbb{N}$ . Since two consecutive iterations are never in the same unstable arc,  $a_n \neq a_{n+1}$  for all  $n \in \mathbb{N}$ . Furthermore, any  $p \in A_\alpha$  has two pre-images of the Kasner circle map  $\mathcal{K}$ : one in  $A_\beta$  and one in  $A_\gamma$ , where  $(\alpha, \beta, \gamma)$  is a permutation of  $(123)$ , see Figure 4. It therefore follows that we can find points visiting a prescribed sequence of expanding arcs, obtained from heteroclinic chains. To describe a finite sequence of arcs we introduce the following notation:  $w_n = a_0 \dots a_{n-1}$ , where  $w_n$  is called a *word*. Consider the set of all words  $w_n$  of length  $n \geq 1$ , also called an *alphabet*, and denote this set by

$$W_n := \left\{ a_0 \dots a_{n-1} \mid \begin{array}{l} a_k \in \{1, 2, 3\} \text{ for } k = 0, \dots, n-1, \\ a_{k+1} \neq a_k \quad \text{for } k = 0, \dots, n-2 \end{array} \right\}. \quad (54)$$

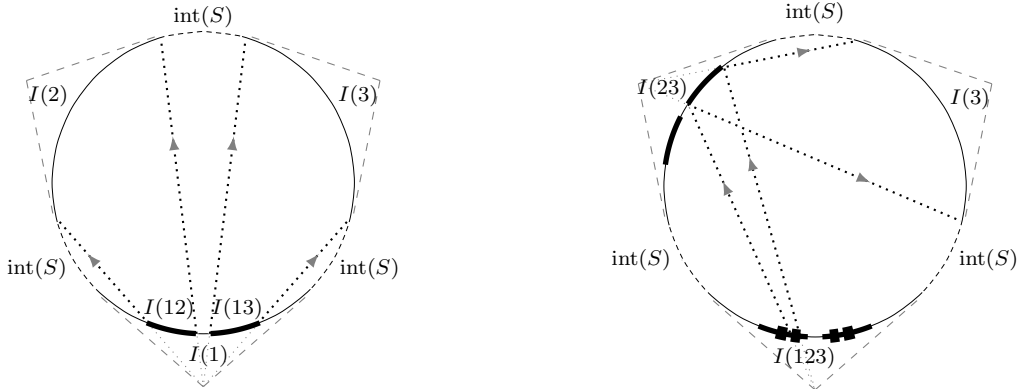
It then follows that the alphabet  $W_n$  consists of  $3 \cdot 2^{n-1}$  words (three possibilities for  $a_0$  and two possibilities for each following  $a_k$  due to the restriction  $a_{k+1} \neq a_k$ ). Points  $p \in C$  are encoded by infinite sequences with  $n = \infty$ , i.e.,  $w_\infty \in W_\infty$ .

To connect words with the iterative construction of  $C$ , we define the set  $I(w_n)$  to be the collection of points on  $K^\circ$  that visits the arcs by iterations of  $\mathcal{K}$  prescribed by  $w_n = a_0 \dots a_{n-1} \in W_n$ . This is formally expressed as

$$I(w_n) := \bigcap_{k=0}^{n-1} \mathcal{K}^{-k}(A_{a_k}), \quad (55)$$

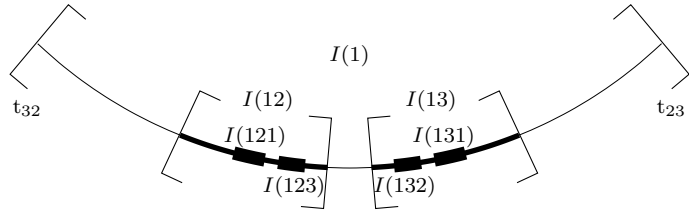
where a specific word  $w_n$  yields a specific connected closed set  $I(w_n)$ , as illustrated in Figure 15. Note that for  $p \in I(w_n) = I(a_0 \dots a_{n-1})$  it follows that  $\mathcal{K}^k(p) \in A_{a_k}$ ,  $k = 0, \dots, n-1$ , and, in particular,  $p \in A_{a_0}$ .

The next lemmata guarantee that the union of  $I(w_n)$  for all words  $w_n \in W_n$  yield the set  $C_n$  in the iterative construction (47), and hence that  $I(w_n)$  are the connected components of  $C_n$ . Moreover, the family  $\{I(w_n)\}_{n \in \mathbb{N}}$  consists of *shrinking nested closed sets*. The veracity of these claims is illustrated by considering a sequence of one of the connected components of the bold sets  $C_n$  for each  $n \geq 1$  in Figure 13 and by a step by step construction of the nested closed sets in Figure 15.



**(a):** The (bold) set  $C_2$  within  $I(1) = A_1$  has two closed connected components given by  $I(w_2)$ , which are encoded by words  $w_2 = a_0a_1 \in W_2$  such that  $a_0 = 1$ . The set  $I(w_2)$  with  $w_2 = 12$  encodes points  $p \in A_1 = I(1)$  such that  $\mathcal{K}(p) \in A_2$ , whereas  $w_2 = 13$  encodes  $p \in A_1 = I(1)$  with  $\mathcal{K}(p) \in A_3 = I(3)$ .

**(b):** The (thicker bold) set  $C_3$  within  $I(1) = A_1$  has four closed connected components  $I(w_3)$ , which are encoded by the words  $w_3 = a_0 a_1 a_2 \in W_3$  such that  $a_0 = 1$ ,  $\mathcal{K}(p) \in A_{a_1}$ ,  $\mathcal{K}^2(p) \in A_{a_2}$ , where  $p \in A_1$ . The sets  $I(w_2)$  and  $I(w_3)$  for the bottom arc are described in detail in Figure **(c)**.



**(c):** The sets  $I(w_n)$ , for  $n = 1, 2, 3$ , in the arc  $A_1$ . The (thin) set  $C_1$  has one closed connected component in  $A_1$  given by  $I(w_1)$  encoded by the word  $w_1 = 1 \in W_1$ , i.e.,  $A_1 = I(1)$ . The (bold) set  $C_2$  has two closed connected components in  $A_1$  given by  $I(w_2)$ , which are encoded by words  $w_2 = a_0a_1 \in W_2$  such that  $a_0 = 1$ . The (thicker bold) set  $C_3$  has four closed connected components in  $A_1$ , given by  $I(w_3)$  encoded by the words  $w_3 = a_0a_1a_2 \in W_3$  such that  $a_0 = 1$ .

**Figure 15:** Illustration of the nested sets  $I(w_n)$  for  $n = 1, 2, 3$ . The (bold) set  $C_1$  has three closed connected component given by arcs  $A_1, A_2, A_3$ , described in equation (12) and Figure 2, and they are encoded by symbolic dynamics as  $I(w_1) = A_{w_1}$ , with the corresponding word  $w_1$  within the alphabet  $W_1 = \{1, 2, 3\}$ .

**Lemma 4.5.** For  $n \geq 1$ , the set  $C_n$  is given by the union of the  $3 \cdot 2^{n-1}$  closed, connected, disjoint sets  $I(w_n)$ :

$$C_n = \bigcup_{w_n \in W_n} I(w_n). \quad (56)$$

*Proof.* First, we show that  $C_n \subseteq \cup_{w_n \in W_n} I(w_n)$ . By the definitions in (47), points  $p \in C_n$  are not in the  $k^{th}$  removed set  $F_k$  for all  $k = 0, \dots, n-1$ . There is thereby a unique symbol  $a_k \in \{1, 2, 3\}$  such that  $\mathcal{K}^k(p) \in A_{a_k}$  for each  $k = 0, \dots, n-1$  and  $a_{k+1} \neq a_k$  for all  $k = 0, \dots, n-2$ . Hence  $p \in I(w_n)$  for the word  $w_n = a_0 \dots a_{n-1} \in W_n$ .

Second,  $I(w_n) \subseteq C_n$  for all  $w_n = a_0 \dots a_{n-1} \in W_n$  since  $p \in I(w_n)$  are not in  $F_k$  for all  $k = 0, \dots, n-1$ , as follows from the definition (55) and the iterative construction defined in (47). Hence  $p \in C_n$ .

To show disjointedness, consider two different words in  $W_n$  given by  $w_n = a_0 \dots a_{n-1}$  and

$\tilde{w}_n = \tilde{a}_0 \dots \tilde{a}_{n-1}$  such that  $a_k \neq \tilde{a}_k$  for some  $k$ . Then any  $p \in I(w_n)$  satisfies  $\mathcal{K}^k(p) \in A_{a_k}$  whereas  $\mathcal{K}^k(p) \notin A_{\tilde{a}_k}$  since  $A_{a_k}$  and  $A_{\tilde{a}_k}$  are disjoint. Hence  $p \notin I(\tilde{w}_n)$ .

Finally, the number of closed connected components of  $C_n$  is given by the cardinality of  $W_n$ , which is  $3 \cdot 2^{n-1}$ .  $\square$

**Lemma 4.6.** *For any  $n \geq 2$ , the set  $I(w_n)$  is a closed nested set of  $K^\circ$ :*

$$I(w_n) \subseteq I(w_{n-1}), \quad (57)$$

where  $w_n = a_0 \dots a_{n-1} \in W_n$  and  $w_{n-1} = a_0 \dots a_{n-2} \in W_{n-1}$ . Moreover,

$$0 < |I(w_n)| < 2\pi\nu^{n-2}, \quad (58)$$

for some constant  $\nu \in (0, 1)$ , where  $|\cdot|$  denotes the Lebesgue measure.

*Proof.* The arcs  $A_\alpha$  for  $\alpha = 1, 2, 3$  are closed, and so are their pre-images under the continuous map  $\mathcal{K}$ . Since  $I(w_n)$  is an intersection of closed sets defined in (55), it follows that  $I(w_n)$  is a closed set in  $K^\circ$ .

The nested inclusion (57) follows from rewriting equation (55) as

$$I(w_n) = I(w_{n-1}) \cap \mathcal{K}^{-(n-1)}(A_{a_{n-1}}). \quad (59)$$

This also implies that  $|I(w_n)| > 0$ , since  $I(w_n)$  is connected and strictly contains two nonempty closed disjoint subsets given by  $I(w_{n+1})$  for  $w_{n+1} = a_0 \dots a_n \in W_{n+1}$ , where the word  $w_{n+1}$  is an extension of  $w_n$  by concatenating a symbol  $a_n \neq a_{n-1}$  at the end, see Figure 15.

Next we show equation (58). The Kasner map restricted to the set  $I(w_n)$ , given by  $\mathcal{K} : I(a_0 \dots a_{n-1}) \rightarrow I(a_1 \dots a_{n-1})$ , see Figure 15, is a diffeomorphism, which implies that  $x = \mathcal{K}(p)$  leads to:

$$\min_{p \in I(w_n)} |D\mathcal{K}(p)| \cdot |I(w_n)| \leq \left| \int_{I(w_n)} D\mathcal{K}(p) dp \right| = \left| \int_{I(a_1 \dots a_{n-1})} dx \right| = |I(a_1 \dots a_{n-1})|. \quad (60)$$

Since the sets  $I(w_n)$  are nested as in (57), and since  $I(w_2)$  is a connected component of  $C_2$  for some  $w_2 \in W_2$ , as described in equation (56), it follows that

$$\min_{p \in I(w_n)} |D\mathcal{K}(p)| \geq \min_{p \in I(w_2)} |D\mathcal{K}(p)| \geq \min_{p \in C_2} |D\mathcal{K}(p)| =: \nu^{-1} > 1, \quad (61)$$

as illustrated by Figure 15. The last inequality, which yields  $\nu < 1$ , follows from that  $C_2$  is bounded away from the tangential points, see Figure 12, and since the derivative then is strictly bigger than one, see (32) and Figure 5.

We then apply the inequality (60) recursively together with (61), which leads to

$$|I(w_n)| \leq \nu^{n-2} \cdot |I(w_2)| \quad (62)$$

for some  $w_2 \in W_2$ . Together with  $|I(w_2)| < |K^\circ| = 2\pi$  this results in equation (58).  $\square$

Finally, note that the shrinking rate of  $|I(w_n)|$  in (58) is not improved by repeating the recursive procedure in (62) once more in order to bound  $|I(w_n)|$  by  $|I(w_1)|$ . Then the right hand side of (61) is replaced with  $\nu^{n-2} \cdot \tilde{\nu} |I(w_1)|$ , where  $\tilde{\nu}^{-1} := \min_{p \in C_1} |D\mathcal{K}(p)|$ . However,  $\tilde{\nu} = 1$ , since  $C_1$  consists of the three arcs  $A_\alpha$ , which contain tangential points for which the minimum 1 is attained, see Figure 5.

## 4.4 Proof of Theorems 4.1 and 4.2

Based on the above ingredients we will now prove Theorems 4.1 and 4.2 in six steps.

### First step: Closedness and nonemptiness of the set $C$ .

Since  $C$  is obtained in equation (48) as the intersection of closed sets  $C_n$ , defined in (47), which in turn is the union of closed arcs  $I(w_n)$  in equation (56),  $C$  is also closed.

Furthermore, given a word  $w_\infty = (a_k)_{k \in \mathbb{N}_0} \in W_\infty$  and its truncations  $w_n = a_0 \dots a_{n-1}$ , the family  $\{I(w_n)\}_{n \in \mathbb{N}}$  consists of shrinking nested closed sets such that its intersection consists of a single point  $p$ , due to Lemma 4.6 and Cantor's intersection Theorem in complete metric spaces when  $\text{diam}(I(w_n)) \rightarrow 0$  as  $n \rightarrow \infty$ . Such a point belongs to  $I(w_n)$  for all  $n \geq 1$ , and also in  $C_n$  for every  $n \geq 0$  due to (56) and  $C_0 = K^\circ$ . Consequently,  $p \in C$ , which is determined by the intersection of all  $C_n$  according to (48). In other words,

$$\bigcap_{n \in \mathbb{N}_0} I(w_n) = p \in C. \quad (63)$$

Note that such a point  $p$  is associated with the word  $w_\infty = a_0 a_1 a_2 \dots \in W_\infty$ , whereas the next point in the heteroclinic chain,  $\mathcal{K}(p)$ , is associated with the sequence  $\tilde{w}_\infty = a_1 a_2 \dots$ , which is the word  $w_\infty$  without the first symbol  $a_0$ . Hence  $\mathcal{K}(p)$  lies in the intersection of the family  $\{I(\tilde{w}_n)\}_{n \in \mathbb{N}_0}$ . Different points in the same heteroclinic chain are therefore distinguished by fixing  $a_0$ . This notion of deleting the first symbol is also called a shift to the left, and is used to prove chaoticity in the sixth step.

### Second step: No isolated points in $C$ .

Consider a point  $p \in C$  and an  $\varepsilon$ -neighborhood of  $p$  in  $K^\circ$ . Let  $w_\infty = (a_k)_{k \in \mathbb{N}_0} \in W_\infty$  be a sequence such that  $\mathcal{K}^k(p) \in A_{a_k}$  for all  $k \in \mathbb{N}_0$ . According to equation (58), there is an  $n \in \mathbb{N}$  such that  $I(w_n) = I(a_0 \dots a_{n-1})$  contains  $p$  and has a length smaller than  $\varepsilon$ .

Next we prove that  $I(w_n)$  contains a point  $q \in C$  different than  $p$  with a distance smaller than an arbitrary  $\varepsilon$ , and hence that  $p$  is not isolated. Let  $\tilde{a}_n \in \{1, 2, 3\}$  be different than  $a_{n-1}$  and  $a_n$ . Hence, the word  $\tilde{w}_{n+1} := a_0 \dots a_{n-1} \tilde{a}_n$  is without repetition and differs from  $w_{n+1} = a_0 \dots a_{n-1} a_n$ . Moreover, the disjoint sets  $I(w_{n+1})$  and  $I(\tilde{w}_{n+1})$  are both contained in  $I(w_n)$ , since such arc sequences are nested (57), see Figure 15. We now show that there is a  $q \in I(\tilde{w}_{n+1})$  which is also in  $C$ , but different than  $p$ , since  $p \in I(w_{n+1})$ . Consider the family  $\{I(\tilde{w}_k)\}_{k \in \mathbb{N}}$  of shrinking nested closed sets, where  $\tilde{w}_k := a_0 \dots a_k$  is the truncation of the word  $\tilde{w}_\infty := a_0 \dots a_{n-1} \tilde{a}_n a_n a_{n+1} \dots \in W_\infty$ . This guarantees that  $a_{n-1}, \tilde{a}_n$  and  $a_n$  are pair-wise disjoint, and hence (63) implies that there is a  $q$ , which lies in  $C$  and in the intersection of  $I(\tilde{w}_k)$  for all  $k \in \mathbb{N}$ , and consequently in  $I(\tilde{w}_{n+1})$ .

### Third step: $\overline{C}$ has an empty interior.

Since  $C$  is closed,  $\overline{C} = C$ , we only have to prove that  $C$  has an empty interior. Consider the same arbitrary point  $p \in C$  and  $I(w_n)$  within an  $\varepsilon$ -neighborhood for any  $\varepsilon > 0$ , as in the second step. We now show that  $I(w_n)$  contains a point  $r \in K^\circ \setminus C$ , and hence that  $p$  is not an interior point and that there thereby are no interior points.

Consider  $r \in \partial I(w_n)$ . Since the restriction  $\mathcal{K} : I(w_n) \rightarrow I(a_1 \dots a_{n-1})$  is a diffeomorphism, it preserves boundaries, i.e.,  $\mathcal{K}(r) \in \partial I(a_1 \dots a_{n-1})$ . After  $n-1$  iterations,  $\mathcal{K}^{n-1}(r) \in$

$\partial I(a_{n-1})$ . Note that  $I(a_{n-1})$  is the arc  $A_{a_{n-1}}$ , and that its boundary consists of the tangential points, which are in  $S$ . Hence  $\mathcal{K}^{n-1}(r) \in S$ , and thus  $r \in K^\circ \setminus C$ , see Figure 12.

**Fourth step:  $C$  has measure zero.**

We prove that  $F = K^\circ \setminus C$  has full measure  $2\pi$ , and hence that  $C$  has measure zero.

Define the relative size of the  $n^{\text{th}}$  removed set of the iterative construction (47) as

$$q_n := \frac{|F_n|}{|C_n|} \in (0, 1), \quad (64)$$

which is well-defined, since  $C_n$  contains the sets  $I_n(w_n)$  of positive length.

Consider the following partial sum of the pairwise disjoint sets  $F_k$ :

$$s_n := \sum_{k=0}^n |F_k|. \quad (65)$$

Then

$$|F| = s_\infty. \quad (66)$$

Applying the definition (47c) of  $C_{n+1}$  recursively leads to

$$|C_{n+1}| = 2\pi - s_n. \quad (67)$$

We then use equations (64), (65) and (67) to obtain

$$s_{n+1} - s_n = |F_{n+1}| = |C_{n+1}|q_{n+1} = (2\pi - s_n)q_{n+1}. \quad (68)$$

Note that the sequence  $(s_n)_{n \in \mathbb{N}_0}$  in (65) is increasing and bounded above by  $2\pi$  and thereby converges to the limit  $|F| \in [0, 2\pi]$ . On the other hand, the sequence  $(q_n)_{n \in \mathbb{N}_0}$  is bounded, and thus admits converging subsequences  $(q_{n_k})_{k \in \mathbb{N}_0}$  with a limit  $q$ . Taking the limit of (68) results in

$$0 = |F| - |F| = (2\pi - |F|)q. \quad (69)$$

Proving that  $F$  has full measure corresponds to excluding  $q = 0$ . We therefore show that  $q_n$  is uniformly bounded away from 0. First, observe that  $|F_n| = |C_n| - |C_{n+1}|$ , as follows from (47c), which enables us to rewrite (64) as

$$q_n = 1 - \frac{|C_{n+1}|}{|C_n|}. \quad (70)$$

We now show that the quotient  $|C_{n+1}|/|C_n|$  is uniformly bounded away from 1, which follows from the expansion property of the Kasner circle map in Lemma 2.1. Note that  $C_{n+1} \subseteq C_2$  for every  $n \geq 1$ , and that  $\mathcal{K}(C_{n+1}) \subseteq C_n$ , from which it follows that

$$\min_{p \in C_2} |D\mathcal{K}(p)| \cdot |C_{n+1}| \leq \min_{p \in C_{n+1}} |D\mathcal{K}(p)| \cdot |C_{n+1}| \leq |C_n|, \quad (71)$$

or, equivalently,

$$\frac{|C_{n+1}|}{|C_n|} \leq \frac{1}{\min_{p \in C_{n+1}} |D\mathcal{K}(p)|} \leq \frac{1}{\min_{p \in C_2} |D\mathcal{K}(p)|} = \nu < 1, \quad (72)$$

where the last inequality was shown in connection with equation (61). Moreover,  $F_1$  removes a whole neighborhood of the tangential points, as follows from (47), see Figure 12. Since  $|C_{n+1}|/|C_n|$  is uniformly bounded away from 1, it follows that  $q_n$  is uniformly bounded away from 0, and hence any converging subsequence of  $(q_n)_{n \in \mathbb{N}_0}$  has a limit  $q > 0$ .

**Fifth step: Bounds on the Hausdorff dimension of  $C$ .**

The bounds (42) follow from Proposition 6 in [73], which we simplify and adapt to our situation and notation.

**Proposition 4.7.** *Consider the iterative construction of  $C$  given by  $C_n$  in (47), with connected components  $I(w_n)$  in (55) for  $w_n \in W_n$ . Suppose there are closed sets  $I_*(w_n)$  and  $I^*(w_n)$  of Lebesgue measure  $|I_*(w_n)| = c/\lambda^*$  and  $|I^*(w_n)| = c/\lambda_*$  for some  $c \in \mathbb{R}_+$  and  $0 < 1/\lambda^* \leq 1/\lambda_* < 1$  such that  $I_*(w_n) \subseteq I(w_n) \subseteq I^*(w_n)$  where the sets  $\text{int}(I_*(w_n))$  and  $\text{int}(I_*(\tilde{w}_n))$  are disjoint for different words  $w_n \neq \tilde{w}_n$ . Then,*

$$\frac{\log(2)}{\log(\lambda^*)} \leq \dim_H(C) \leq \frac{\log(2)}{\log(\lambda_*)}. \quad (73)$$

Recall that  $C_n$  in (47) is obtained by a non-uniform contraction of  $C_{n-1}$  with a contraction rate given by the inverse of the expansion rate (32). We exclude the case  $n = 1$ , which only divides  $K^\circ$  into the three physically equivalent arcs  $A_\alpha$  and  $C$  into three identical parts with the same dimension, one in each arc, see Figure 2. Then the following sets satisfy the above hypothesis: for  $n > 1$  let  $I_*(w_n)$  and  $I^*(w_n)$  be uniform contractions of the set  $I(w_{n-1})$  with respective contraction rates being the inverse of the expansion rates given by  $\lambda^* := M = \max_{p \in C} |D\mathcal{K}(p)|$  and  $\lambda_* := m = \min_{p \in C} |D\mathcal{K}(p)|$  so that  $c := |I(w_{n-1})|$ . Disjointness follows from the proof of Lemma 4.5, which showed that  $I(w_n)$  and  $I(w_k)$  are disjoint, while Lemma 4.4 gave the desired bounds  $M$  and  $m < M$ . Note also that  $C$  lies within  $K^\circ$  and contains no interval, and thus that its Hausdorff dimension has to be less than 1.

Although the bounds (42) now have been proven, it is useful to provide an intuitive non-rigorous reasoning of this proof: our Cantor set lies between two standard Cantor sets with removed sets being uniformly scaled by the inverse of the minimum and maximum expansion of the Kasner map in (32).

The Cantor set  $C$  can be divided into three identical parts: the intersection of  $C$  with each arc  $A_\alpha$  for  $\alpha = 1, 2, 3$ , which are the three connected components of the first iterate  $C_1$  in the construction (47) of  $C$ . Since those three sets are disjoint,

$$d_H(C) = d_H(C \cap A_\alpha). \quad (74)$$

After such a first iterate, the construction is similar to the standard Cantor set in an interval: three parts of each arc  $A_\alpha$  are removed, yielding two remaining subarcs, which are the two connected components of  $C_2 \cap A_\alpha$ . The left and right parts of  $C$  in the two connected components of  $C_2 \cap A_\alpha$  are called  $C^L$  and  $C^R$ , in analogy with the ternary Cantor set argument in (46), see Figure 13. Then,

$$\mu^d(C \cap A_\alpha) = \mu^d(C^L) + \mu^d(C^R) = 2\delta^d \mu^d(C \cap A_\alpha), \quad (75)$$

where the first equality holds since the sets  $C^L$  and  $C^R$  are disjoint; the second since such sets have the same measure and are obtained by contracting  $C \cap A_\alpha$  with a factor  $\delta < 1$ , which is the inverse of the expansion of the set  $C^L$  according to the Kasner circle map, scaled with the power of the dimension  $d$ .

Note that the contraction rate  $\delta < 1$  is not uniform, since the expansion of the Kasner circle map is not uniform. Moreover, each iteration has a different contraction rate given by  $|C_{k+1}|/|C_k|$ . We therefore obtain the following bounds:

$$2M^{-d}\mu^d(C \cap A_\alpha) \leq \mu^d(C \cap A_\alpha) \leq 2m^{-d}\mu^d(C \cap A_\alpha). \quad (76)$$

If  $\mu^d(C \cap A_\alpha) \neq 0$  and  $\infty$  for some  $d \geq 0$ , which we refrain from proving, we obtain

$$2M^{-d} \leq 1 \leq 2m^{-d}, \quad (77)$$

where the logarithm implies the desired bounds (42). There remains to show that  $\mu^{d_M}(C \cap A_\alpha) < \infty$  and  $\mu^{d^*}(C_1^i \cap C) \geq \epsilon > 0$  in order to make the above proof rigorous. This, however, follows in a similar manner as for the usual ternary Cantor set, or, alternatively, see [73].

### Sixth step: Chaoticity of $\mathcal{K}$ on $C$ .

To determine chaoticity of  $\mathcal{K}$  on the Cantor set  $C$ , we establish topological conjugacy with the *shift map*,  $\sigma : W_\infty \rightarrow W_\infty$ , which shifts a sequence to the right, i.e.,  $\sigma(a_0a_1a_2\dots) := a_1a_2a_3\dots$ , since the shift map is well-known to be chaotic, see Chapter 1.6 in [21]. To accomplish this we construct an *encoding map*, which is a homeomorphism  $h : C \rightarrow W_\infty$  such that  $h \circ \mathcal{K} = \sigma \circ h$ , i.e., we need to establish the following commutative diagram:

$$\begin{array}{ccc} C & \xrightarrow{\mathcal{K}} & C \\ h \downarrow & & \downarrow h \\ W_\infty & \xrightarrow{\sigma} & W_\infty \end{array} \quad (78)$$

If such a map  $h$  exists, we say that the discrete dynamical systems  $\mathcal{K}$  and  $\sigma$  are *topologically conjugate*. Note that the dynamics of  $\mathcal{K}$  and  $h$  are equivalent, since  $\mathcal{K} = h^{-1} \circ \sigma \circ h$ , and hence fixed points and periodic heteroclinic chains can be translated from one system to the other, see Chapter 1.7 in [21].

We construct the map  $h$  so that it encodes each point  $p \in C$  into an infinite sequence of three symbols 1, 2, 3 without consecutive repetitions, which accounts for the arcs  $A_1, A_2, A_3$  the iterations of  $\mathcal{K}^n(p)$  visits, i.e.,

$$\begin{aligned} h : C &\rightarrow W_\infty \\ p &\mapsto h(p) := w_\infty = (a_k)_{k \in \mathbb{N}_0}, \end{aligned} \quad (79)$$

where for each  $k$ , we define  $a_k$  by  $\mathcal{K}^k(p) \in A_{a_k}$ . Note that  $W_\infty$  is the alphabet of words of infinite length, i.e., the set (54) when  $n = \infty$ , and that periodic heteroclinic chains yield infinite periodic sequences.

Following the heteroclinic orbit that takes  $p$  to  $\mathcal{K}(p)$  corresponds to a shift to the right given by  $\sigma(a_0a_1a_2\dots) := a_1a_2a_3\dots$ . In other words, the diagram in (78) commutes. However, we also have to show that  $h$  is bijective, continuous, and that  $h^{-1}$  is also continuous.

This follows from the definition of  $I(w_n)$  in (55) and its properties given in Lemma 4.6, as shown next.

The map  $h$  is bijective since for any sequence  $w_\infty \in W_\infty$  there is a unique point  $p \in C$  such that  $h(p) = w_\infty$ . This point is  $p = \bigcap_{n \in \mathbb{N}_0} I(w_n)$ , as in (63), where  $w_n$  is the  $n^{\text{th}}$  truncation of the infinite word  $w_\infty$ .

The map  $h$  is continuous at any point  $p \in C$ , since the neighborhood  $I(w_n) \cap C$  of  $p$ , for any  $n \in \mathbb{N}_0$ , only contains points  $q \in C$  whose corresponding sequences of symbols  $h(q)$  coincide with  $h(p)$  for the first  $n$  symbols.

The map  $h^{-1}$  is also continuous. For any  $\varepsilon > 0$ , there is an  $n \in \mathbb{N}_0$  such that any two given sequences  $w_\infty, \tilde{w}_\infty \in W_\infty$  for which the first  $n$  symbols coincide, both  $h^{-1}(w_\infty)$  and  $h^{-1}(\tilde{w}_\infty)$  are in  $I(w_n) = I(\tilde{w}_n)$  with  $|I(w_n)| < \varepsilon$ , due to (58) in Lemma 4.6.

Note that the above proof does not carry over to the critical case with  $v = 1/2$  since the map  $h$  in (79) only encodes the Cantor set  $C$ , i.e., it does not encode the set  $S$ , which includes the tangential points and the Taub points. To deal with  $v \in (1/2, 1)$  and  $v = 1/2$  in a unified manner, we make an appropriate modification in Appendix C.

## 5 Subcritical case

In the subcritical case,  $v \in (0, 1/2)$ , each point in the set  $K^\circ$  admits at least one unstable direction and hence the following Lemma holds:

**Lemma 5.1.** *Every point in the set  $K^\circ$  admits at least one infinite heteroclinic chain.*

More precisely, all points in  $K^\circ \setminus \text{int}(A_\alpha \cap A_\beta)$  have one unstable direction, whereas points in  $\text{int}(A_\alpha \cap A_\beta)$  have two unstable directions, see Figure 2. A point within  $\text{int}(A_\alpha \cap A_\beta)$  thereby admits two different heteroclinic connections on the hemispheres  $\text{II}_\alpha$  and  $\text{II}_\beta$  given by (16), which induces a multivalued Kasner circle map  $\mathcal{K}$ , see Figure 4. To deal with this situation we interpret  $\mathcal{K}$  as a collection of maps on the Kasner circle  $K^\circ$ , i.e., we will reformulate  $\mathcal{K}$  as a so-called expansive iterated function system.

Recall that the Kasner circle map (24) is expanding due to equation (32). However, the usual definition of an *iterated function system* (IFS) is based on a family of contractions in a metric space  $X$ , i.e.,  $\mathcal{F} := \{f_i : X \rightarrow X \mid i = 1, \dots, N, f_i \in C^1 \text{ and } |f'_i| < 1\}$ . According to [41], there exists a unique nonempty compact set  $\mathcal{A} \subseteq X$  called the *attractor* of  $\mathcal{F}$ , which satisfies  $\mathcal{A} = \overline{\bigcup_{i=1}^N f_i(\mathcal{A})}$ .

An example is the ternary Cantor set  $T$ , iteratively constructed in (43), which can be seen as the attractor of the IFS given by  $\{f_L, f_R : [0, 1] \rightarrow [0, 1]\}$ , where the left and right maps are  $f_L(x) := x/3$  and  $f_R(x) := x/3 + 2/3$ , respectively. Then the  $n^{\text{th}}$ -step of the construction  $T_n$  consists of the union of all its connected components given by the image  $f_{i_n} \circ \dots \circ f_{i_1}([0, 1])$  for some  $i_1, \dots, i_n \in \{L, R\}$ , see Figure 11.

Fewer efforts have been made in understanding families that are not contractions, although see the construction of Koch curves using expansions in [74] and the more recent work [59]. Both these investigations focus on generating patterns occurring outside fractal sets and

understanding iterates, which in a non-compact space escape to infinity. Since we are dealing with expansive iterates of a compact set, the Kasner circle  $K^\circlearrowright$ , we propose a theory of expansive iterated function system (eIFS) on compact metric spaces<sup>9</sup>. We define an *expansive iterated function system* (eIFS) as a family of expansions in a compact metric space  $X$ ,

$$\mathcal{F} := \left\{ f_i : X \rightarrow X \mid i = 1, \dots, N, \begin{array}{l} f_i \in C^1 \text{ almost everywhere,} \\ |f'_i| > 1 \text{ on dense open sets} \end{array} \right\}. \quad (80)$$

In the spirit of [41], we define the iterates of  $\mathcal{F}$  by the Hutchinson operator:

$$\mathcal{F}^n(p) := \bigcup_{i_1, \dots, i_n \in \{1, \dots, N\}} f_{i_n} \circ \dots \circ f_{i_1}(p), \quad (81)$$

where the  $n^{th}$  iterate yields a set consisting of at most  $N^n$  points, since the Hutchinson operator  $\mathcal{F}^n(p)$  is defined as the union over all possible iterates.

We now consider the Kasner circle map (24) as an expansive iterated function system and state a conjecture regarding its dynamics. The *Kasner circle eIFS* is defined as a collection of eight maps as follows:

$$\mathcal{K} := \{\mathcal{K}_{\mu\nu\zeta}(p) : K^\circlearrowright \rightarrow K^\circlearrowright \mid \mu = 1, 2; \nu = 1, 3; \zeta = 2, 3\}, \quad (82)$$

where each individual map is given by

$$\mathcal{K}_{\mu\nu\zeta}(p) := \begin{cases} f_1(p) & \text{for } p \in A_1 \setminus \{(A_1 \cap A_2) \cup (A_1 \cap A_3)\} \\ f_2(p) & \text{for } p \in A_2 \setminus \{(A_2 \cap A_1) \cup (A_2 \cap A_3)\} \\ f_3(p) & \text{for } p \in A_3 \setminus \{(A_3 \cap A_1) \cup (A_3 \cap A_2)\} \\ f_\mu(p) & \text{for } p \in A_1 \cap A_2 \\ f_\nu(p) & \text{for } p \in A_2 \cap A_3 \\ f_\zeta(p) & \text{for } p \in A_1 \cap A_3 \end{cases} \quad (83)$$

where  $f_*(p) := g(p)p + (g(p) - 1)T_*/v$  such that the symbol  $*$  is to be replaced by 1, 2, 3 or  $\mu \in \{1, 2\}$ ,  $\nu \in \{2, 3\}$ ,  $\zeta \in \{1, 3\}$ .

Any point that is not in the overlap regions, e.g.  $p \in A_1 \setminus \{(A_1 \cap A_2) \cup (A_1 \cap A_3)\}$ , has the same image under all maps  $\mathcal{K}_{\mu\nu\zeta}(p)$ , independently of the indices  $\mu, \nu, \zeta$ . On the other hand, points in the overlap regions, e.g.  $p \in A_1 \cap A_2$ , have two different maps with different images:  $\mathcal{K}_{1\nu\zeta}(p)$  and  $\mathcal{K}_{2\nu\zeta}(p)$ , independently of the indices  $\nu$  and  $\zeta$ . This combinatorial problem of choosing between two maps for each of the three overlapping arcs yields the eight maps in (82).

Due to (24), each map (83) is expanding and  $C^1$  everywhere in  $K^\circlearrowright$ , except at certain tangential boundary points  $\partial(A_\alpha \cap A_\beta)$  where the derivative is one. Nevertheless, if  $\mathcal{K}_{\mu\nu\zeta}(p)$  is discontinuous at such a tangential point, there is another  $\mathcal{K}_{\mu'\nu'\zeta'}(p)$  that is both  $C^1$  and strictly expanding at this point.

---

<sup>9</sup>Alternatively, one can consider the usual physical time direction (i.e., the reverse of the present time direction), for which the Kasner map becomes a contraction almost everywhere, and seek an attractor  $\mathcal{A}$  and its properties for a non-hyperbolic IFS, see [4, 63] and references therein.

The iterates of the Kasner eIFS are given by its Hutchinson operator:

$$\mathcal{K}^n(p) := \bigcup_{\substack{\mu_k=1,2; \nu_k=2,3; \zeta_k=1,3 \\ \text{for } k=1,\dots,n}} \mathcal{K}_{\mu_n \nu_n \zeta_n} \circ \dots \circ \mathcal{K}_{\mu_1 \nu_1 \zeta_1}(p). \quad (84)$$

This allows us to formulate the following conjecture:

**Conjecture 5.2.** *The Kasner circle eIFS is chaotic when  $v \in (0, 1/2)$ .*

We expect that the Kasner circle eIFS is chaotic due to the expanding properties of each map of the Kasner circle eIFS (82). However, the notion of chaos still has to be further developed for multivalued maps. We suggest two different approaches to tackle this problem. First, one can attempt to generalize the notion of chaotic discrete dynamical systems to eIFS using the Hausdorff distance between sets, since the image under the Hutchinson operator of the Kasner map in (84) is a set of points. Second, one can try to incorporate different symbols  $\mu\nu\zeta$  in the definition of chaos, and require that topological mixing occurs for some, for generic, or for all symbols  $\mu\nu\zeta$ . Roughly speaking, this means that there are chaotic realizations of the eIFS.

We also expect that there are two special iterations in the Hutchinson operator (84) which dictate the chaotic dynamics. Whenever some iterate of a point  $p$  reaches the overlap  $A_\alpha \cap A_\beta$ , there are two choices of maps: one corresponding to orbits originating from the auxiliary point  $Q_\alpha/v$  and one from  $Q_\beta/v$ . Consider the iteration  $\mathcal{K}_{\mu_n \nu_n \zeta_n} \circ \dots \circ \mathcal{K}_{\mu_1 \nu_1 \zeta_1}(p)$ , related to a symbolic sequence  $(\mu_k, \nu_k, \zeta_k)_{k \in \mathbb{N}_0}$  that always selects the map with minimum expansion rate among the two choices, and define it to be  $\mathcal{K}_m^n(p)$ . Similarly, denote by  $\mathcal{K}_M^n(p)$  the iteration that always selects the map with maximum expansion among the two choices. These maps are uniquely determined for each point that is not a Taub point. We expect the dynamics of  $\mathcal{K}_m^n$  and  $\mathcal{K}_M^n$  to quantify how chaotic the full dynamics turns out to be, although there are several technical problems which need to be resolved, especially in connection with the Taub points.

Note that there is redundancy in the iteration of the maps (83) in the Hutchinson operator (84), e.g., a point that is not in any overlap region  $p \in A_\alpha \setminus \{(A_\alpha \cap A_\beta) \cup (A_\alpha \cap A_\gamma)\}$  is mapped by  $\mathcal{K}_{\mu\nu\zeta}(p)$  for all  $\mu\nu\zeta$  in the Hutchinson operator (84). Nevertheless, all these images coincide and consist of a single point. To avoid redundancy, one can give alternative descriptions of the multivalued Kasner circle map (24), which affect the number of maps in an eIFS. For instance, instead of considering the maps (82) within the eIFS framework in (80), one can consider a family of *three*  $C^1$  maps such that the domain of each map corresponds to  $A_\alpha$ . In this and similar descriptions, one has to be careful about how images of some maps should be contained within the domain of a different map in order to have a well-defined iteration. To circumvent this problem, and have the whole Kasner circle  $K^\circ$  as the domain, we choose the maps in (82). The drawback with this choice is that each map (83) is discontinuous at certain tangential points.

Even though the overall dynamical structure is far from being understood, there are still special features which can be compared with the supercritical case. Consider the set  $\tilde{C}$  of points in  $K^\circ$  for which all iterates of the Kasner circle map  $\mathcal{K}$  consist of exactly one

positive eigenvalue in the  $N_\alpha$  variables<sup>10</sup>, see Figures 2 and 4, i.e.,

$$\tilde{C} := \{p \in K^\circ \mid \mathcal{K}^n(p) \notin \text{int}((A_1 \cap A_2) \cup (A_1 \cap A_3) \cup (A_2 \cap A_3)) \text{ for all } n \in \mathbb{N}_0\}. \quad (85)$$

This set is given by the points that never reach the overlaps  $\text{int}(A_\alpha \cap A_\beta)$ . The map  $\mathcal{K}$  is thereby not a multivalued map on the set  $\tilde{C}$ , and thus  $\mathcal{K}$  is well-defined. Furthermore, the set  $\tilde{C}$  is not empty since, e.g., there are two (physically equivalent) period 3 cycles, given by Lemma 2.2 and depicted in Figure 7, since the three vertices of each triangle do not lie in any of the overlap regions  $A_\alpha \cap A_\beta$ .

The complement of the set  $\tilde{C}$  in  $K^\circ$  is given by

$$\tilde{F} := \{p \in K^\circ \mid \mathcal{K}^n(p) \in \text{int}((A_1 \cap A_2) \cup (A_1 \cap A_3) \cup (A_2 \cap A_3)) \text{ for some } n \in \mathbb{N}_0\}. \quad (86)$$

Splitting the dynamics in  $K^\circ$  into two disjoint invariant sets,  $\tilde{C}$  and  $\tilde{F}$ , is a first step to tackle Conjecture 5.2. The properties of the set  $\tilde{C}$ , and how they depend on  $v$ , are not clear: Is it a Cantor set or not? What is its Lebesgue measure and Hausdorff dimension? Does  $\tilde{C}$  or  $\tilde{F}$  dominate the dynamics in the subcritical case?

## 6 First principles and the dynamical hierarchy

We now investigate the dynamical consequences summarized in Table 2 of first principles, which for the vacuum  $\lambda$ - $R$  class A Bianchi models reduce to the scale-automorphism groups for the Lie contraction hierarchy in Figure 1.

The scale-automorphism group for each level of the hierarchy yields monotone functions and conserved quantities derived in Appendix B.1. As we will see, these monotone functions and conserved quantities restrict and push the dynamics toward the initial singularity from the highest level of the class A Bianchi hierarchy, Bianchi type IX and VIII, to the lowest levels of the hierarchy, Bianchi type II and I. In particular, they completely determine the dynamics for Bianchi types I and II<sup>11</sup>. The next level in the hierarchy are the Bianchi type VI<sub>0</sub> and VII<sub>0</sub> models, where the scale-automorphism group give rise to several quantities that limit the asymptotic dynamics. These quantities yield a complete qualitative description for this level of the hierarchy, which we focus on in this section. The asymptotic dynamics of type VIII and IX form a considerable challenge and we only present some limited results.

### Bianchi type VI<sub>0</sub> and VII<sub>0</sub>

To obtain the equations for the type VI<sub>0</sub> and VII<sub>0</sub> vacuum  $\lambda$ - $R$  models we set, without loss of generality,  $N_1 = 0$ ,  $N_2 > 0$ ,  $N_3 < 0$  for type VI<sub>0</sub>, and  $N_1 = 0$ ,  $N_2 > 0$ ,  $N_3 > 0$  for type VII<sub>0</sub>. Since  $N_1 = 0$  selects a special direction, it is natural to replace  $(\Sigma_1, \Sigma_2, \Sigma_3)$

<sup>10</sup>Note that the set  $C$  in (40) for  $v \in (1/2, 1)$  can also be described by this formulation. Thus the properties of such a set (of points with exactly one positive eigenvalue for all iterates) depend on  $v$ .

<sup>11</sup>In Appendix B.1 we derive the Kasner circle  $K^\circ$  of fixed points from the scale-automorphism group of Bianchi type I. We also show that the heteroclinic type II orbits, given in (23), follow from the Bianchi type II scale-automorphism group.

with the  $\Sigma_{\pm}$  Misner variables given in (26). Setting  $N_1 = 0$  in (134) and (135) yields the evolution equations

$$\Sigma'_+ = 2(1 - \Sigma^2)(1 + 2v\Sigma_+), \quad (87a)$$

$$\Sigma'_- = 4v(1 - \Sigma^2)\Sigma_- + 2\sqrt{3}(N_2^2 - N_3^2), \quad (87b)$$

$$N'_2 = -2(2v\Sigma^2 + \Sigma_+ + \sqrt{3}\Sigma_-)N_2, \quad (87c)$$

$$N'_3 = -2(2v\Sigma^2 + \Sigma_+ - \sqrt{3}\Sigma_-)N_3, \quad (87d)$$

and the constraint

$$1 - \Sigma^2 - (N_2 - N_3)^2 = 0, \quad \text{where} \quad \Sigma^2 := \Sigma_+^2 + \Sigma_-^2. \quad (87e)$$

Due to the constraint (87e), the state spaces for the type VI<sub>0</sub> and VII<sub>0</sub> models with  $N_1 = 0$  are 3-dimensional with a 2-dimensional boundary given by the union of the invariant type II<sub>2</sub>, II<sub>3</sub> and K<sup>○</sup> sets. Type VI<sub>0</sub> has a relatively compact state-space, whereas type VII<sub>0</sub> has an unbounded one. Equation (87e) implies that  $\Sigma_+^2 + \Sigma_-^2 \leq 1$ . For type VI<sub>0</sub>,  $(N_2 - N_3)^2 = N_2^2 + N_3^2 + 2|N_2N_3|$ , and hence (87e) yields  $N_2^2 \leq 1 - \Sigma^2$  and  $N_3^2 \leq 1 - \Sigma^2$ , where the equalities hold individually for the II<sub>2</sub> and II<sub>3</sub> boundary sets, respectively. For type VII<sub>0</sub>, on the other hand, introducing  $N_{\pm} := N_2 \pm N_3$  results in that the constraint (87e) can be written as  $\Sigma^2 + N_-^2 = 1$ , and thus  $\Sigma_{\pm}$  and  $N_-$  are bounded, while  $N_+$  is unbounded.

The analysis of the Bianchi type VI<sub>0</sub> and VII<sub>0</sub> scale-automorphism group of the vacuum  $\lambda$ - $R$  models in Appendix B.1 resulted in three quantities that are essential for the asymptotics of the dynamical system (87):

$$1 + 2v\Sigma_+, \quad Z_{\text{sup}} := \frac{(2v + \Sigma_+)^2}{|N_2N_3|} \quad Z_{\text{sub}} := \frac{(1 + 2v\Sigma_+)^2}{|N_2N_3|}, \quad (88)$$

where  $Z_{\text{sup}} = Z_{\text{sub}} = Z_{\text{crit}} = (1 + \Sigma_+)^2/|N_2N_3|$  when  $v = 1/2$ . Due to (87), these quantities satisfy

$$(1 + 2v\Sigma_+)' = 4v(1 - \Sigma^2)(1 + 2v\Sigma_+), \quad (89a)$$

$$Z'_{\text{sup}} = 4 \left[ \frac{(1 + 2v\Sigma_+)^2 + (4v^2 - 1)\Sigma_-^2}{2v + \Sigma_+} \right] Z_{\text{sup}}, \quad (89b)$$

$$Z'_{\text{sub}} = 4(2v + \Sigma_+)Z_{\text{sub}}, \quad (89c)$$

and hence  $Z'_{\text{crit}} = 4(1 + \Sigma_+)Z_{\text{crit}}$ .

These functions behave differently for the subcritical, critical and supercritical cases, and they have different asymptotic consequences for the type VI<sub>0</sub> and VII<sub>0</sub> vacuum  $\lambda$ - $R$  models, primarily because the state space of the type VII<sub>0</sub> models is unbounded. Nevertheless, the two Bianchi types share the same  $\text{II}_2 \cup \text{II}_3 \cup \text{K}^{\circ}$  boundary, and thus several dynamical asymptotic features. These shared features include the stable set in the Kasner circle set  $\text{K}^{\circ}$ , given by  $S_{\text{VI}_0} = S_{\text{VII}_0} = S_{\text{VI}_0, \text{VII}_0} := \text{K}^{\circ} \setminus \text{int}(A_2 \cup A_3)$ , which, due to that  $N_1 = 0$ , is different than the set  $S$  in the supercritical Bianchi type VIII and IX models, cf. Figures 2 and 16, although both  $S_{\text{VI}_0, \text{VII}_0}$  and  $S$  are defined as the sets where type II heteroclinic chains end. In the subcritical case, type VI<sub>0</sub> and VII<sub>0</sub> also share the region  $A_2 \cap A_3$  in

$K^\circlearrowright$ , where both  $N_2$  and  $N_3$  are unstable in  $\text{int}(A_2 \cap A_3)$ . In the critical case,  $A_2 \cap A_3$  reduces to the Taub point  $T_1$ . These features are illustrated in Figure 16.

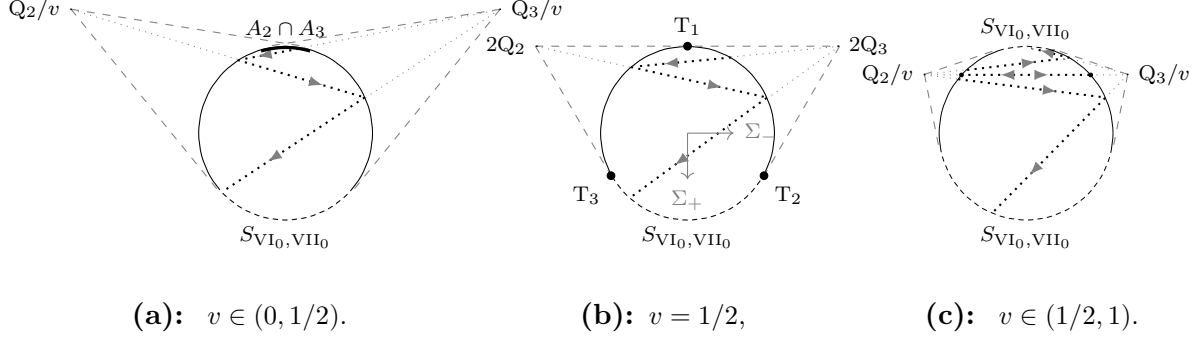


**Figure 16:** The common stable set  $S_{VI_0, VII_0}$  for Bianchi type  $VI_0$  and  $VII_0$ . In addition, projected onto  $(\Sigma_+, \Sigma_-)$ -space, there are illustrative heteroclinic chains located on the  $\Pi_2 \cup \Pi_3 \cup K^\circlearrowright$  boundary. In particular,  $v \in (1/2, 1)$  admits a heteroclinic cycle/chain with period 2, which resides on the projected line between  $Q_2/v$  and  $Q_3/v$  characterized by  $\Sigma_+ = -1/(2v)$ .

**Proposition 6.1.** *In Bianchi type  $VI_0$  the limit sets (in  $\tau_-$ ) are as follows:*

- (i) *When  $v \in (0, 1/2]$ , the  $\alpha$ -limit set for all orbits resides in the set  $A_2 \cap A_3$  in  $K^\circlearrowright$ , where  $A_2 \cap A_3$  reduces to the Taub point  $T_1$  when  $v = 1/2$ . The  $\omega$ -limit set for all orbits resides in the set  $S_{VI_0}$ .*
- (ii) *When  $v \in (1/2, 1)$ , the  $\alpha$ -limit set for all orbits is the fixed point  $p_{VI_0}$  given by*

$$p_{VI_0} := \left\{ (\Sigma_+, \Sigma_-, N_2, N_3) = \left( -\frac{1}{2v}, 0, \frac{\sqrt{1 - 1/(4v^2)}}{2}, -\frac{\sqrt{1 - 1/(4v^2)}}{2} \right) \right\}. \quad (90)$$

*Apart from  $p_{VI_0}$ , the  $\omega$ -limit set of all orbits on the invariant subset  $\Sigma_+ = -1/(2v)$  consists of the heteroclinic chain with period 2, while the  $\omega$ -limit set of all orbits with  $\Sigma_+ \neq -1/(2v)$  resides in the set  $S_{VI_0}$ .<sup>12</sup>*

*Proof.* All type  $VI_0$  orbits satisfy  $\Sigma^2 < 1$ , and thereby  $|\Sigma_+| < 1$ , while  $\Sigma^2 = 1$  corresponds to the type I boundary set  $K^\circlearrowright$ , since the constraint (87e) yields  $(N_2 - N_3)^2 = N_2^2 + N_3^2 + 2|N_2 N_3| = 0$ , and thus  $N_2 = N_3 = 0$ , when  $\Sigma^2 = 1$ .

For the subcritical and critical type  $VI_0$  models, with  $v \in (0, 1/2]$ , the function  $1 + 2v\Sigma_+$  is bounded according to  $0 \leq 1 - 2v < 1 + 2v\Sigma_+ \leq 1 + 2v$ , and, due to (89a), it is monotonically increasing. Thus  $\lim_{\tau_- \rightarrow \pm\infty} (1 - \Sigma^2) = 0$  in (89a), and hence  $\lim_{\tau_- \rightarrow \pm\infty} (N_2, N_3) = (0, 0)$ . Therefore both the  $\alpha$ - and  $\omega$ -limit sets for all type  $VI_0$  orbits belong to the set  $K^\circlearrowright$ . It then follows from the stability properties of  $K^\circlearrowright$  that the  $\alpha$ -limit set for these orbits resides in the set  $A_2 \cap A_3$  in the subcritical case,  $v \in (0, 1/2)$ , while it consists of the Taub point  $T_1$  with  $\Sigma_+ = -1$  in the critical case  $v = 1/2$ . It also follows for both the subcritical and critical cases that the  $\omega$ -limit set of all type  $VI_0$  orbits lies in the set  $S_{VI_0}$ .

<sup>12</sup>Therefore, the invariant set  $\Sigma_+ = -1/(2v)$  is a co-dimension one stable set for the heteroclinic chain with period 2. In particular, this set is equivalent to a Bowen's eye, where the fixed point  $p_{VI_0}$  is surrounded by spiraling orbits toward the heteroclinic chain with period 2, see [86] and [22].

In the supercritical case,  $v \in (1/2, 1)$ , the function  $Z_{\sup} > 0$  in (88) is strictly monotonically increasing in the type VI<sub>0</sub> state space, except at the fixed point  $p_{\text{VI}_0}$ , given by (90), where  $Z_{\sup}$  attains its global minimum,  $Z_{\sup}(p_{\text{VI}_0}) = 4(4v^2 - 1) > 0$ . Since  $Z_{\sup}$  is strictly monotonically increasing for all non- $p_{\text{VI}_0}$  type VI<sub>0</sub> orbits, it follows that their  $\alpha$ -limits reside at the minimum of  $Z_{\sup}$  at  $p_{\text{VI}_0}$ , see the monotonicity principle in [95]. Moreover,  $Z_{\sup} \rightarrow \infty$  as  $\tau_- \rightarrow \infty$ , for all non- $p_{\text{VI}_0}$  orbits. Since the numerator  $(1 + 2v\Sigma_+)^2$  of  $Z_{\sup}$  in (88) is bounded, it follows that  $\lim_{\tau_- \rightarrow \infty} N_2 N_3 = 0$ , and thus that the  $\omega$ -limit set of all non- $p_{\text{VI}_0}$  supercritical type VI<sub>0</sub> orbits resides in the  $\text{II}_2 \cup \text{II}_3 \cup \text{K}^\circ$  boundary. According to (89a),  $1 + 2v\Sigma_+ = 0$  describes an invariant separatrix surface, which divides the remaining state space into two disjoint sets,  $1 + 2v\Sigma_+ < 0$  and  $1 + 2v\Sigma_+ > 0$ , on which  $1 + 2v\Sigma_+$  is monotone.<sup>13</sup> It follows that the  $\omega$ -limit set of all non- $p_{\text{VI}_0}$  orbits on the invariant set  $\Sigma_+ = -1/(2v)$  is the heteroclinic cycle/chain with period 2. With similar reasoning as in the subcritical and critical cases, equation (89a) yields that the  $\omega$ -limit set for all orbits in the subset  $1 + 2v\Sigma_+ < 0$  ( $1 + 2v\Sigma_+ > 0$ ) resides in the connected component of the set  $S_{\text{VI}_0}$  with  $1 + 2v\Sigma_+ < 0$  ( $1 + 2v\Sigma_+ > 0$ ).  $\square$

Let us now turn to type VII<sub>0</sub>, but before presenting asymptotic results we first consider the locally rotationally symmetric (LRS) type VII<sub>0</sub> subset (for additional information about the LRS models, see Appendix B.1). This invariant set is given by  $N_- = 0$  and  $\Sigma_- = 0$ , where the constraint (87e) divides the LRS subset into two disjoint invariant sets consisting of the two lines at  $\Sigma_+ = 1$  and  $\Sigma_+ = -1$ , i.e.,

$$\text{LRS}^\pm := \left\{ (\Sigma_+, 0, N_2, N_3) \in \mathbb{R}^4 \mid \begin{array}{l} \Sigma_+ = \pm 1, \\ N_2 = N_3 \neq 0 \end{array} \right\}, \quad (91\text{a})$$

where the superscript of  $\text{LRS}^\pm$  is determined by the sign of  $\Sigma_+$ . Let  $N := N_2 = N_3 > 0$ . Then the flow on the  $\text{LRS}^\pm$  subsets is determined by

$$N' = -2\Sigma_+(2v\Sigma_+ + 1)N, \quad \Sigma_+ = \pm 1. \quad (92)$$

On  $\text{LRS}^+$ , where  $\Sigma_+ = +1$ , the variable  $N \in (0, \infty)$  monotonically decreases from  $\lim_{\tau_- \rightarrow -\infty} N = \infty$  to 0, and hence the orbit in the invariant line ends at  $Q_1$  in the set  $\text{K}^\circ$  for all  $v \in (0, 1)$ . On  $\text{LRS}^-$ , where  $\Sigma_+ = -1$ , there are three  $v$ -dependent cases: the critical case,  $v = 1/2$ , which results in a line of fixed points; the subcritical case,  $v \in (0, 1/2)$ , which yields an orbit that emanates from  $T_1$ , where  $N \in (0, \infty)$  subsequently monotonically increases, which results in  $\lim_{\tau_- \rightarrow \infty} N = \infty$ ; the supercritical case,  $v \in (1/2, 1)$ , reverses the flow and leads to an orbit for which  $\lim_{\tau_- \rightarrow -\infty} N = \infty$ , while it ends at  $T_1$ .

The next Propositions address the  $\alpha$ -limit and  $\omega$ -limit sets for the type VII<sub>0</sub> models.

**Proposition 6.2.** *The  $\omega$ -limit set (in  $\tau_-$ ) for all Bianchi type VII<sub>0</sub> orbits resides in the stable set  $S_{\text{VII}_0}$  in the Kasner circle set  $\text{K}^\circ$ , apart from three exceptions:*

(i) *When  $v \in (0, 1/2)$ , the  $\text{LRS}^-$  set consists of an orbit for which  $\lim_{\tau_- \rightarrow \infty} N = \infty$ .*

---

<sup>13</sup>As described in Appendix B.1, the existence of the invariant set  $1 + 2v\Sigma_+ = 0$  follows from a discrete symmetry, which also results in that the flow of (89a) is equivariant under a change of sign of  $1 + 2v\Sigma_+$ .

- (ii) When  $v = 1/2$ , the LRS<sup>-</sup> set is a line of fixed points  $N_2 = N_3 = \text{constant}$ .
- (iii) When  $v \in (1/2, 1)$ , there is an invariant set of co-dimension one, characterized by  $\Sigma_+ = -1/(2v)$ , for which the heteroclinic cycle with period 2 on the  $\text{II}_2 \cup \text{II}_3 \cup \text{K}^\circ$  boundary is the  $\omega$ -limit set.

*Proof.* The first two exceptions follow from the previous analysis of the LRS type VII<sub>0</sub> subset, due to (92). Consider therefore type VII<sub>0</sub> non-LRS orbits, i.e., orbits for which  $\Sigma_-^2 + N_-^2 > 0$  and thereby  $|\Sigma_+| < 1$ . Note that in contrast to the type VII<sub>0</sub> state space, the  $\text{II}_2 \cup \text{II}_3 \cup \text{K}^\circ$  boundary is compact.

In the subcritical and critical cases,  $Z_{\text{sub}} > 0$  for all non-LRS<sup>-</sup> orbits. In the LRS<sup>-</sup> case the orbit satisfies  $\lim_{\tau_- \rightarrow \infty} N_2 N_3 = \infty$  in the subcritical case, while LRS<sup>-</sup> yields a line of fixed points with constant  $N_2 = N_3$  in the critical case. Then note that

$$(1 + 2v\Sigma_+)' = 4vN_-^2(1 + 2v\Sigma_+), \quad N_- := N_2 - N_3, \quad (93a)$$

$$(1 + 2v\Sigma_+)^{\prime\prime}|_{N_-=0} = 0, \quad (93b)$$

$$(1 + 2v\Sigma_+)^{\prime\prime\prime}|_{N_-=0} = 96(N_2 + N_3)^2\Sigma_-^2(1 + 2v\Sigma_+). \quad (93c)$$

Thus  $(1 + 2v\Sigma_+)$  is monotonically increasing for all non-LRS orbits (i.e., orbits such that  $\Sigma_-^2 + N_-^2 > 0$ ), except when  $N_- = 0$  (and thereby  $\Sigma_- \neq 0$ ), which corresponds to an inflection point in the growth of the positive quantity  $(1 + 2v\Sigma_+)$ , due to (93). Thus all non-LRS<sup>-</sup> orbits eventually enter the (positively) invariant set  $\Sigma_+ > -2v$ . Since, due to (89c),  $Z_{\text{sub}} > 0$  is strictly monotonically increasing in the invariant set  $\Sigma_+ > -2v$ , it follows that  $\lim_{\tau_- \rightarrow \infty} Z_{\text{sub}} = \infty$  and thereby  $\lim_{\tau_- \rightarrow \infty} N_2 N_3 = 0$ . Thus the  $\omega$ -limit set of all non-LRS<sup>-</sup> orbits in the subcritical and critical cases resides in the  $\text{II}_2 \cup \text{II}_3 \cup \text{K}^\circ$  boundary set. The same analysis as in type VI<sub>0</sub> of this boundary set yields the same result for the non-LRS<sup>-</sup> orbits in type VII<sub>0</sub>.

In the supercritical case,  $\Sigma_+ = -1/(2v)$  forms an invariant separatrix surface, which divides the VII<sub>0</sub> state space into two disjoint invariant subsets with  $1 + 2\Sigma_+ \neq 0$  on which  $1 + 2v\Sigma_+$  is monotone, just as in type VI<sub>0</sub>. Due to (89b),  $Z_{\text{sup}} > 0$  in (88) is strictly monotonically increasing everywhere in the type VII<sub>0</sub> state space, except at two lines where  $\Sigma_+ = -1/(2v)$ ,  $\Sigma_- = 0$ , and  $N_2 = N_3 \pm \sqrt{1 - (1/2v)^2}$ , due to the constraint (87e). However, these lines, denoted by  $L_{\text{VII}_0}^\pm$ , in contrast to the fixed point  $p_{\text{VI}_0}$  in type VI<sub>0</sub>, are not invariant sets. When an orbit passes through one of the lines  $L_{\text{VII}_0}^\pm$  this therefore only results in an inflection point in the growth of  $Z_{\text{sup}}$ . Moreover,  $\lim_{\tau_- \rightarrow \infty} Z_{\text{sup}} = \infty$ , since  $Z_{\text{sup}}$  can only be asymptotically bounded if an orbit asymptotically approaches a line  $L_{\text{VII}_0}^\pm$ . This, however, requires that  $\lim_{\tau_- \rightarrow \infty} (\Sigma_-, \Sigma'_-) = (0, 0)$ , but this is impossible since equation (87b) then implies that  $N_2 + N_3 = 0$ , and hence  $N_2 = N_3 = 0$ , asymptotically, which is in contradiction with  $N_2 = N_3 \pm \sqrt{1 - (1/2v)^2}$  asymptotically. Since the numerator  $(2v + \Sigma_+)^2$  of  $Z_{\text{sup}}$  in (88) is bounded, the unbounded growth of  $Z_{\text{sup}}$  implies that  $\lim_{\tau_- \rightarrow \infty} N_2 N_3 = 0$ . Thus at least one of  $N_2$  or  $N_3$  decays to zero, while the other variable is asymptotically bounded due to the constraint (87e). Hence the  $\omega$ -limit set for all non-LRS<sup>-</sup> type VII<sub>0</sub> orbits resides in the  $\text{II}_2 \cup \text{II}_3 \cup \text{K}^\circ$  boundary set. This in turn leads to the same conclusions for the  $\omega$ -limit sets as for the non- $p_{\text{VI}_0}$  orbits in type VI<sub>0</sub>.  $\square$

**Proposition 6.3.** *The  $\alpha$ -limit set (in  $\tau_-$ ) for all Bianchi type VII<sub>0</sub> orbits are as follows:*

- (i) When  $v \in (0, 1/2)$ , the  $\alpha$ -limit set of all non-LRS<sup>+</sup> orbits reside in  $A_2 \cap A_3$ . The LRS<sup>+</sup> set consists of an orbit such that  $\lim_{\tau_- \rightarrow -\infty} N = \infty$ , where  $N := N_2 = N_3$ .
- (ii) When  $v = 1/2$ , the  $\alpha$ -limit set of all non-LRS orbits is the line of fixed points, LRS<sup>-</sup>. The LRS<sup>+</sup> set consists of an orbit for which  $\lim_{\tau_- \rightarrow -\infty} N = \infty$ .
- (iii) When  $v \in (1/2, 1)$ , all non-LRS orbits asymptotically satisfy

$$\lim_{\tau_- \rightarrow -\infty} \Sigma_+ = -\frac{1}{2v}, \quad \lim_{\tau_- \rightarrow -\infty} N_2 N_3 = \infty, \quad (94)$$

whereas  $\Sigma_-$  and  $N_-$ ,  $(\Sigma_-, N_-) = (\sqrt{1 - \Sigma_+^2} \cos \psi, \sqrt{1 - \Sigma_+^2} \sin \psi)$ , are asymptotically oscillatory, since  $\psi$  is strictly monotonic as  $\tau_- \rightarrow -\infty$ .

*Proof.* The reasoning in the proof of the previous proposition about  $\omega$ -limits also yield the basic elements when  $\tau_- \rightarrow -\infty$ , but, due to the unboundedness of the type VII<sub>0</sub> state space, there are some new issues, which did not occur when  $\tau_- \rightarrow \infty$ .

In the subcritical and critical cases, similar arguments as in the previous discussion about  $\omega$ -limit sets lead to the following:  $(1 + 2v\Sigma_+)$  is monotonically decreasing when  $\tau_- \rightarrow -\infty$ , which shows that the  $\alpha$ -limit set for all non-LRS<sup>+</sup> orbits resides in the set  $A_2 \cap A_3$  for the subcritical case, and in the line of fixed points LRS<sup>-</sup> for the critical case.<sup>14</sup>

For the non-LRS orbits in the supercritical case,  $(1 + 2v\Sigma_+)^2 > 0$  is monotonically decreasing as  $\tau_- \rightarrow -\infty$ , and orbits thereby approach the invariant set  $\Sigma_+ = -1/(2v)$ . Similar reasoning as in the proposition for the  $\omega$ -limit using the monotone function  $Z_{\text{sup}}$  results in  $\lim_{\tau_- \rightarrow -\infty} N_2 N_3 = \infty$  for the non-LRS orbits. Since  $N_+^2 = N_-^2 + 4N_2 N_3$ ,  $N_{\pm} = N_2 \pm N_3$ , and since  $N_-^2$  is bounded ( $N_-^2 = 1 - \Sigma^2 < 1$ ) it follows that  $\lim_{\tau_- \rightarrow -\infty} N_+ = \infty$ . To study the asymptotic behaviour of  $\Sigma_-$  and  $N_-$ , we introduce polar coordinates for  $N_-$  and  $\Sigma_-$  and solve the constraint (87e). This leads to the following set of new variables:

$$(\Sigma_+, \Sigma_-, N_-, N_+) = \left( \Sigma_+, \sqrt{1 - \Sigma_+^2} \cos \psi, \sqrt{1 - \Sigma_+^2} \sin \psi, \frac{1}{\sqrt{3}M} \right), \quad (95)$$

which result in the unconstrained dynamical system

$$\Sigma'_+ = (1 - \Sigma_+^2)(1 + 2v\Sigma_+)[1 - \cos(2\psi)], \quad (96a)$$

$$M' = (2\Sigma_+(1 + 2v\Sigma_+) + (1 - \Sigma_+^2)[2v(1 + \cos(2\psi)) + 3M \sin(2\psi)]) M, \quad (96b)$$

$$\psi' = -\frac{2}{M} - (2v + \Sigma_+) \sin(2\psi). \quad (96c)$$

We have already shown that  $\lim_{\tau_- \rightarrow -\infty} \Sigma_+ = -1/(2v)$  and  $\lim_{\tau_- \rightarrow -\infty} N_+ = \infty$ , from which it follows that  $\lim_{\tau_- \rightarrow -\infty} M = 0$ . Due to this, and since  $2v + \Sigma_+$  is bounded, equation (96c) implies that  $\psi$  is strictly monotonic as  $\tau_- \rightarrow -\infty$ .<sup>15</sup>  $\square$

<sup>14</sup>A more detailed analysis of the critical GR case was performed in [31], which showed that each fixed point on the LRS<sup>-</sup> subset is the  $\alpha$ -limit set for a one-parameter set of orbits.

<sup>15</sup>For brevity we will refrain from deriving explicit asymptotic expressions for  $\Sigma_+$ ,  $M$  and  $\psi$ , and thereby  $\Sigma_{\pm}$  and  $N_2$ ,  $N_3$  in the supercritical type VII<sub>0</sub> case. However, to derive such expressions there are several different methods one can use, e.g. those in [93, 47], or in [77], or the asymptotic averaging method used in [1].

We now compare the ingredients for the proof given here for the critical case with well-known proofs in GR. In our approach,  $Z_{\text{sup}}$  and  $Z_{\text{sub}}$  in (88) become identical in the critical case:

$$Z_{\text{crit}} := Z_{\text{sup}} = Z_{\text{sub}} = \frac{(1 + \Sigma_+)^2}{|N_2 N_3|}, \quad (97)$$

where

$$Z'_{\text{crit}} = 4(1 + \Sigma_+)Z_{\text{crit}}. \quad (98)$$

In the traditional approach to the GR case, see [13, 94, 76, 79], two monotone functions  $Z_+$  and  $Z_-$  were respectively used for type  $\text{VI}_0$  and  $\text{VII}_0$ :

$$Z_{\pm} := \frac{\Sigma_{\pm}^2 + N_{\pm}^2}{|N_2 N_3|}, \quad (99)$$

where

$$Z'_{\pm} = \frac{4(1 + \Sigma_+)\Sigma_{\pm}^2}{\Sigma_{\pm}^2 + N_{\pm}^2} Z_{\pm}. \quad (100)$$

Even though the equation for the type  $\text{VII}_0$  function  $Z_-$  can be simplified to  $Z'_- = 4\Sigma_-^2(1 - \Sigma_+)^{-1}Z_-$ , the functions  $Z_{\pm}$  arguably gives a more cumbersome analysis than the function  $Z_{\text{crit}} = Z_{\text{sup}} = Z_{\text{sub}}$  in (97), which naturally arises from the scale-automorphism symmetry of these models.

## Bianchi types VIII and IX

In Appendix B.1, we derive the following monotone function from the scale symmetry of the vacuum  $\lambda$ - $R$  type VIII and IX models:

$$\Delta := 3|N_1 N_2 N_3|^{2/3}, \quad (101)$$

which, due to (4), satisfy

$$\Delta' = -8v\Sigma^2\Delta. \quad (102)$$

Thus  $\Delta$  is monotonically decreasing when  $\Sigma^2 > 0$ , and has an inflection point when  $\Sigma^2 = 0$ , since

$$\Delta''|_{\Sigma^2=0} = 0, \quad \Delta'''|_{\Sigma^2=0} = -\frac{8}{3}v(\mathcal{S}_1^2 + \mathcal{S}_2^2 + \mathcal{S}_3^2)\Delta, \quad (103)$$

where  $\mathcal{S}_1^2 + \mathcal{S}_2^2 + \mathcal{S}_3^2 > 0$ . Therefore,

$$\lim_{\tau_- \rightarrow \infty} \Delta = 0, \quad (104)$$

and consequently

$$\lim_{\tau_- \rightarrow \infty} \Sigma^2 \leq 1, \quad (105)$$

since the definition of  $\Omega_k$  in (5b) implies  $\Omega_k + \Delta \geq 0$ ,<sup>16</sup> and hence  $\Sigma^2 \leq 1 + \Delta$ , due to the constraint (4c). Moreover, because of (104) it follows that at least one of the variables

<sup>16</sup>In type VIII,  $\Omega_k > 0$  since the curvature scalar  $R < 0$ , while  $R$  can be positive in type IX. Using that  $R = e^{-4v\beta^{\lambda}}\bar{R}$  and that  $\bar{R}$  is a function of  $\beta^{\pm}$ , as given in (153a) in Appendix A, shows that  $\bar{R}$  has a negative minimum when  $\beta^{\pm} = 0$ . Adding a constant so that the minimum becomes zero, corresponds to adding  $\Delta$  to  $\Omega_k$ , where  $\Omega_k + \Delta = 0$  when  $N_1 = N_2 = N_3$ , which corresponds to  $\beta^{\pm} = 0$ . Thus  $\Omega_k + \Delta \geq 0$ .

$N_\alpha$  must decay to 0, for all  $v \in (0, 1)$ . Thus the  $\omega$ -limit set of all Bianchi type IX orbits resides in the union of the closure of the type  $\text{VII}_0$  subsets, whereas the  $\omega$ -limit set of all type VIII orbits lies in closure of the union of the single type  $\text{VII}_0$  subset and the two type  $\text{VI}_0$  subsets.<sup>17</sup>

Next we turn to some dynamical conjectures for Bianchi type VIII and IX. We expect that the above features will be important ingredients in future proofs of these conjectures, both in the  $\lambda$ - $R$  case and for more general HL models.

## 7 Dynamical conjectures

Apart from the previous section, the main part of the paper has focussed on the discrete dynamics of the Kasner circle map  $\mathcal{K}$ , associated with the heteroclinic chains obtained by concatenation of Bianchi type II heteroclinic orbits in the  $\lambda$ - $R$  Bianchi type VIII and IX models with  $v \in (0, 1)$ . In particular, we have shown that the critical case to which GR belongs,  $v = 1/2$ , represents a bifurcation, where non-generic chaos on a Cantor set for the supercritical case,  $v \in (1/2, 1)$ , is replaced by generic chaos for the critical and subcritical cases,  $v \in (0, 1/2]$ .

It remains to connect the discrete dynamics of  $\mathcal{K}$  with asymptotic continuous dynamics in Bianchi type VIII and IX, described by the dynamical system (4). We therefore conclude with some dynamical conjectures, which reflect an expected hierarchy of difficulty as regards possible proofs. The conjectures can be divided into two classes: (i) if and how many type VIII and IX solutions have an infinite heteroclinic chain on the Bianchi type I and II boundary as their  $\omega$ -limit set, (ii) if generic solutions of type VIII and IX asymptotically approach the type I boundary or the union of the type I and II boundary sets, and how this depends on the parameter  $v$ .

**Conjecture 7.1.** *In the Bianchi type VIII and IX supercritical case,  $v \in (1/2, 1)$ , each heteroclinic cycle with period 2 has a stable invariant set (as  $\tau_- \rightarrow \infty$ ) of co-dimension one.*

It should be possible to prove this conjecture with, e.g., the methods used in [51, 52, 10], but the situation for the period 2 cycle is arguably more special than the problems in the aforementioned references, and other types of proofs might therefore be possible. Conjecture 7.1 can be regarded as a first step toward the next more ambitious one.

**Conjecture 7.2.** *In the Bianchi type VIII and IX supercritical case,  $v \in (1/2, 1)$ , each infinite heteroclinic chain associated with the Cantor set  $C$  has a stable invariant set (as  $\tau_- \rightarrow \infty$ ) of co-dimension one.*

---

<sup>17</sup>All initially expanding vacuum  $\lambda$ - $R$  Bianchi type I–VIII models are forever expanding, due to that the spatial curvature of these models satisfies  $R \leq 0$ . However, all initially expanding type IX solutions reach a point of maximum expansion and then recollapse. This has been proven in [31] for GR, and a similar proof can be given for the  $\lambda$ - $R$  models. We thereby assume that initial data in type IX correspond to initially expanding solutions, where we are interested in the initial singularity when  $\tau_- \rightarrow \infty$ .

Loosely speaking, the heteroclinic chains with period 2 form the ‘boundary’ of the infinite heteroclinic chains associated with the Cantor set  $C$ . It thus seems natural to establish if the period 2 chain has an attracting set of co-dimension one before addressing Conjecture 7.2.

Incidentally, the special role of  $C$  illustrates that it may not be sufficient to establish the existence of a stable set for the full global understanding of asymptotics of a given model, such as the models with dimension 11 or higher in [19]. Models with a stable set may thereby be more complicated than one expects, and in quite interesting ways.

**Conjecture 7.3.** *In the Bianchi type VIII and IX subcritical case,  $v \in (0, 1/2)$ , each infinite heteroclinic chain associated with the set  $\tilde{C} \subset K^\circ$  in (85) has a stable invariant set (as  $\tau_- \rightarrow \infty$ ) of co-dimension one.*

Note that the physically equivalent heteroclinic chains/cycles with period 3 in Figure 7 are examples of infinite heteroclinic chains associated with the Cantor set  $C$  when  $v \in (1/2, 1)$  and  $\tilde{C}$  when  $v \in (0, 1/2)$ . Instead of attempting to prove the two previous conjectures, one could instead try to more modestly prove that the heteroclinic chains with period 3 have  $\omega$ -limit sets of a co-dimension one in type VIII and IX, e.g., by using the methods for the critical GR case in [51, 52]. To address the more general issues in the two following conjectures, presumably requires more general methods, see [10, 14, 22].

**Conjecture 7.4.** *In the Bianchi type VIII and IX supercritical case,  $v \in (1/2, 1)$ , the stable set  $S$  on  $K^\circ$  is the attractor  $\mathcal{A}_-$  (as  $\tau_- \rightarrow \infty$ ).*

There are subtleties in how to define an attractor, as discussed in [64]. In the present context we are interested in the behaviour of most orbits in the state space, and thus we deal with an attractor that attracts generic sets of orbits in the state space. This set is called the *likely limit set* in [64], which is the unique maximal attractor. The Kasner circle consists of six physically equivalent subsets, related by axis permutations (7), which thereby are the six elements in the unique equivalence class of the quotient of the attractor  $\mathcal{A}_-$  under the action of the dihedral group  $D_3$  according to (7). Combining this feature with the above conjecture suggests that we refer to the quotient space  $\mathcal{A}_-/D_3$  as the *physical attractor*.

It is clear from the local analysis of  $K^\circ$  that  $S$  attracts all nearby orbits. To prove Conjecture 7.4 requires establishing that all generic sets of solutions only have points on  $S$  as their  $\omega$ -limit. Even though we expect that there is a set of solutions that has the heteroclinic chains associated with the Cantor set  $C$  as their  $\omega$ -limits, and thereby not  $S$ , we believe that this set is non-generic, as suggested by Conjecture 7.2.

**Conjecture 7.5.** *In the Bianchi type VIII and IX subcritical and critical cases,  $v \in (0, 1/2]$ , the attractor  $\mathcal{A}_-$  (as  $\tau_- \rightarrow \infty$ ) consists of the set  $\text{II}_1 \cup \text{II}_2 \cup \text{II}_3 \cup K^\circ$ .*

Conjecture 7.5 is supported by the heuristic moving wall arguments in Appendix A, in combination with the result that  $\lim_{\tau_- \rightarrow \infty} \Delta = 0$  in equation (104), which shows that the  $\omega$ -limits of the type IX (VIII) solutions reside on the union of the type VII<sub>0</sub> (VII<sub>0</sub> and VI<sub>0</sub>), type II and type I boundary sets. Moreover, the heuristic analysis in Appendix A

suggests that the type VII<sub>0</sub> and VI<sub>0</sub> cross terms  $N_1N_2$ ,  $N_2N_3$ ,  $N_3N_1$  tend to zero in the subcritical and critical type IX and VIII models when  $\tau_- \rightarrow \infty$  in some generic sense, where a new definition of genericity is required, involving statistical measures and taking into account the evolutionary history of solutions; for further details, see Appendix A<sup>18</sup>. It is worth noticing that the situation is somewhat reminiscent of that in Bianchi type VI<sub>-1/9</sub> and when using an Iwasawa frame in GR, see [89, 90, 37] and references therein.

Presumably, the most difficult conjecture to prove of the above conjectures is Conjecture 7.5 for the subcritical case, especially when  $v$  becomes increasingly small (if true; when  $v = 0$  the unstable region for each of the cross terms is half of  $K^\circlearrowright$ , and thus the considerations in Appendix A concerning this bifurcation value should come as no surprise). Nevertheless, can the methods in [79, 31] for the GR Bianchi type IX case be developed and adapted to the  $\lambda$ - $R$  Bianchi type IX subcritical models with  $v \in (0, 1/2)$ ? Note that these methods do not establish the conjecture for type VIII in GR, although see [78] for some limited type VIII results, and also [14, 22]. The difficulties in GR for type VIII presumably also lead to difficulties for the subcritical type VIII case and possibly also for type IX.

All the above conjectures rely on that  $\lim_{\tau_- \rightarrow \infty} (N_1N_2, N_2N_3, N_3N_1) = (0, 0, 0)$ , and the behaviour of the individual terms  $N_1$ ,  $N_2$  and  $N_3$ . Possible proofs using the dynamical systems approach presumably involve the growth and decay of these quantities, which we therefore now take a closer look at. Without loss of generality, we describe the evolution equations using the  $\Sigma_\pm$  variables in (26), which are adapted to the  $\Sigma_1$ -direction. In Appendix A we derive a system of evolution equations, which can be written as follows,

$$\Sigma'_+ = 2(1 - \Sigma^2)(1 + 2v\Sigma_+) - 6N_1(2N_1 - N_2 - N_3), \quad (106a)$$

$$\Sigma'_- = 4v(1 - \Sigma^2)\Sigma_- + 2\sqrt{3}(N_2 - N_3)(N_2 + N_3 - N_1), \quad (106b)$$

$$N'_1 = -4v \left[ \left( \Sigma_+ - \frac{1}{2v} \right)^2 + \Sigma_-^2 - \left( \frac{1}{2v} \right)^2 \right] N_1. \quad (106c)$$

$$N'_2 = -v \left[ \left( \Sigma_+ + \sqrt{3}\Sigma_- + \frac{1}{v} \right)^2 + \left( \sqrt{3}\Sigma_+ - \Sigma_- \right)^2 - \frac{1}{v^2} \right] N_2, \quad (106d)$$

$$N'_3 = -v \left[ \left( \Sigma_+ - \sqrt{3}\Sigma_- + \frac{1}{v} \right)^2 + \left( \sqrt{3}\Sigma_+ + \Sigma_- \right)^2 - \frac{1}{v^2} \right] N_3, \quad (106e)$$

and the constraint

$$1 = \Sigma^2 + \Omega_k, \quad (106f)$$

where

$$\Sigma^2 := \Sigma_+^2 + \Sigma_-^2, \quad (106g)$$

$$\Omega_k := N_1^2 + N_2^2 + N_3^2 - 2N_1N_2 - 2N_2N_3 - 2N_3N_1. \quad (106h)$$

---

<sup>18</sup>The Hamiltonian description in Appendix A gives a better account of this feature than the dynamical systems approach, since the latter represents a projection of the full state space, where the solution history is hidden and only appears explicitly in the decoupled variable  $p_\lambda$ .

It follows that, e.g.,  $N_1$  is monotonically decreasing (increasing) when  $(\Sigma_+, \Sigma_-)$  is outside (inside) the circle

$$\left(\Sigma_+ - \frac{1}{2v}\right)^2 + \Sigma_-^2 = \left(\frac{1}{2v}\right)^2. \quad (107)$$

which has its center at  $(\Sigma_+, \Sigma_-) = (1/2v, 0)$  and a radius  $1/2v$ . It also follows from (106) that the terms  $N_2$  and  $N_3$  decrease (increase) outside (inside) similar circles, obtained by axis permutations, see Figure 17.

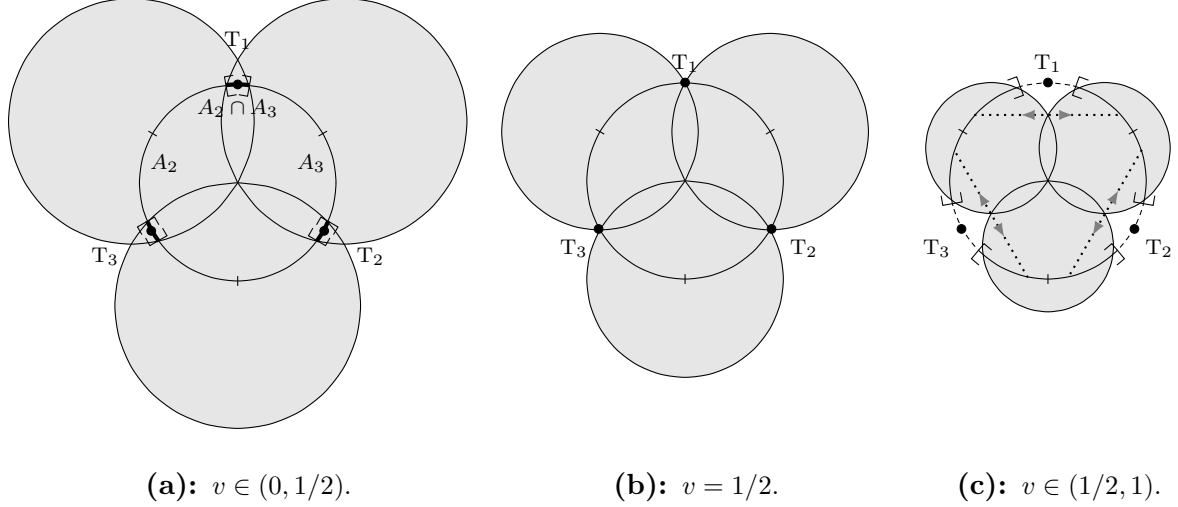


**Figure 17:** The interior of the (light gray) disk opposite to the location of the Taub point  $T_\alpha \in K^\circlearrowleft$  in  $(\Sigma_1, \Sigma_2, \Sigma_3)$ -space indicates growth of each individual  $N_\alpha$ ,  $\alpha = 1, 2, 3$ . Outside their growth region the individual terms decay. As  $v \in (0, 1)$  increases, the disks radii decrease and they move toward the middle, where  $\Sigma^2 = 0$ . For  $v \in (0, 1/2)$  the disks cover the whole region inside  $\Sigma^2 = 1$ . At  $v = 1/2$  the disks only intersect with  $\Sigma^2 = 1$  at the  $\Sigma_\alpha$  values of the Taub points  $T_\alpha$ . For  $v \in (1/2, 1)$  the disks intersect at the  $\Sigma_\alpha$  values of the heteroclinic chains with period two, and there is a neighborhood of the location of the Taub points in  $(\Sigma_1, \Sigma_2, \Sigma_3)$ -space with decay.

Expressing the evolution of the cross terms in the  $\Sigma_\pm$  variables results in the equations

$$(N_1 N_2)' = -8v \left[ \left(\Sigma_+ - \frac{1}{8v}\right)^2 + \left(\Sigma_- + \frac{\sqrt{3}}{8v}\right)^2 - \left(\frac{1}{4v}\right)^2 \right] (N_1 N_2), \quad (108a)$$

$$(N_3 N_1)' = -8v \left[ \left(\Sigma_+ - \frac{1}{8v}\right)^2 + \left(\Sigma_- - \frac{\sqrt{3}}{8v}\right)^2 - \left(\frac{1}{4v}\right)^2 \right] (N_3 N_1), \quad (108b)$$

$$(N_2 N_3)' = -8v \left[ \left(\Sigma_+ + \frac{1}{4v}\right)^2 + \Sigma_-^2 - \left(\frac{1}{4v}\right)^2 \right] (N_2 N_3), \quad (108c)$$

Hence, e.g.,  $N_2 N_3$  is monotonically decreases (increases) when  $(\Sigma_+, \Sigma_-)$  is outside (inside) the following circle

$$\left(\Sigma_+ + \frac{1}{4v}\right)^2 + \Sigma_-^2 = \left(\frac{1}{4v}\right)^2, \quad (109)$$

which has its center at  $(\Sigma_+, \Sigma_-) = (-1/4v, 0)$  and a radius  $1/4v$ . It also follows from (108) that the other cross terms decrease (increase) outside (inside) similar circles, obtained by axis permutations. In particular,  $N_1N_2$  and  $N_3N_1$  decay when  $\Sigma_+ < -1/(8v)$  while  $N_2N_3$  decays when  $\Sigma_+ < -1/(2v)$ . These decay and growth regions are depicted in Figure 18.

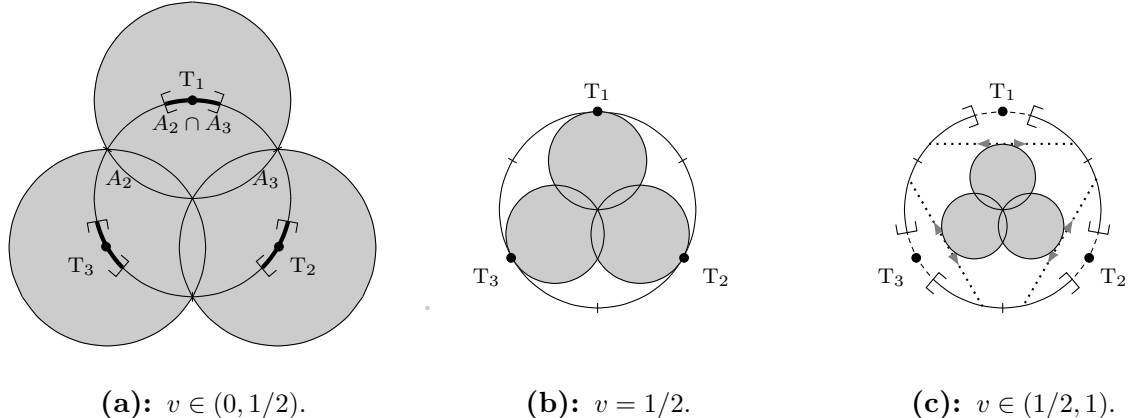


**Figure 18:** The interior of the (dark gray) disk closest to the location of the Taub point  $T_\alpha$  in  $(\Sigma_1, \Sigma_2, \Sigma_3)$ -space indicates growth of the cross term  $N_\beta N_\gamma$ ,  $(\alpha, \beta, \gamma) = (123)$  or a permutation thereof. Outside their growth region the cross terms decay. As  $v \in (0, 1)$  increases, the (gray) disks radii decrease and they move toward the middle, where  $\Sigma^2 = 0$ . For  $v \in (0, 1/2)$ , the disks have parts both outside and inside  $\Sigma^2 = 1$ , and in particular, for  $v = 1/4$ , their boundary circles intersect at the  $\Sigma_\alpha$  location of the  $Q_\alpha$  points. At  $v = 1/2$  the disks only intersect with  $\Sigma^2 = 1$  at the  $\Sigma_\alpha$  values of the Taub points  $T_\alpha$ . For  $v \in (1/2, 1)$  the disks lie inside  $\Sigma^2 = 1$ .

All the above conjectures are about the dynamical system (4), which describes the dynamics of the vacuum  $\lambda$ - $R$  class A models. In Appendix A.2 we show how to derive dynamical systems for the more general HL models, and how the discrete statements about the dynamical system (4) translate to these systems. Moreover, similar heuristic arguments as those in the  $\lambda$ - $R$  case suggest that dynamical conjectures, analogous to those above, can be stated for broad classes of HL models. The results in Appendix A.2 also indicate that if one is not able to obtain proofs for the  $\lambda$ - $R$  case, then one is not likely to be able to prove analogous results for more general HL models. In other words, the  $\lambda$ - $R$  models is a necessary step that needs to be overcome before attempting to tackle more general HL models.

The above rigorous dynamical conjectures implicitly suggest that one uses a dynamical systems formulation of the type discussed in this work. However, there are other possible approaches. In [75] the authors used metric variables as the starting point for their analysis. Arguably the most efficient way to do this is to use a Lagrangian or Hamiltonian approach, as done in Appendix A, and use a time variable defined by setting  $\mathcal{N} = -1$  in this appendix. Alternatively, one can use the billiard (metric configuration space) formulation of Chitré and Misner [17, 65, 66], see p. 812 in [67], and also [18, 37, 20], and attempt to estimate the terms that are heuristically neglected, and which contain the history of the solutions.

## A Hořava-Lifshitz models

In this appendix we derive the evolution equations (4) for the vacuum spatially homogeneous  $\lambda$ - $R$  class A Bianchi models. We also obtain a regular constrained dynamical system for the Hořava-Lifshitz (HL) class A Bianchi models. In addition, we heuristically argue that the heteroclinic structure these models exhibit on the union of the Bianchi type I and II sets describes the relevant asymptotic dynamical structure toward the singularity for the  $\lambda$ - $R$  models and a wide range of more general HL models. This is further supported by the existence of a ‘dominant’ Bianchi type I and II invariant set in the HL dynamical systems formulation which can be identified with the Bianchi type I and II invariant set for the  $\lambda$ - $R$  models. The main part of the paper is therefore also relevant for a broad set of HL models.

Recall that the dynamics of HL gravity is based on the action (3a), where the kinetic part is given by (3b) and the potential by (3c). We consider vacuum spatially homogeneous HL class A Bianchi models, for which the Bianchi type VIII and IX models are the most general ones. These models admit a symmetry-adapted spatial (left-invariant) co-frame  $\{\omega^1, \omega^2, \omega^3\}$ , described in equation (1), which we repeat for the reader’s convenience:

$$d\omega^1 = -n_1 \omega^2 \wedge \omega^3, \quad d\omega^2 = -n_2 \omega^3 \wedge \omega^1, \quad d\omega^3 = -n_3 \omega^1 \wedge \omega^2, \quad (110)$$

where the structure constants  $n_1, n_2, n_3$  determine the Lie algebras of the three-dimensional simply transitive symmetry groups, which describe the class A Bianchi models, see e.g. [95], and Table 1.

Expressing the components of the spatial metric in the symmetry adapted spatial co-frame (110) leads to that they become purely time-dependent. Since the GR and HL class A Bianchi models share the same spatial symmetry adapted frame, they also have the same automorphism groups. In the present context, automorphisms are linear transformations of the spatial left-invariant frame that leave the structure constants of the Bianchi symmetry groups unchanged. Since the automorphisms are what is left of the symmetry generating spatial diffeomorphisms, it should come as no surprise that there is a close connection between them and the momentum/Codazzi vacuum constraints, which are the same for all GR and HL models, see e.g. [38]. In particular, the momentum/Codazzi constraints can be set to zero by means of the class A off-diagonal automorphisms, which at the same time can be used to diagonalize the spatially homogeneous spatial metric, see [95, 43, 62] and references therein.<sup>19</sup> We will use the symmetry adapted co-frame with diagonal class A metrics throughout, and we also set the shift vector  $N_i$  in (2) to zero. The only remaining constraint is the Hamiltonian/Gauss constraint.

The diagonalized vacuum spatially homogeneous class A metrics are given by

$$\mathbf{g} = -N^2(t) dt \otimes dt + g_{11}(t) \omega^1 \otimes \omega^1 + g_{22}(t) \omega^2 \otimes \omega^2 + g_{33}(t) \omega^3 \otimes \omega^3, \quad (111)$$

where the lapse  $N = N(t)$  is a non-zero function determining the particular choice of time variable. Due to the diagonal time-dependent spatial metric (111), the extrinsic

---

<sup>19</sup>Diagonalization and the role of the automorphism group also depends on the spatial topology, an issue which we neglect. For an investigation about the role of spatial topology in a Hamiltonian description of Bianchi models, see [5].

curvature is also diagonal, given by  $(K_{11}, K_{22}, K_{33}) = (\dot{g}_{11}, \dot{g}_{22}, \dot{g}_{33})/(2N)$ , where  $\cdot$  denotes a derivative with respect to  $t$ . Alternatively, raising one of the indices, it takes the form

$$(K_1^1, K_2^2, K_3^3) = \frac{1}{2N} \left( \frac{\dot{g}_{11}}{g_{11}}, \frac{\dot{g}_{22}}{g_{22}}, \frac{\dot{g}_{33}}{g_{33}} \right). \quad (112)$$

For the HL class A Bianchi models, the action (3a) expressed in terms of the symmetry adapted co-frame (1) yields the field equations for the associated metric (111). In order to simplify this action as much as possible and thereby obtain simple Hamiltonian equations, we focus on the kinetic part  $\mathcal{T}$  in equation (3b), which can be written as

$$\mathcal{T} = (K_1^1)^2 + (K_2^2)^2 + (K_3^3)^2 - \lambda(K_1^1 + K_2^2 + K_3^3)^2. \quad (113)$$

It follows that  $\mathcal{T}$  is a quadratic form in the time derivatives of the metric. To simplify  $\mathcal{T}$ , we make a variable transformation from the metric components to the variables  $\beta^0, \beta^+, \beta^-$ , first introduced by Misner [65, 66, 67],

$$g_{11} = e^{2(\beta^0 - 2\beta^+)}, \quad (114a)$$

$$g_{22} = e^{2(\beta^0 + \beta^+ + \sqrt{3}\beta^-)}, \quad (114b)$$

$$g_{33} = e^{2(\beta^0 + \beta^+ - \sqrt{3}\beta^-)}. \quad (114c)$$

This results in that  $\mathcal{T}$  in equation (113) takes the form

$$\mathcal{T} = \frac{6}{N^2} \left[ -\left( \frac{3\lambda - 1}{2} \right) (\dot{\beta}^0)^2 + (\dot{\beta}^+)^2 + (\dot{\beta}^-)^2 \right]. \quad (115)$$

Note that the character of the quadratic form (115) changes when  $\lambda = 1/3$ . Since we are interested in continuously deforming the GR case  $\lambda = 1$ , we restrict considerations to  $\lambda > 1/3$ . To simplify the kinetic part further, we introduce a new variable  $\beta^\lambda$  and a density-normalized lapse function  $\mathcal{N}$ , defined by

$$\beta^\lambda := \sqrt{\frac{3\lambda - 1}{2}} \beta^0, \quad (116a)$$

$$\mathcal{N} := \frac{N}{12\sqrt{g}}, \quad (116b)$$

where  $g = g_{11}g_{22}g_{33} = \exp(6\beta^0)$  is the determinant of the spatial metric in the symmetry adapted co-frame, which leads to,

$$\sqrt{g}N\mathcal{T} = \frac{1}{2\mathcal{N}} \left[ -(\dot{\beta}^\lambda)^2 + (\dot{\beta}^+)^2 + (\dot{\beta}^-)^2 \right]. \quad (117)$$

It is convenient to define

$$T := \frac{\sqrt{g}N}{\mathcal{N}} \mathcal{T} = 12g\mathcal{T}, \quad (118)$$

so that  $\mathcal{N}T$  is the kinetic part of the Lagrangian for the present spatially homogeneous models, in analogy with the GR case, see e.g., ch. 10 in [95]. The density-normalized lapse

$\mathcal{N}$  is kept in the kinetic term  $\mathcal{N}T$ , since it is needed in order to obtain the Hamiltonian constraint, which is accomplished by varying  $\mathcal{N}$  in the Hamiltonian.

To proceed to a Hamiltonian description, we introduce the canonical momenta

$$p_\lambda := -\frac{\dot{\beta}^\lambda}{\mathcal{N}}, \quad p_\pm := \frac{\dot{\beta}^\pm}{\mathcal{N}}. \quad (119)$$

This leads to that  $T$  takes the form

$$T = \frac{1}{2} (-p_\lambda^2 + p_+^2 + p_-^2). \quad (120)$$

Similarly to the treatment of the kinetic part, we define

$$V := \sqrt{g}N\mathcal{V}/\mathcal{N} = 12g\mathcal{V}. \quad (121)$$

Due to (3c),

$$V = {}^1V + {}^2V + {}^3V + {}^4V + {}^5V + {}^6V + \dots, \quad (122)$$

where

$${}^1V := 12k_1gR, \quad {}^2V := 12k_2gR^2, \quad {}^3V := 12k_3gR_j^iR_i^j, \quad (123a)$$

$${}^4V := 12k_4gR_j^iC_i^j, \quad {}^5V := 12k_5gC_j^iC_i^j, \quad {}^6V := 12k_6gR^3. \quad (123b)$$

The superscripts on  ${}^AV$  (where  $A = 1, \dots, 6$ ) thereby coincide with the subscripts of the constants  $k_A$  in (3c).

Based on (3a), this leads to a Hamiltonian  $H$  given by

$$H := \sqrt{g}N(\mathcal{T} + \mathcal{V}) = \mathcal{N}(T + V) = 0, \quad (124)$$

where  $T$  only depends on the canonical momenta  $p_\lambda, p_\pm$ , given by (120), and  $V$  only depends on  $\beta^\lambda, \beta^\pm$ , given by (122) and (123).

In order to derive the ordinary differential equations for these models via the Hamiltonian equations in terms of the variables  $\beta^\lambda, \beta^\pm$  and the canonical momenta  $p_\lambda, p_\pm$ , we need to compute each  ${}^AV(\beta^\lambda, \beta^\pm)$ . We proceed with two cases: one which minimally modifies vacuum GR in the present context, the vacuum  $\lambda$ - $R$  models in Section A.1; one which more generally modifies GR, the HL models in Section A.2. Both cases have a Hamiltonian with the same kinetic part, given in (120), but they have different potentials in (122) and (123). The vacuum  $\lambda$ - $R$  models are obtained by setting  $k_1 = -1, k_2 = k_3 = k_4 = k_5 = k_6 = 0$  in (123) and thus (122) yields  $V = {}^1V = -12gR$ , i.e., the same potential as in GR. The more general vacuum HL models are determined by the potentials  ${}^AV$  with  $A = 1, \dots, 6$ , and combinations thereof.

## A.1 $\lambda$ - $R$ Class A models

The vacuum  $\lambda$ - $R$  models minimally modify the vacuum GR models [28, 11, 58]. They are obtained from an action that consists of the generalized kinetic part in (3b), i.e., by keeping  $\lambda$  (GR is obtained by setting  $\lambda = 1$ ), and the vacuum GR potential in (3c), i.e., a potential arising from  $-R$  only, and hence when  $k_1 = -1$  and  $k_2 = k_3 = k_4 = k_5 = k_6 = 0$  in (3c). These models suffice for our goal of illustrating the role of first principles and their connection with the structure of generic spacelike singularities.

## Derivation of the $\lambda$ - $R$ evolution equations

To obtain succinct expressions for the spatial curvature, and thereby the potential  $V = {}^1V = -12gR$ , we introduce the following auxiliary quantities (see [32] for a discussion when one, or several, of the constants  $n_1, n_2, n_3$  is zero),

$$m_1 := n_1 g_{11} = n_1 e^{2(2v\beta^\lambda - 2\beta^+)}, \quad (125a)$$

$$m_2 := n_2 g_{22} = n_2 e^{2(2v\beta^\lambda + \beta^+ + \sqrt{3}\beta^-)}, \quad (125b)$$

$$m_3 := n_3 g_{33} = n_3 e^{2(2v\beta^\lambda + \beta^+ - \sqrt{3}\beta^-)}. \quad (125c)$$

Here we have introduced the parameter  $v$ , which is defined by the relation

$$v := \frac{1}{\sqrt{2(3\lambda - 1)}}, \quad (126)$$

and hence  $\beta^0 = 2v\beta^\lambda$  due to (116). The parameter  $v$  plays a prominent role in this and the next Appendix, and in the evolution equations (4). Since we are interested in continuous deformations of GR with  $\lambda = 1$ , and thus  $v = 1/2$ , we restrict attention to  $v \in (0, 1)$ , although  $v = 0$  and  $v = 1$ , which result in bifurcations, will sometimes also be considered. Specializing the general expression for the spatial curvature in [23] to the diagonal class A Bianchi models leads to<sup>20</sup>

$$R_1^1 = \frac{1}{2g}(m_1^2 - (m_2 - m_3)^2), \quad (127)$$

where  $R_1^1 = g^{11}R_{11} = g_{11}^{-1}R_{11}$ , and similarly by permutations for  $R_2^2$  and  $R_3^3$ . It follows that the spatial scalar curvature  $R = R_1^1 + R_2^2 + R_3^3$  is given by

$$R = -\frac{1}{2g}(m_1^2 + m_2^2 + m_3^2 - 2m_1m_2 - 2m_2m_3 - 2m_3m_1). \quad (128)$$

This thereby yields the potential in (122) and (123) with  $k_1 = -1$ :

$$V = {}^1V = -12gR = 6(m_1^2 + m_2^2 + m_3^2 - 2m_1m_2 - 2m_2m_3 - 2m_3m_1), \quad (129)$$

where  $V$  depends on  $\beta^\lambda$  and  $\beta^\pm$  via  $m_1, m_2$  and  $m_3$ , according to equation (125).

The evolution equations for  $\beta^\lambda, \beta^\pm, p_\lambda, p_\pm$  are obtained from Hamilton's equations, where  $T$  and  $V$  in the Hamiltonian (124) are given by (120) and (129), respectively, which yields

$$\dot{\beta}^\lambda = \frac{\partial H}{\partial p_\lambda} = -\mathcal{N}p_\lambda, \quad \dot{p}_\lambda = -\frac{\partial H}{\partial \beta^\lambda} = -\mathcal{N}\frac{\partial V}{\partial \beta^\lambda}, \quad (130a)$$

$$\dot{\beta}^\pm = \frac{\partial H}{\partial p_\pm} = \mathcal{N}p_\pm, \quad \dot{p}_\pm = -\frac{\partial H}{\partial \beta^\pm} = -\mathcal{N}\frac{\partial V}{\partial \beta^\pm}, \quad (130b)$$

---

<sup>20</sup>Note that the expressions for the extrinsic and the spatial curvature with one upper and one lower index coincide when using either the presently introduced spatial co-frame or an associated orthonormal frame for the diagonal class A models, as in [23].

while the Hamiltonian constraint  $T + V = 0$  is obtained by varying  $\mathcal{N}$ .

Next, we choose a new time variable  $\tau_- := -\beta^\lambda$ , which is directed toward the physical past, since we are considering expanding models. This is accomplished by setting  $\mathcal{N} = p_\lambda^{-1}$  in the first equation in (130a), and thereby  $N = 12\sqrt{g}/p_\lambda$ , which results in the following evolution equations:

$$\frac{d\beta^\lambda}{d\tau_-} = -1, \quad \frac{dp_\lambda}{d\tau_-} = -\frac{1}{p_\lambda} \frac{\partial V}{\partial \beta^\lambda}, \quad (131a)$$

$$\frac{d\beta^\pm}{d\tau_-} = \frac{p_\pm}{p_\lambda}, \quad \frac{dp_\pm}{d\tau_-} = -\frac{1}{p_\lambda} \frac{\partial V}{\partial \beta^\pm}. \quad (131b)$$

We then rewrite the system (131) and the constraint  $T + V = 0$  using the non-canonical variable transformation,

$$\Sigma_\pm := -\frac{p_\pm}{p_\lambda}, \quad N_\alpha := -2\sqrt{3} \left( \frac{m_\alpha}{p_\lambda} \right), \quad (132)$$

while keeping  $p_\lambda$ . Note that  $\Sigma_\pm = d\beta^\pm/d\beta^\lambda = -d\beta^\pm/d\tau_-$ .

These variables lead to a decoupling<sup>21</sup> of the evolution equation for the variable  $p_\lambda$ ,

$$p'_\lambda = -4v(1 - \Sigma^2)p_\lambda, \quad (133)$$

where ' denotes the derivative  $d/d\tau_-$ . This yields the following reduced system of evolution equations

$$\Sigma'_\pm = 4v(1 - \Sigma^2)\Sigma_\pm + \mathcal{S}_\pm, \quad (134a)$$

$$N'_1 = -2(2v\Sigma^2 - 2\Sigma_+)N_1, \quad (134b)$$

$$N'_2 = -2(2v\Sigma^2 + \Sigma_+ + \sqrt{3}\Sigma_-)N_2, \quad (134c)$$

$$N'_3 = -2(2v\Sigma^2 + \Sigma_+ - \sqrt{3}\Sigma_-)N_3, \quad (134d)$$

while the Hamiltonian constraint  $T + V = 0$  results in

$$1 - \Sigma^2 - \Omega_k = 0, \quad (134e)$$

where

$$\Sigma^2 := \Sigma_+^2 + \Sigma_-^2, \quad (135a)$$

$$\Omega_k := N_1^2 + N_2^2 + N_3^2 - 2N_1N_2 - 2N_2N_3 - 2N_3N_1, \quad (135b)$$

$$\mathcal{S}_+ := 2[(N_2 - N_3)^2 - N_1(2N_1 - N_2 - N_3)], \quad (135c)$$

$$\mathcal{S}_- := 2\sqrt{3}(N_2 - N_3)(N_2 + N_3 - N_1). \quad (135d)$$

Note that the variables  $\Sigma_\pm$ ,  $N_1$ ,  $N_2$  and  $N_3$ , defined in (132), are *dimensionless*. Dimensions can be introduced in various ways, but terms in a sum must all have the same

---

<sup>21</sup>More precisely, the variables result in a skew-product dynamical system where the base dynamics acts in  $(\Sigma_\pm, N_1, N_2, N_3)$  while the fiber dynamics acts in  $p_\lambda$ . This notion was introduced in connection with ergodic theory in [3].

dimension. The constraint (134e) is such a sum. Since this sum contains 1, which obviously is dimensionless, it follows that  $\Sigma_+$ ,  $\Sigma_-$ ,  $N_1$ ,  $N_2$  and  $N_3$  are dimensionless, and so is the time variable  $\tau_-$ , as follows from inspection of (134).

The introduction of the Misner parametrization and the associated  $\Sigma_\pm$  variables breaks an axis permutation symmetry, which can be restored by introducing the variables

$$\Sigma_1 := -2\Sigma_+, \quad \Sigma_2 := \Sigma_+ + \sqrt{3}\Sigma_-, \quad \Sigma_3 := \Sigma_+ - \sqrt{3}\Sigma_-. \quad (136)$$

By multiplying the equation for  $\Sigma_+$  with  $-2$  and setting  $\mathcal{S}_1 = -2\mathcal{S}_+$ , we obtain the equation for  $\Sigma_1$ . Replacing (123) with  $(\alpha\beta\gamma)$  then allows us to write the above system of evolution equations (134) as the system (4), which is invariant under the axis permutations in (7). Note that we only need the equation for  $\Sigma_+$  and not the one for  $\Sigma_-$  to obtain the system (4), a strategy we will use for the HL models. The vacuum equations for GR are obtained by setting  $v = 1/2$ .<sup>22</sup>

### Heuristic $\lambda$ - $R$ considerations

To obtain some motivation for some of the Conjectures in Section 7, we use Misner's heuristic approximation scheme, which he introduced in order to understand the initial Bianchi type IX singularity in GR, see [65, 66, 43] and ch. 10 in [95], and apply it to the class A Bianchi  $\lambda$ - $R$  models. In this scheme, a class A Bianchi solution toward the past initial singularity (i.e. when  $\tau_- = -\beta^\lambda \rightarrow \infty$ ) is described as a 'particle' moving in a potential well in  $(\beta^+, \beta^-) \in \mathbb{R}^2$  space.

Let us begin with the  $\lambda$ - $R$  Bianchi type I models for which  $n_1 = n_2 = n_3 = 0$ , according to Table 1, and thus  $m_1 = m_2 = m_3 = 0$  in equation (125). Hence the spatial curvature (128) is identically zero, and so is the potential (129), which implies that the kinetic part (120) in the Hamiltonian (124) determines the dynamics. It therefore follows that any type I solution can be described as a 'cosmological particle' that is moving with the *constant* velocity

$$\vec{V} = (V_+, V_-) = \left( \frac{d\beta^+}{d\tau_-}, \frac{d\beta^-}{d\tau_-} \right) = (-\Sigma_+, -\Sigma_-), \quad (137)$$

in  $\beta^\pm$ -space, due to (131) and (132). Note that  $\vec{V}$ ,  $V_\pm$  should not be confused with the potential  $V$ . Since the Hamiltonian/Gauss constraint in Bianchi type I reduces to  $T = 0$ , it follows that  $\Sigma_+^2 + \Sigma_-^2 = 1$ , and hence that the speed  $|\vec{V}|$  of the 'cosmological particle' is  $|\vec{V}| = 1$ . Thus the fixed points in the Kasner circle set  $K^\circ$  are interpreted in this picture as a particle with a constant velocity  $\vec{V} = (-\Sigma_+, -\Sigma_-)$  and speed  $|\vec{V}| = 1$  in  $\beta^\pm$ -space.

The  $\lambda$ - $R$  Bianchi type II<sub>1</sub> models are characterized by  $n_1 \neq 0, n_2 = n_3 = 0$ , see Table 1, and thus  $m_1 \neq 0, m_2 = m_3 = 0$ , as follows from (125). Similar statements hold for II<sub>2</sub> and II<sub>3</sub>. The evolution of the II<sub>1</sub> models is determined by

$$T + V = \frac{1}{2} (-p_\lambda^2 + p_+^2 + p_-^2) + 6m_1^2 = 0, \quad (138)$$

---

<sup>22</sup>For a similar derivation of the GR case, see ch. 10 in [95], but note that the present variables  $N_\alpha$  differ from those in [95] by a factor  $2\sqrt{3}$ .

where we recall due to (125) that

$$m_1 = n_1 e^{2(2v\beta^\lambda - 2\beta^+)} = n_1 e^{-4(v\tau_- + \beta^+)}, \quad (139)$$

where the time variable is given by  $\tau_- := -\beta^\lambda$ .

The steep exponential potential (139) is approximated by setting it to be identically zero when the exponential in  $6m_1^2$  is sufficiently small, and replacing it with an *infinite potential wall* when the smallness condition is violated. For a chosen sufficiently small constant  $C \ll 1$ , the potential attains this small value  $C = 6n_1^2 e^{-8(v\tau_- + \beta_0^+)}$  for some  $\beta_0^+ \in \mathbb{R}$ , which determines its location in  $\beta^+ \in \mathbb{R}$  as a function of the constants  $n_1, v, C$  and the time  $\tau_-$ , given by  $\beta_0^+ := \log(6n_1^2/C)^{1/8} - v\tau_-$ . The steep potential (139) is thereby approximated by a potential that is set to zero when  $\beta^+ > \beta_0^+$ , since then  $6n_1^2 e^{-8(v\tau_- + \beta^+)} < C$ , and an infinite potential wall at  $\beta^+ = \beta_0^+$ . As  $\tau_-$  increases toward the singularity, the location of the wall at  $\beta_0^+$  moves in the negative  $\beta^+$ -direction according to  $\beta_0^+ := \log(6n_1^2/C)^{1/8} - v\tau_-$ , with a velocity

$$\vec{v}_1 = (v_+, v_-) = \left( \frac{d\beta_0^+}{d\tau_-}, \frac{d\beta_0^-}{d\tau_-} \right) = (-v, 0), \quad (140)$$

and thus the wall has a speed  $|\vec{v}_1| = v$  in the negative  $\beta^+$ -direction. If  $V_+ < v_+ = -v < 0$  (and hence  $|V_+| > v > 0$ ), then the cosmological particle eventually reaches and bounces against the infinite potential wall given by the Bianchi type  $\text{II}_1$  potential  $6m_1^2$ , see Figure 19. This occurs if  $-\Sigma_+ < -v$ , which corresponds to  $\Sigma_1 < -2v$  in the coordinates (136). This coincides with the instability criterion on  $K^\circlearrowleft$  in the  $\Sigma_1$ -direction, which defines the unstable arc  $\text{int}(A_1)$  in equation (12).

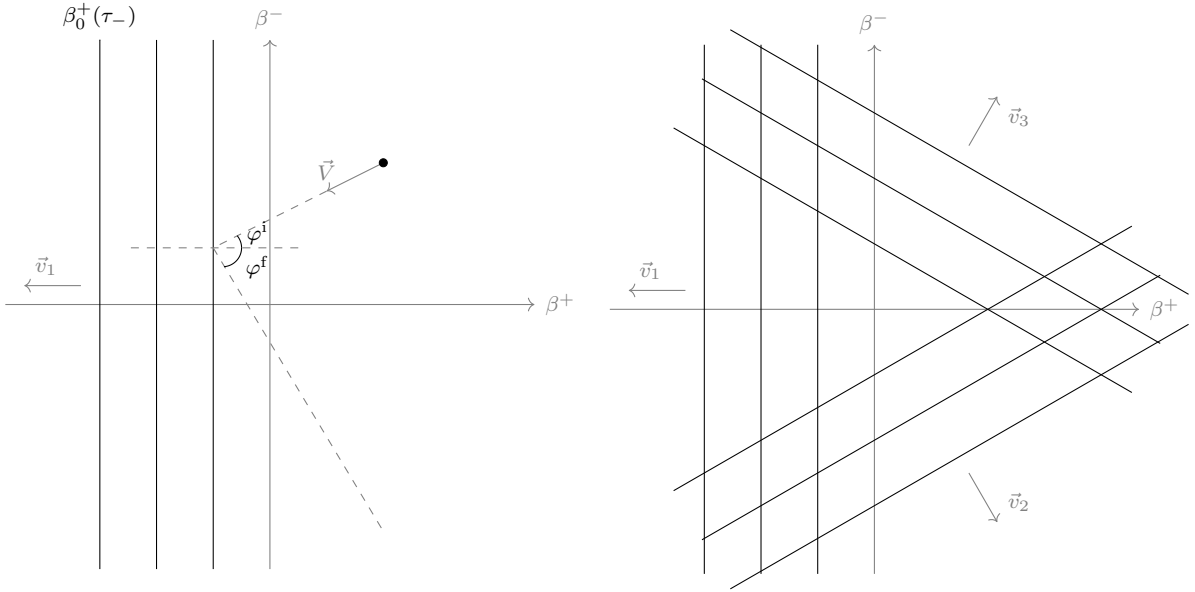
Similarly, one can construct the infinite potential walls for the Bianchi type  $\text{II}_2$  and  $\text{II}_3$  models, and obtain analogous results by adapting the  $\beta^\pm$  variables to those directions. Such walls, with respective potentials given by  $6m_2^2$  and  $6m_3^2$ , have the following velocities in the present  $\beta^\pm$  coordinates:

$$\vec{v}_2 = \frac{1}{2}(1, \sqrt{3})v, \quad \vec{v}_3 = \frac{1}{2}(1, -\sqrt{3})v. \quad (141)$$

The general picture is therefore that a cosmological particle moves in a Bianchi type I potential  $V = 0$ , with velocity  $\vec{V} = (-\Sigma_+, -\Sigma_-)$ , until it encounters a Bianchi type II moving wall and bounces, thereby obtaining new values of  $\Sigma_\pm$ , determined by the Kasner circle map, see Figure 19. As follows from (27b), a bounce against the  $\text{II}_1$  wall corresponds to

$$\sin \varphi^f = \frac{(1 - v^2) \sin \varphi^i}{1 + v^2 - 2v \cos \varphi^i}, \quad (142)$$

where  $\varphi^i$  is the angle the straight line motion of the particle makes with the  $\beta^+$ -axis, while  $\varphi^f$  describes the outgoing motion after the bounce, which is given by the subsequent Kasner solution. The bounce law (142) can also be obtained in the present description by making boost in the  $\beta^+$ -direction in  $(\beta^\lambda, \beta^\pm)$ -space so that the potential wall does not move and using that the ingoing and outgoing bounce angles then are equal. We will perform such a boost in the next appendix. Finally, note that (142) reduces to the GR case when  $v = 1/2$ , e.g. given in ch. 10 in [95].



**(a):** Incoming ‘particle’ with velocity  $\vec{V}$  and moving potential  $\text{II}_1$  walls. **(b):** Moving potential  $\text{II}_1$ ,  $\text{II}_2$  and  $\text{II}_3$  walls with respective velocities  $\vec{v}_1$ ,  $\vec{v}_2$  and  $\vec{v}_3$ .

**Figure 19:** The cosmological particle with velocity  $\vec{V}$ , determined by the Kasner solutions, and the level sets of the type  $\text{II}_1$  potential described by a moving wall at  $\beta_0^+(\tau_-)$  with velocity  $\vec{v}_1$ , and similarly for  $\text{II}_2$  and  $\text{II}_3$ . The particle reaches the moving wall  $\text{II}_1$  and bounces with the law given by (142) when  $|V_+| > v$ .

Next, consider the Bianchi type VIII and IX models. According to (129), the potential consists of the three combined Bianchi type II potentials given by  $6m_1^2, 6m_2^2, 6m_3^2$ , which together form a *triangular potential well* in  $\beta^\pm$ -space, plus the three ‘cross terms’  $-12m_1m_2, -12m_2m_3, -12m_3m_1$ , which form *cross term walls*. The cross terms are all negative in type IX, while two are positive and one is negative in type VIII. They are given by exponentials, which can be approximated by a region where each individual term can be set to zero and a negative or positive (depending on its sign) infinite potential wall moving in  $\beta^\pm$ -space depending on time  $\tau_-$ . For example, the reasoning that resulted in equation (140) for the type  $\text{II}_1$  potential can be replicated for the cross term  $-12m_2m_3 = -12n_2n_3 \exp[4(-2v\tau_- + \beta^+)]$ . This leads to a wall with a velocity  $\vec{v}_{2,3} = (2v, 0)$ , and thus a speed  $2v$  in the positive  $\beta^+$ -direction. By means of permutation symmetry, similar statements hold for the other cross terms. According to (141), the Bianchi type  $\text{II}_2$  and  $\text{II}_3$  potentials yield walls moving with a component of the velocity given by  $v/2$  in the positive  $\beta^+$ -direction. For sufficiently large  $\tau_-$ , the cross term walls will therefore be ‘hidden’ behind the type II walls, and hence should not affect the asymptotic dynamics, since particles will bounce off the type II walls before reaching the cross term walls. It is therefore expected that only Bianchi type II potentials play a role for the asymptotic limit  $\tau_- \rightarrow \infty$ .

The overall picture is thereby that the asymptotic dynamics is described by free motion of a cosmological particle in  $\beta^\pm$ -space with speed  $|\vec{V}| = 1$  in a Bianchi type I zero potential, followed by bounces against Bianchi type II walls moving with speed  $v$ , if the

particle catches up with the moving walls, which depends on the direction of the cosmological particle and the speed  $v$  of the wall. The Bianchi type II<sub>1</sub>, II<sub>2</sub> and II<sub>3</sub> potentials form a triangular potential well that is increasing in size in  $\beta^\pm$ -space as  $\tau_- \rightarrow \infty$ . The above heuristic picture amounts to the claim that generic solutions of the evolution equations (134) asymptotically follow heteroclinic Bianchi type II chains, or end in the set  $S$  in  $K^\circ$  in the supercritical case  $v > 1/2$ .

There is, however, a subtlety at the corners of the triangular potential well. Take the corner at  $\beta^- = 0$ . In this case, the type II walls described by  $m_2^2 = m_3^2 \propto \exp(4(-2v\tau_- + \beta^+))$  have the same velocity  $2v$  in the  $\beta^+$ -direction, as has the cross term wall given by  $-m_2 m_3$ . Consider therefore a possibly ‘dangerous’ region where the cross term  $-m_2 m_3$  near the corner of the triangular well might affect the asymptotic dynamics. To understand this better, define

$$\bar{V}(\beta^\pm) := e^{-8v\beta^\lambda} V = e^{8v\tau_-} V. \quad (143)$$

Note that the asymptotic dynamics for large times is described by  $\tau_- \rightarrow \infty$ , and consequently for large values of  $\bar{V}(\beta^\pm)$ .

Without loss of generality we set  $n_1 = n_2 = n_3 = 1$  in type IX;  $n_1 = n_2 = 1, n_3 = -1$  in type VIII;  $n_1 = 0, n_2 = n_3 = 1$  in type VII<sub>0</sub>;  $n_1 = 0, n_2 = 1, n_3 = -1$  in type VI<sub>0</sub>;  $n_1 = 1, n_2 = n_3 = 0$  in type II. Due to (129) and (125), this leads to the following potentials

$$\bar{V}_{\text{II}} = 6e^{-8\beta^+}, \quad \text{for type II,} \quad (144a)$$

$$\bar{V}_{\text{VI}_0} = 24e^{4\beta^+} \cosh^2(2\sqrt{3}\beta^-), \quad \text{for type VI}_0, \quad (144b)$$

$$\bar{V}_{\text{VII}_0} = 24e^{4\beta^+} \sinh^2(2\sqrt{3}\beta^-), \quad \text{for type VII}_0, \quad (144c)$$

$$\bar{V}_{\text{VIII}} = 6 \left[ e^{-8\beta^+} - 4e^{-2\beta^+} \sinh(2\sqrt{3}\beta^-) + 4e^{4\beta^+} \cosh^2(2\sqrt{3}\beta^-) \right], \quad \text{for type VIII,} \quad (144d)$$

$$\bar{V}_{\text{IX}} = 6 \left[ e^{-8\beta^+} - 4e^{-2\beta^+} \cosh(2\sqrt{3}\beta^-) + 4e^{4\beta^+} \sinh^2(2\sqrt{3}\beta^-) \right], \quad \text{for type IX,} \quad (144e)$$

with level sets of  $\bar{V}$  depicted in Figures 19, 20 and 21.

Note that a translation in  $\beta^+$  simply rescales the potentials  $\bar{V}_{\text{VI}_0}$  and  $\bar{V}_{\text{VII}_0}$  in (144), and hence all the potential level curves of  $\bar{V}_{\text{VI}_0}$  and  $\bar{V}_{\text{VII}_0}$  have the same shape, see Figure 20. Furthermore,  $\bar{V}_{\text{VI}_0}$  and  $\bar{V}_{\text{VII}_0}$  approach the type II<sub>2</sub> and II<sub>3</sub> potentials exponentially fast as  $|\beta^-|$  increases. Thus  $\bar{V}_{\text{VI}_0}$  and  $\bar{V}_{\text{VII}_0}$  can be approximated by the type II<sub>2</sub> and II<sub>3</sub> potentials when  $|\beta^-| > \epsilon$ , for some  $\epsilon > 0$  sufficiently small. The region  $|\beta^-| < \epsilon$ , denoted by the  $\epsilon$ -corner region, is where the approximating infinite type II wall description breaks down. In particular, it is at this region where the cross-term  $N_2 N_3$  has a significant role in the dynamical system picture.

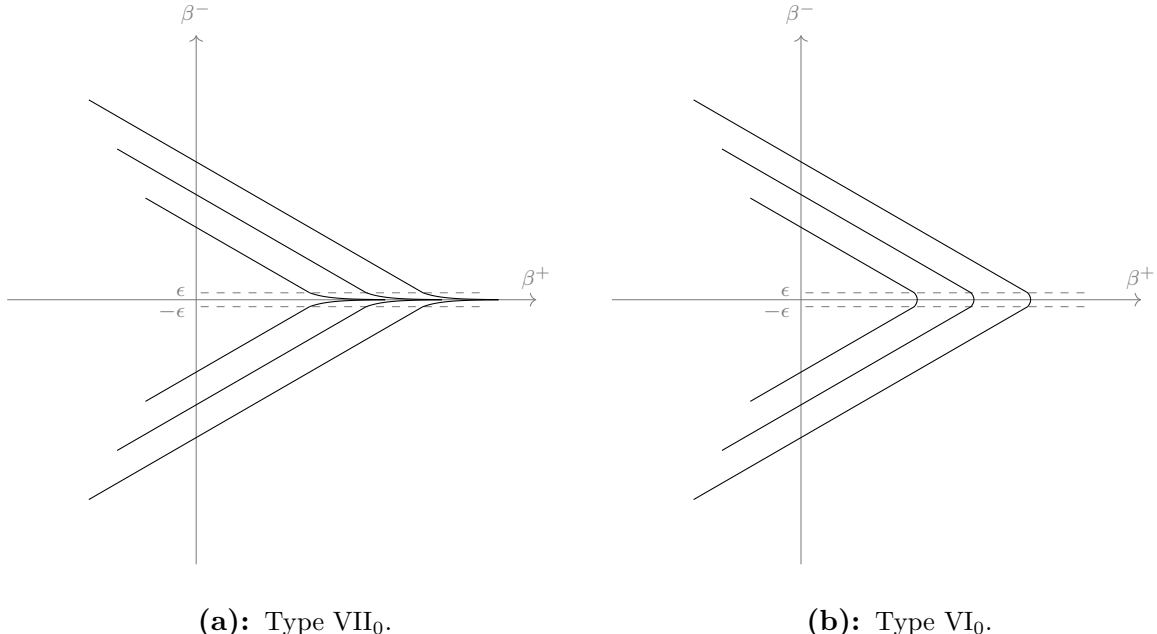


**Figure 20:** Level curves of  $\bar{V}$  in (144) for type VII<sub>0</sub> and VI<sub>0</sub>. Each level curve have the same shape under translation in  $\beta^+$ . Note that the  $\epsilon$ -corner region, where the type II approximation fails, has a fixed size  $2\epsilon$  independently of the level curves of  $\bar{V}$ .

As derived from first principles in Appendix B, in the dynamical systems picture the asymptotics as  $\tau_- \rightarrow \infty$  for solutions of type VIII and IX for all  $v \in (0, 1)$  reside on the union of the disjoint relevant type VI<sub>0</sub> and VII<sub>0</sub> boundary sets, and the union of the type II and I boundary sets. This corresponds to that the level curves of the potentials  $\bar{V}_{\text{VIII}}$  and  $\bar{V}_{\text{IX}}$  increasingly possess the same shape for large values of the potential, and that they are locally described by the relevant type VI<sub>0</sub> and VII<sub>0</sub> potentials. The level curves of the potentials  $\bar{V}_{\text{VIII}}$  and  $\bar{V}_{\text{IX}}$  are thereby asymptotically shape invariant, see Figure 21.

In a similar way as for the individual type II potential, we approximate the type VIII and IX potentials  $V = e^{-8v\tau_-} \bar{V}(\beta^\pm)$  by setting them to be identically zero when  $V < C$  for some chosen small constant  $C \ll 1$  (i.e.,  $\tau_-$  and  $\bar{V}$  are large), and an *infinite potential wall* when  $V = C$ , consisting of the associated three infinite type II potential walls. This results in an equilateral triangular potential well, which yields an increasingly good approximation as  $\tau_-$  increases, except at the  $\epsilon$ -corner regions, which are asymptotically described by type VI<sub>0</sub>, VII<sub>0</sub>, see Figures 19 and 21.

According to the above heuristic approximation scheme, a type VIII or IX solution is described as a free particle moving with unit speed  $|\vec{V}| = 1$  in a triangular potential well with the  $\epsilon$ -corners cut out (i.e., for now, we assume that the particle does not enter the corner regions). Similarly to each single type II wall, the three approximating infinite type II potential walls move with a speed  $|\vec{v}_\alpha| = v$ , where each individual  $\text{II}_\alpha$  walls have velocities  $\vec{v}_1, \vec{v}_2, \vec{v}_3$  in (140) and (141), respectively. If the particle hits an infinite type II wall, it bounces according to that type II wall's bounce law, which is determined by the wall's velocity, given by (142), unless it enters a corner region. In the critical and subcritical cases,  $v \in (0, 1/2]$ , as  $v$  decreases the increasingly slow wall motion implies that

the particle on average bounces against the walls increasingly often. In the subcritical case,  $v \in (0, 1/2)$ , the regions  $A_\alpha \cap A_\beta$  correspond to directions where the particle might hit the corner region between  $\Pi_\alpha$  and  $\Pi_\beta$ . In the supercritical case,  $v \in (1/2, 1)$ , the walls move faster and the particle bounces against walls less often. Note, however, that the particle bounces against the type II walls infinitely if the velocity directions are associated with the Cantor set  $C$ . Otherwise, after a finite number of bounces, the particle acquires a velocity direction so that it does not catch up with any wall, and thereby it enters a final Kasner state described by the final velocity direction.<sup>23</sup>

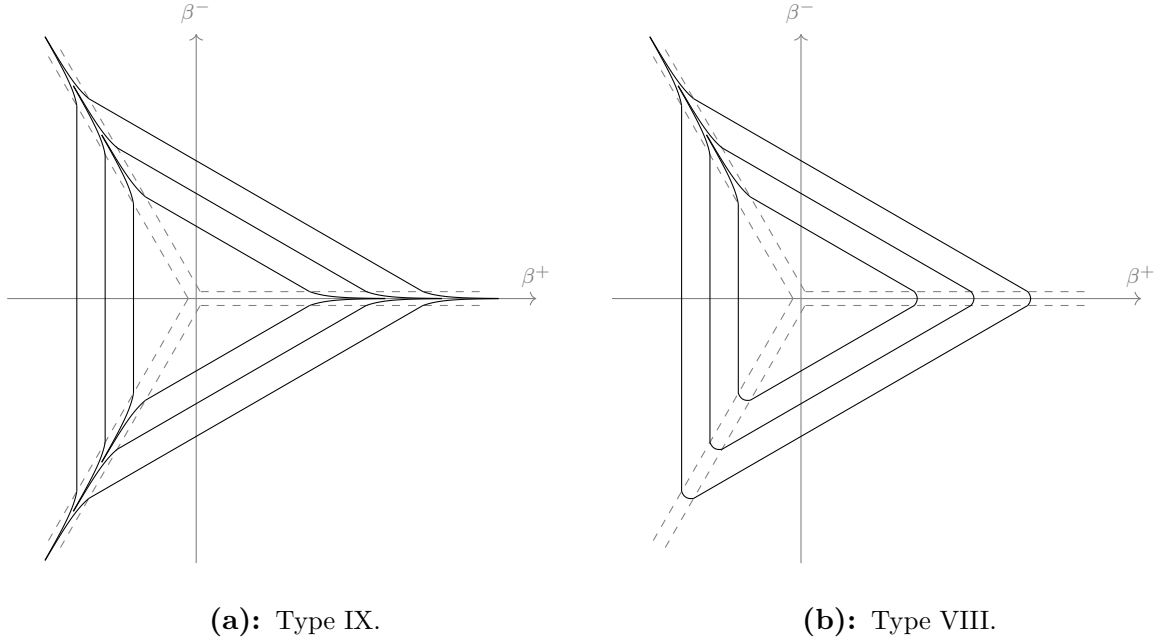


**Figure 21:** Level curves for large  $\bar{V}$  in (144) for Bianchi type IX and VIII. As  $\tau_-$  increases (and thus  $\bar{V}$  becomes larger), each level curve has a larger perimeter, whereas the  $\epsilon$ -corners have fixed size  $2\epsilon$ , which asymptotically becomes negligible compared to the remaining perimeter length given by the type II triangle of length  $3L(\tau_-)$ .

The above heuristic picture assumes that the particle does not enter an  $\epsilon$ -corner region. However, consider a starting point at some  $(\tau_-)_0$  where the length of the equilateral type II triangle is  $3L_0$ , and the  $\epsilon$ -regions have fixed length  $6\epsilon$ . Since the sides of the triangle are moving apart with speed  $v$ , its size  $3L(\tau_-)$  increases as  $\tau_- \rightarrow \infty$ , whereas the  $\epsilon$ -corners have fixed size  $6\epsilon$  independent of  $\tau_-$ , which means that the size of the corner regions becomes asymptotically negligible, i.e.,  $\lim_{\tau_- \rightarrow \infty} (2\epsilon/L(\tau_-)) = 0$ . This suggests that the probability that a generic particle (corresponding to non-locally rotationally symmetric solutions) enters an  $\epsilon$ -corner region tends to zero as  $\tau_- \rightarrow \infty$ , which corresponds to that the ‘cross terms’ asymptotically tend to zero, in some statistically generic sense.

The above suggest that the type II heteroclinic chains describe the asymptotic dynamics in the subcritical and critical cases,  $v \in (0, 1/2]$ , in some statistically generic sense, and

---

<sup>23</sup>This might also happen before the wall description has become a good approximation. This corresponds to that a solution ends at the stable set  $S$  before starting to shadow the type II and I boundaries.

that solutions associated with the Cantor set  $C$  in the supercritical case,  $v \in (1/2, 1)$ , also asymptotically shadow type II heteroclinic chains.

In the above discussion, we have assumed that the potential wall is not affected by the bounce. This is not quite the case, but we will argue that the effect is asymptotically negligible. During the Bianchi type I motion,  $p_\lambda$  and  $p_\pm$  are all constants (for simplicity set  $\mathcal{N}$  to a constant, and then note that  $\beta^\lambda$  and  $\beta^\pm$  are all cyclic variables). Then write the Hamiltonian type II<sub>1</sub> constraint as

$$\Sigma_+^2 + \Sigma_-^2 + \frac{12n_1^2}{p_\lambda^2} e^{-8(v\tau_- + \beta^+)} = 1, \quad (145)$$

where the Bianchi type I regime is determined by a wall  $6n_1^2 e^{-8(v\tau_- + \beta_0^+)} p_\lambda^{-2} = C \ll 1$ , where  $p_\lambda$ , which we previously neglected, is a constant during the Bianchi type I motion of the cosmological particle. However,  $p_\lambda$  changes during a bounce against the wall, where the difference is determined by the relevant Bianchi type II<sub>1</sub> solution, as seen as follows. Equations (19) and (133) result in that  $p_\lambda \propto 1/\eta$ . Since we are considering expanding models,  $p_\lambda$  is negative, see (130a), and it is monotonically decreasing when  $\tau_-$  is increasing, due to (133). Also, since  $p_\lambda \propto 1/\eta$ , then  $\eta^i = 1$  and  $\eta^f = g$  according to Section 2.2. Therefore,

$$\frac{p_\lambda^f - p_\lambda^i}{p_\lambda^i} = \frac{1}{g-1}, \quad (146)$$

due to a Bianchi type II bounce. In other words, the wall moves because of the bounce, apart from its movement during the cosmological particle's Bianchi type I motion. However, we will now argue that this effect is asymptotically negligible for generic solutions.

Equation (133) yields  $p_\lambda \propto \exp(\int [-4v(1 - \Sigma^2)] d\tau_-)$ . In the dynamical systems picture, the above heuristic cosmological particle description corresponds to that solutions to an increasing extent shadow the heteroclinic Bianchi type II orbits. They thereby stay increasingly long times  $\tau_-$  near the Kasner circle  $K^\circ$  where  $1 - \Sigma^2 = 0$ , while the effects on  $p_\lambda$  of a given type II bounce according to (146) are not affected by when a bounce takes place in the evolution of the solution. However, the increasing size of the triangular potential well shows that solutions have a 'memory' of their evolution, which is not locally seen, not in (146) nor in the local eigenvalue analysis of  $K^\circ$ . Due to increasingly accurate shadowing, the time  $\tau_-$  spent by the particle during bounces becomes asymptotically negligible compared to the time spent in Bianchi type I motion. This is due to that the time spent during a bounce is determined by the time it takes the particle to move the extra distance the wall has moved because of the bounce. Since this distance is increasingly small when compared to the size of the increasing triangular well, the (average) time during a bounce when compared to the (average) time between bounces, which is increasing due to the increasing size of the triangular well, becomes asymptotically negligible (this has been illustrated numerically in GR, see, e.g., Figure 11.1 in [95]).

The above heuristic discussion suggests that the following 'dominant'  $\lambda$ - $R$  Hamiltonian captures the asymptotic dynamics of the original Hamiltonian:

$$H_{\text{Dom}} := \mathcal{N} \left( \frac{1}{2} (-p_\lambda^2 + p_+^2 + p_-^2) + V_{\text{Dom}} \right), \quad V_{\text{Dom}} := 6m_1^2 + 6m_2^2 + 6m_3^2. \quad (147)$$

In other words, the potential  $V_{\text{Dom}}$  consists of the three type II potentials, without the cross terms in the original potential  $V$  in (129). Expressing the Hamiltonian equations obtained from  $H_{\text{Dom}}$  in the variables  $(\Sigma_{\pm}, N_1, N_2, N_3)$  and time  $\tau_-$  yields the same evolution equations as for the  $\lambda$ - $R$  models in (134), except that the cross terms  $N_1 N_2$ ,  $N_2 N_3$ , and  $N_3 N_1$  are absent. This system has the same heteroclinic Bianchi type I and II structure as the  $\lambda$ - $R$  models. The above heuristic reasoning suggests that both dynamical systems, associated with (124) and (147), respectively, are asymptotically described by  $K^\circlearrowright$  and the Bianchi type II heteroclinic chains, in a manner that supports the conjectures in Section 7. The same conclusion is obtained from the billiard formulation of Chitré and Misner [17, 65, 66], see p. 812 in [67], and also [18, 37, 20]. Incidentally, it seems plausible that the symbolic dynamics methods used in the main text could be used in this billiard formulation. Also, it would be interesting to see if deforming first principles in some restricted sense in more general models (such as those discussed in [18], e.g., by considering string theory inspired modifications) can lead to bifurcations that are related to those in the present case.

## A.2 Hořava-Lifshitz Class A models

The vacuum spatially homogeneous Hořava-Lifshitz (HL) class A Bianchi models have a Hamiltonian with the same kinetic part as the vacuum  $\lambda$ - $R$  models, but a potential  $V$  in (122) consisting of a sum of the potentials  ${}^A V$  with  $A = 1, \dots, 6$ , where the superscript  ${}^A$  reflects the constants  $k_A$  in (3c), which multiply the spatial curvature expressions in (122) and (123), determined by the spatial Ricci curvature  $R_j^i$  and the Cotton (Cotton-York) tensor  $C_j^i$ .

For the diagonal class A models the only non-zero components of  $R_j^i$  are the diagonal terms  $R_1^1$ ,  $R_2^2$  and  $R_3^3$ , and similarly for  $C_j^i$ . The reason for writing these tensors with one upper and lower index is that the orthonormal frame expressions coincide with those obtained when using the left-invariant frame in (111). This allows us to specialize the general orthonormal frame expressions for the spatial curvature and the Cotton tensor in [23] to the present diagonal class A Bianchi models, where  $R_1^1$  is given in (127), the curvature scalar  $R$  in (128), and

$$C_1^1 = -\frac{1}{2g^{3/2}} (2m_1^3 - (m_2 + m_3) [m_1^2 + (m_2 - m_3)^2]), \quad (148)$$

where  $m_1, m_2, m_3$  are defined in (125). The remaining components  $R_2^2$ ,  $R_3^3$  and  $C_2^2$ ,  $C_3^3$  are obtained by permutation of indices 1, 2, 3 in the respective formulas for  $R_1^1$  and  $C_1^1$ .

As stated in the derivation of the dynamical system (134) for the  $\lambda$ - $R$  models, we only need to compute the equation for  $\Sigma_+$  and use permutations to obtain the equations for the  $\Sigma_\alpha$  variables, as argued after (136). In addition, we will exploit that each potential term in  $V$  can be written as an exponential in  $\beta^\lambda$  times a function of  $\beta^+$  and  $\beta^-$ , since each potential term  ${}^A V$  has a certain dimensional weight under conformal scalings of the

spatial metric. To make this weight explicit, we define

$$\bar{m}_1 := g^{-1/3} m_1 = n_1 e^{-4\beta^+}, \quad (149a)$$

$$\bar{m}_2 := g^{-1/3} m_2 = n_2 e^{2\beta^+ + 2\sqrt{3}\beta^-}, \quad (149b)$$

$$\bar{m}_3 := g^{-1/3} m_3 = n_3 e^{2\beta^+ - 2\sqrt{3}\beta^-}. \quad (149c)$$

Here we have introduced the convention that variables with an overbar are functions of  $\beta^\pm$  only. Denoting  $R_1^1$  and  $C_1^1$  with  $R_1$  and  $C_1$ , respectively, leads to that the equations (127) and (148) can be written as follows, by means of (149) and  $g = \exp(12v\beta^\lambda)$ ,

$$R_1 = e^{-4v\beta^\lambda} \bar{R}_1, \quad \bar{R}_1 = \frac{1}{2}(\bar{m}_1^2 - \bar{m}_-^2), \quad (150a)$$

$$C_1 = e^{-6v\beta^\lambda} \bar{C}_1, \quad \bar{C}_1 = -\frac{1}{2} (2\bar{m}_1^3 - \bar{m}_+ (\bar{m}_1^2 + \bar{m}_-^2)), \quad (150b)$$

where we define  $\bar{m}_\pm$  as

$$\bar{m}_\pm := \bar{m}_2 \pm \bar{m}_3. \quad (151)$$

The terms  $R_2 = R_2^2$ ,  $R_3 = R_3^3$ ,  $C_2 = C_2^2$  and  $C_3 = C_3^3$  are again obtained by permutations. To obtain succinct expressions, we not only introduce  $\bar{m}_\pm$ , but also the following (Misner-like) parametrization of the diagonal components of  $\bar{R}_j^i$  and  $\bar{C}_j^i$ :

$$\bar{A}_1 = \frac{1}{3}(\bar{A} - 2\bar{A}_+), \quad \bar{A} := \bar{A}_1 + \bar{A}_2 + \bar{A}_3, \quad (152a)$$

$$\bar{A}_2 = \frac{1}{3}(\bar{A} + \bar{A}_+ + \sqrt{3}\bar{A}_-), \quad \text{where} \quad \bar{A}_+ := \frac{1}{2}(\bar{A}_2 + \bar{A}_3 - 2\bar{A}_1), \quad (152b)$$

$$\bar{A}_3 = \frac{1}{3}(\bar{A} + \bar{A}_+ - \sqrt{3}\bar{A}_-), \quad \bar{A}_- := \frac{\sqrt{3}}{2}(\bar{A}_2 - \bar{A}_3). \quad (152c)$$

The Cotton tensor  $C_j^i$  is trace-free, and hence  $\bar{C} = \bar{C}_1 + \bar{C}_2 + \bar{C}_3 = 0$  when replacing  $\bar{A}$  with  $\bar{C}$ . Using the expressions in (150) for  $\bar{R}_1$ ,  $\bar{C}_1$ , and permutations thereof, in (152) gives

$$\bar{R} = -\frac{1}{2}(\bar{m}_1^2 - 2\bar{m}_1\bar{m}_+ + \bar{m}_-^2), \quad (153a)$$

$$\bar{R}_+ = -\frac{1}{2}(2\bar{m}_1^2 - \bar{m}_1\bar{m}_+ - \bar{m}_-^2), \quad (153b)$$

$$\bar{R}_- = -\frac{\sqrt{3}}{2}\bar{m}_-(\bar{m}_1 - \bar{m}_+), \quad (153c)$$

$$\bar{C}_+ = \frac{3}{4}(2\bar{m}_1^3 - \bar{m}_1^2\bar{m}_+ - \bar{m}_+\bar{m}_-^2), \quad (153d)$$

$$\bar{C}_- = \frac{\sqrt{3}}{4}\bar{m}_- (\bar{m}_1^2 + 2\bar{m}_1\bar{m}_+ - 2\bar{m}_+^2 - \bar{m}_-^2). \quad (153e)$$

The above parametrization leads to that potentials  ${}^A V$  in (123) take the form:

$${}^1 V = e^{8v\beta^\lambda} ({}^1 \bar{V}), \quad {}^1 \bar{V} = 12k_1 \bar{R}, \quad (154a)$$

$${}^2 V = e^{4v\beta^\lambda} ({}^2 \bar{V}), \quad {}^2 \bar{V} = 12k_2 \bar{R}^2, \quad (154b)$$

$${}^3 V = e^{4v\beta^\lambda} ({}^3 \bar{V}), \quad {}^3 \bar{V} = 12k_3 \bar{R}_j^i \bar{R}_i^j = 4k_3 (\bar{R}^2 + 2\bar{R}_+^2 + 2\bar{R}_-^2), \quad (154c)$$

$${}^4 V = e^{2v\beta^\lambda} ({}^4 \bar{V}), \quad {}^4 \bar{V} = 12k_4 \bar{R}_j^i \bar{C}_i^j = 8k_4 (\bar{R}_+ \bar{C}_+ + \bar{R}_- \bar{C}_-), \quad (154d)$$

$${}^5 V = {}^5 \bar{V}, \quad {}^5 \bar{V} = 12k_5 \bar{C}_j^i \bar{C}_i^j = 8k_5 (\bar{C}_+^2 + \bar{C}_-^2), \quad (154e)$$

$${}^6 V = {}^6 \bar{V}, \quad {}^6 \bar{V} = 12k_6 \bar{R}^3, \quad (154f)$$

which follows from (123) and (152). Thus all potentials  ${}^A V$  depend explicitly on  $\beta^\lambda$  as described in (154), whereas  ${}^A \bar{V}$  are functions of  $\bar{m}_1, \bar{m}_2, \bar{m}_3$  due to (153) and (151), and thereby of  $\beta^\pm$  according to (149).

Assigning a weight under spatial conformal scalings according to the scale  $g^{1/6} = e^{2v\beta^\lambda}$  results in that the potentials  ${}^A V$  in (154) have the following weights, denoted by  $[{}^A V]$ ,

$$[{}^1 V] = 4, \quad [{}^2 V] = [{}^3 V] = 2, \quad [{}^4 V] = 1, \quad [{}^5 V] = [{}^6 V] = 0. \quad (155)$$

In other words, all potentials  ${}^A V$  have an exponential dependence on  $\beta^\lambda$ , but with different powers of  $g^{1/6} = e^{2v\beta^\lambda}$  according to (155). The integer relations between the weights for the different potential terms,  $[{}^1 V] = [({}^2 V)^2] = [({}^3 V)^2] = [({}^4 V)^4]$  play a role below.

All HL models share some common features. First, all HL models have the same automorphism group and associated symmetries at each level of the class A Bianchi hierarchy, IX, VIII; VII<sub>0</sub>, VI<sub>0</sub>; II; I, see Figure 1. Second, each individual curvature term yields a potential with a certain weight (155), which results in that each individual potential has a scale-symmetry which can be combined with the automorphism group to yield a scale-automorphism group.<sup>24</sup> For this reason, we now describe the potentials at each level of the class A Bianchi hierarchy below type VIII and IX (the potentials of type VIII and IX where given in (154)).

The type VI<sub>0</sub> and VII<sub>0</sub> models are characterized by a single vanishing structure constant  $n_1, n_2, n_3$ . Without loss of generality, let  $n_1 = 0$  (and hence  $\bar{m}_1 = 0$ ) describe these models. Equations (149) and (151) then motivate the definitions

$$\tilde{m}_\pm := e^{-2\beta^+} m_\pm = n_2 e^{2\sqrt{3}\beta^-} \pm n_3 e^{-2\sqrt{3}\beta^-}, \quad (156)$$

where we introduce the convention that variables with a  $\sim$  on top are functions of  $\beta^-$  only. It follows that  $d\tilde{m}_\pm/d\beta^- = 2\sqrt{3}\tilde{m}_\pm$ . Equations (154) and (153) imply that the type VII<sub>0</sub>

---

<sup>24</sup>In Appendix B, this group is central for the dynamical properties at each level in the class A Bianchi hierarchy, for both the  $\lambda$ -R and HL models.

and VI<sub>0</sub> potentials with  $n_1 = 0$  can be written as

$${}^1V_{\text{VII}_0, \text{VI}_0} = e^{4(2v\beta^\lambda + \beta^+)}({}^1\tilde{V}), \quad {}^1\tilde{V} = -6k_1\tilde{m}_-^2, \quad (157\text{a})$$

$${}^2V_{\text{VII}_0, \text{VI}_0} = e^{4(v\beta^\lambda + 2\beta^+)}({}^2\tilde{V}), \quad {}^2\tilde{V} = 3k_2\tilde{m}_-^4, \quad (157\text{b})$$

$${}^3V_{\text{VII}_0, \text{VI}_0} = e^{4(v\beta^\lambda + 2\beta^+)}({}^3\tilde{V}), \quad {}^3\tilde{V} = 3k_3\tilde{m}_-^2(2\tilde{m}_+^2 + \tilde{m}_-^2), \quad (157\text{c})$$

$${}^4V_{\text{VII}_0, \text{VI}_0} = e^{2(v\beta^\lambda + 5\beta^+)}({}^4\tilde{V}), \quad {}^4\tilde{V} = -6k_4\tilde{m}_+\tilde{m}_-^2(\tilde{m}_+^2 + \tilde{m}_-^2), \quad (157\text{d})$$

$${}^5V_{\text{VII}_0, \text{VI}_0} = e^{12\beta^+}({}^5\tilde{V}), \quad {}^5\tilde{V} = \frac{3}{2}k_5(7\tilde{m}_+^2\tilde{m}_-^4 + 4\tilde{m}_-^2\tilde{m}_+^4 + \tilde{m}_-^6), \quad (157\text{e})$$

$${}^6V_{\text{VII}_0, \text{VI}_0} = e^{12\beta^+}({}^6\tilde{V}), \quad {}^6\tilde{V} = -\frac{3}{2}k_6\tilde{m}_-^6. \quad (157\text{f})$$

To describe the HL Bianchi type II models, we consider, without loss of generality, the II<sub>1</sub> models, which are characterized by  $n_2 = n_3 = 0$ , which yields  $\bar{m}_2 = \bar{m}_3 = 0$  and  $\bar{m}_\pm = 0$ . The Bianchi type II<sub>1</sub> potentials in (154) with curvature terms (153) are thereby given by

$${}^1V_{\text{II}_1} = -6k_1e^{8v\beta^\lambda}\bar{m}_1^2 = -6k_1n_1^2e^{8(v\beta^\lambda - \beta^+)} = -6k_1n_1^2e^{-8(v\tau_- + \beta^+)}, \quad (158\text{a})$$

$${}^2V_{\text{II}_1} = 3k_2e^{4v\beta^\lambda}\bar{m}_1^4 = 3k_2n_1^4e^{4(v\beta^\lambda - 4\beta^+)} = 3k_2n_1^4e^{-4(v\tau_- + 4\beta^+)}, \quad (158\text{b})$$

$${}^3V_{\text{II}_1} = 9k_3e^{4v\beta^\lambda}\bar{m}_1^4 = 9k_3n_1^4e^{4(v\beta^\lambda - 4\beta^+)} = 9k_3n_1^4e^{-4(v\tau_- + 4\beta^+)}, \quad (158\text{c})$$

$${}^4V_{\text{II}_1} = -12k_4e^{2v\beta^\lambda}\bar{m}_1^5 = -12k_4n_1^5e^{2(v\beta^\lambda - 10\beta^+)} = -12k_4n_1^5e^{-2(v\tau_- + 10\beta^+)}, \quad (158\text{d})$$

$${}^5V_{\text{II}_1} = 18k_5\bar{m}_1^6 = 18k_5n_1^6e^{-24\beta^+}, \quad (158\text{e})$$

$${}^6V_{\text{II}_1} = -\frac{3}{2}k_6\bar{m}_1^6 = -\frac{3}{2}k_6n_1^6e^{-24\beta^+}. \quad (158\text{f})$$

The common dimensional weight in (155) for  ${}^2V$  and  ${}^3V$ , and for  ${}^5V$  and  ${}^6V$ , motivates that these two pairs of potentials are treated collectively, i.e.,

$${}^{2,3}V := {}^2V + {}^3V = e^{4v\beta^\lambda}({}^{2,3}\bar{V}) = e^{4v\beta^\lambda}[4(3k_2 + k_3)\bar{R}^2 + 8k_3(\bar{R}_+^2 + \bar{R}_-^2)], \quad (159\text{a})$$

$${}^{2,3}V_{\text{VII}_0, \text{VI}_0} = e^{4(v\beta^\lambda + 2\beta^+)}({}^{2,3}\tilde{V}) = 3e^{4(v\beta^\lambda + 2\beta^+)}\tilde{m}_-^2[2k_3\tilde{m}_+^2 + (k_2 + k_3)\tilde{m}_-^2], \quad (159\text{b})$$

$${}^{2,3}V_{\text{II}_1} = 3(k_2 + 3k_3)n_1^4e^{4(v\beta^\lambda - 4\beta^+)}, \quad (159\text{c})$$

and

$${}^{5,6}V := {}^5V + {}^6V = {}^{5,6}\bar{V} = 8k_5(\bar{C}_+^2 + \bar{C}_-^2) + 12k_6\bar{R}^3, \quad (160\text{a})$$

$${}^{5,6}V_{\text{VII}_0, \text{VI}_0} = e^{12\beta^+}({}^{5,6}\tilde{V}) = \frac{3}{2}e^{12\beta^+}[k_5(7\tilde{m}_+^2\tilde{m}_-^4 + 4\tilde{m}_-^2\tilde{m}_+^4) + (k_5 - k_6)\tilde{m}_-^6], \quad (160\text{b})$$

$${}^{5,6}V_{\text{II}_1} = \frac{3}{2}(12k_5 - k_6)n_1^6e^{-24\beta^+}, \quad (160\text{c})$$

which follows from (154), (157) and (158).

To obtain a unified description of the various potentials, we refer to them with a superscript  $A$ , i.e.,  ${}^AV$ , where  $A = 1, \{2, 3\}, 4, \{5, 6\}$ ; thus  $A = 2, 3$  and  $A = 5, 6$  corresponds

to  ${}^{2,3}V = {}^2V + {}^3V$  and  ${}^{5,6}V = {}^5V + {}^6V$ , respectively. We also introduce the constants

$${}^1v = v := \frac{1}{\sqrt{2(3\lambda - 1)}}, \quad {}^{2,3}v = \frac{v}{4}, \quad {}^4v = \frac{v}{10}, \quad {}^{5,6}v = 0, \quad (161a)$$

$${}^1a = 2, \quad {}^{2,3}a = 4, \quad {}^4a = 5, \quad {}^{5,6}a = 6, \quad (161b)$$

$${}^1c = -12k_1, \quad {}^{2,3}c = 6(k_2 + 3k_3), \quad {}^4c = -24k_4, \quad {}^{5,6}c = 36k_5 - 3k_6. \quad (161c)$$

The models with  ${}^1v, {}^{2,3}v, {}^4v \in (0, 1)$  thereby correspond to  $\lambda \in (\frac{1}{2}, \infty), (\frac{11}{32}, \infty), (\frac{67}{200}, \infty)$ , respectively.

The constants (161) allow us to write the HL potentials at each level of the class A Bianchi hierarchy as follows:

$${}^AV = e^{4av\beta^\lambda}({}^A\bar{V}), \quad \text{for types IX and VIII}, \quad (162a)$$

$${}^AV_{VII_0, VI_0} = e^{2a(2v\beta^\lambda + \beta^+)}({}^A\tilde{V}), \quad \text{for types VII}_0 \text{ and VI}_0, \text{ with } n_1 = 0, \quad (162b)$$

$${}^AV_{II_1} = \frac{1}{2}c n_1^a e^{4a(v\beta^\lambda - \beta^+)}, \quad \text{for type II}_1, \quad (162c)$$

where we refrain from writing the superscript  $A$  on  ${}^Aa$ ,  ${}^Av$  and  ${}^Ac$  for notational brevity, e.g.,  ${}^AV_{II_1} = \frac{1}{2}c n_1^a e^{4a(v\beta^\lambda - \beta^+)} = \frac{1}{2}({}^Ac)(n_1)({}^Aa)e^{4({}^Aa)(({}^Av)\beta^\lambda - \beta^+)}$ . As can be seen by inspection, inserting (161) into the above expressions yield (154), (157), with  $n_1 = 0$  for the type VII<sub>0</sub> and VI<sub>0</sub> potentials, and (158) for type II<sub>1</sub>.

We will now derive a regular constrained dynamical system for the HL case, and then perform a heuristic analysis of the HL models. In the latter case, when there are several potential terms (154), we heuristically argue that there is a single dominant potential, and that the scale-automorphism group for this dominant potential is intimately linked to the asymptotic dynamics toward the singularity, in the same manner as for the GR and  $\lambda$ - $R$  models.

## Derivation of the HL evolution equations

To obtain a *regular* dynamical system for the HL models, we first consider the Hamiltonian equations with the Hamiltonian (124) for the variables  $\beta^\lambda, \beta^\pm$  and the canonical momenta  $p_\lambda, p_\pm$ . The kinetic part  $T$  depends on  $p_\lambda, p_\pm$  and is given by (120), while the potential  $V$  depends on  $\beta^\lambda, \beta^\pm$  according to (122) and (154). We then use the same  $\Sigma_\pm$  and  $\Sigma_\alpha$  variables as in the  $\lambda$ - $R$  case, defined in (132) and (136), and the time variable  $\tau_- := -\beta^\lambda$ . The Hamiltonian equations then result in the evolution equations

$$\frac{d\beta^\lambda}{d\tau_-} = -1, \quad \frac{dp_\lambda}{d\tau_-} = -\Omega_\lambda p_\lambda, \quad (163a)$$

$$\frac{d\beta^\pm}{d\tau_-} = -\Sigma_\pm, \quad \frac{d\Sigma_\pm}{d\tau_-} = \Omega_\lambda \Sigma_\pm + \mathcal{S}_\pm, \quad (163b)$$

subjected to the constraint

$$\Sigma_+^2 + \Sigma_-^2 + \Omega_k = 1, \quad (164)$$

where we have introduced the following dimensionless quantities

$$\Omega_k := \frac{2}{p_\lambda^2} V, \quad \Omega_\lambda := \frac{1}{p_\lambda^2} \frac{\partial V}{\partial \beta^\lambda}, \quad \mathcal{S}_\pm := -\frac{2}{p_\lambda^2} \frac{\partial V}{\partial \beta^\pm}. \quad (165)$$

The different quantities in (165) can be decomposed into objects that are related to the individual potentials  ${}^A V$  for  $A = 1, \{2, 3\}, 4, \{5, 6\}$  as follows

$$\Omega_k = {}^1 \Omega_k + {}^{2,3} \Omega_k + {}^4 \Omega_k + {}^{5,6} \Omega_k, \quad (166a)$$

$$\Omega_\lambda = {}^1 \Omega_\lambda + {}^{2,3} \Omega_\lambda + {}^4 \Omega_\lambda + {}^{5,6} \Omega_\lambda, \quad (166b)$$

$$\mathcal{S}_\pm = {}^1 \mathcal{S}_\pm + {}^{2,3} \mathcal{S}_\pm + {}^4 \mathcal{S}_\pm + {}^{5,6} \mathcal{S}_\pm, \quad (166c)$$

where  ${}^A \Omega_k := 2p_\lambda^{-2}({}^A V)$ ,  ${}^A \Omega_\lambda := p_\lambda^{-2} \partial_{\partial \beta^\lambda}({}^A V)$  and  ${}^A \mathcal{S}_\pm := -2p_\lambda^{-2} \partial_{\partial \beta^\pm}({}^A V)$ . Due to (154),  $\Omega_\lambda$  is given by

$$\Omega_\lambda = 4v({}^1 \Omega_k) + 2v({}^{2,3} \Omega_k) + v({}^4 \Omega_k), \quad (167)$$

where the coefficients are related to the scaling weights in (155). Note that all  ${}^A \bar{V}$  are homogeneous polynomials in  $\bar{m}_1$ ,  $\bar{m}_2$  and  $\bar{m}_3$ , which are invariant under permutations of indices, as follows from (154), which is a consequence of that the potentials have been constructed from curvature scalars. It follows from the definitions that  ${}^A \Omega_k$  for  $A = 1, \{2, 3\}, 4, \{5, 6\}$  are also homogeneous polynomials in  $\bar{m}_\alpha$  and that  ${}^A \Omega_k$ ,  $\Omega_k$  and  $\Omega_\lambda$  are invariant under permutations.

To compute the equation for  $\Sigma_+$ , we need to compute  ${}^A \mathcal{S}_+$  and  $\mathcal{S}_+$ . To do so, note that the equations (149) and (151) yield

$$\frac{\partial \bar{m}_1}{\partial \beta^+} = -4\bar{m}_1, \quad \frac{\partial \bar{m}_\pm}{\partial \beta^+} = 2\bar{m}_\pm, \quad (168)$$

which together with the chain rule and (153) gives

$$\frac{\partial \bar{R}}{\partial \beta^+} = 2(2\bar{m}_1^2 - \bar{m}_1 \bar{m}_+ - \bar{m}_-^2), \quad (169a)$$

$$\frac{\partial \bar{R}_+}{\partial \beta^+} = 8\bar{m}_1^2 - \bar{m}_1 \bar{m}_+ + 2\bar{m}_-^2, \quad (169b)$$

$$\frac{\partial \bar{R}_-}{\partial \beta^+} = \sqrt{3}(\bar{m}_1 + 2\bar{m}_+) \bar{m}_-, \quad (169c)$$

$$\frac{\partial \bar{C}_+}{\partial \beta^+} = -\frac{9}{2} (4\bar{m}_1^3 - \bar{m}_1^2 \bar{m}_+ + \bar{m}_+ \bar{m}_-^2), \quad (169d)$$

$$\frac{\partial \bar{C}_-}{\partial \beta^+} = -\frac{3\sqrt{3}}{2} (\bar{m}_1^2 + 2\bar{m}_+^2 + \bar{m}_-^2) \bar{m}_-. \quad (169e)$$

These expressions in combination with the chain rule applied to (154) yields each  ${}^A \mathcal{S}_+$  as a homogeneous polynomial in  $\bar{m}_1$ ,  $\bar{m}_2$  and  $\bar{m}_3$  of the same degree as in  ${}^A \Omega_k$ . The polynomials are multiplied with  $p_\lambda^{-2}$  and exponentials in  $\beta^\lambda$ , determined by the weights of  ${}^A V$  in the same way as for  ${}^A \Omega_k$ . We then change the  $\Sigma_\pm$  variables to  $\Sigma_\alpha$ ,  $\alpha = 1, 2, 3$ ,

$$(\Sigma_1, {}^A \mathcal{S}_1, \mathcal{S}_1) := -2(\Sigma_+, {}^A \mathcal{S}_+, \mathcal{S}_+). \quad (170)$$

This leads to

$$\Sigma'_\alpha = \Omega_\lambda \Sigma_\alpha + \mathcal{S}_\alpha, \quad \alpha = 1, 2, 3, \quad (171)$$

where the equations for  $\alpha = 2$  and  $\alpha = 3$  are obtained by cyclic permutations of (123) in the expressions involving  $\bar{m}_1$ ,  $\bar{m}_2$  and  $\bar{m}_3$  when  $\alpha = 1$ . There is thereby no need to compute  $\mathcal{S}_-$ .

Our next step is to introduce dimensionless variables that replace  $\beta^\lambda$ ,  $\beta^\pm$  in (163) and  $p_\lambda$  in order to obtain a *regular* dynamical system. In the  $\lambda$ - $R$  case, the single potential term given by  $V = {}^1V$  had a specific weight under conformal scaling transformations, which yielded a symmetry that decoupled the evolution equation for  $p_\lambda$ . We now have potential terms in (154) with different weights (155), where adding them breaks this symmetry. We therefore introduce separate dimensionless variables  ${}^A N_\alpha$ ,  $A = 1, \{2, 3\}, 4, \{5, 6\}$ , that respect the different weights and the polynomial nature of the potential in terms of  $\bar{m}_\alpha$ . This leads to twelve variables  ${}^A N_\alpha$ , three for each value of  $A$ , replacing the four variables  $\beta^\lambda$ ,  $\beta^\pm$  and  $p_\lambda$ . Due to the construction, the equation for the dimensional variable  $p_\lambda$ ,

$$p'_\lambda = -\Omega_\lambda p_\lambda \quad (172)$$

decouples, but the redundancy of variables  ${}^A N_\alpha$  results in constraints between them.

To explicitly define the variables  ${}^A N_\alpha$ , which will lead to explicit constraints, we first consider the type II<sub>1</sub> potentials  ${}^A V_{\text{II}_1}$  in equation (158) and define  ${}^A \Omega_{\text{II}_1} := 2({}^A V_{\text{II}_1})/(-p_\lambda)^2$ . Permutation of axis allows us to obtain the dimensionless expression

$${}^A \Omega_{\text{II}_\alpha} = \frac{2({}^A V_{\text{II}_\alpha})}{(-p_\lambda)^2} = ce^{4a v \beta^\lambda} \frac{\bar{m}_\alpha^a}{(-p_\lambda)^2}, \quad (173)$$

where we refrain from writing the superscript  $A$  on  ${}^A c$ ,  ${}^A a$ ,  ${}^A v$  for brevity. We recall that  $p_\lambda < 0$  for an expanding model.

Throughout we will restrict considerations to HL models for which  $({}^A c)(n_\alpha)^({}^A a) \geq 0$  when  $n_\alpha \neq 0$ , i.e., models with non-negative Bianchi type II potentials and non-negative  ${}^A \Omega_{\text{II}_\alpha}$ . This amounts to sign conditions on the constants  $k_A$  in (158). For example,  $k_1 \leq 0$  in  ${}^1 V_{\text{II}_1}$  when  $n_1 \neq 0$ , whereas

$$k_{2,3} := k_2 + 3k_3 \geq 0, \quad k_{5,6} := 12k_5 - k_6 \geq 0, \quad (174)$$

are associated with  ${}^1 V_{\text{II}_{2,3}}$  and  ${}^1 V_{\text{II}_{5,6}}$ , respectively. Note that the term  ${}^4 V_{\text{II}_1}$  when  $n_1 \neq 0$  is special: it is positive if  $k_4$  is negative and  $n_1$  is chosen to be positive. But in Bianchi type VIII, one of the potentials  ${}^4 V_{\text{II}_1}$ ,  ${}^4 V_{\text{II}_2}$ ,  ${}^4 V_{\text{II}_3}$  by necessity has an opposite sign compared to the other two, irrespective of the sign of  $k_4$ . This occurs since two of the constants  $n_1$ ,  $n_2$ ,  $n_3$  have opposite signs compared to the third, as in Table 1, and these constants appear with odd powers in (158d). For this reason, we exclude the type VIII models with  $k_4 \neq 0$ , except when  $k_{5,6} > 0$ , since  ${}^{5,6} V$  asymptotically ‘dominates’ over  ${}^4 V$ , as will be seen below.

We then define new dimensionless variables that are linear in  $\bar{m}_\alpha$ , as in the  $\lambda$ - $R$  case. This can be done because the potentials  ${}^A V$  are homogeneous polynomials in  $\bar{m}_\alpha$ ,  $\alpha = 1, 2, 3$ ,

and thus the evolution equations has variables that respect these polynomial relationships. We therefore introduce the following variables,

$${}^A N_\alpha := \sqrt[{}^A]{\Omega_{\text{II}\alpha}} = \sqrt[{}^A]{c} e^{4v\beta^\lambda} \frac{\bar{m}_\alpha}{\sqrt[{}^A]{(-p_\lambda)^2}}, \quad (175)$$

where we again drop the superscript  $A$  on  ${}^A v$ ,  ${}^A a$ ,  ${}^A c$ . This leads to the following:

$${}^1 N_\alpha := \sqrt{-12k_1} e^{4v\beta^\lambda} \left( \frac{\bar{m}_\alpha}{-p_\lambda} \right), \quad (176a)$$

$${}^{2,3} N_\alpha := \sqrt[4]{6k_{2,3}} e^{v\beta^\lambda} \left( \frac{\bar{m}_\alpha}{\sqrt{-p_\lambda}} \right), \quad (176b)$$

$${}^4 N_\alpha := \sqrt[5]{-24k_4} e^{2v\beta^\lambda/5} \left( \frac{\bar{m}_\alpha}{\sqrt[5]{p_\lambda^2}} \right), \quad (176c)$$

$${}^{5,6} N_\alpha := \sqrt[6]{3k_{5,6}} \left( \frac{\bar{m}_\alpha}{\sqrt[3]{-p_\lambda}} \right). \quad (176d)$$

As in the  $\lambda$ - $R$  case, considering the Hamiltonian/Codazzi constraint in these variables shows that they are dimensionless. Note that the dimension of  $k_A$  determines how both  $\beta^\lambda$  and  $p_\lambda$  enter the definitions, once one has decided to adapt the variables to the polynomials in  $\bar{m}_\alpha$  (or, equivalently,  $m_\alpha$ ). Finally we choose to fix the remaining dimensionless constants that can multiply the  ${}^A N_\alpha$  variables by requiring that the coefficients for the Bianchi type II terms in each  ${}^A \Omega_k$  are equal to one.

The evolution equations for the variables  ${}^A N_\alpha$ , expressed in the variables  $\Sigma_\alpha$ , are obtained from the above definitions, (163), (170), and are given by

$${}^A N'_\alpha = -2 \left[ 2({}^A v) + \Sigma_\alpha - \frac{\Omega_\lambda}{{}^A a} \right] ({}^A N_\alpha), \quad (177)$$

or, explicitly,

$${}^1 N'_\alpha = (\Omega_\lambda - 4v - 2\Sigma_\alpha) ({}^1 N_\alpha), \quad (178a)$$

$${}^{2,3} N'_\alpha = \frac{1}{2} (\Omega_\lambda - 2v - 4\Sigma_\alpha) ({}^{2,3} N_\alpha), \quad (178b)$$

$${}^4 N'_\alpha = \frac{2}{5} (\Omega_\lambda - v - 5\Sigma_\alpha) ({}^4 N_\alpha), \quad (178c)$$

$${}^{5,6} N'_\alpha = \frac{1}{3} (\Omega_\lambda - 6\Sigma_\alpha) ({}^{5,6} N_\alpha), \quad (178d)$$

where  $\alpha = 1, 2, 3$ , and where  ${}^A v$  has been replaced with  $v$ , defined in (6), according to (161a).

As mentioned, there are twelve variables  ${}^A N_\alpha$ , since  $\alpha = 1, 2, 3$  and  $A = 1, \{2, 3\}, 4, \{5, 6\}$ , and thus they are not all independent since they are functions of four variables,  $\beta^\lambda$ ,  $\beta^\pm$ ,  $p_\lambda$ . The above evolution equations (178) are therefore constrained. Using that there are integer weight relations between the different potentials  ${}^A V$ ,  $A = 1, \{2, 3\}, 4, \{5, 6\}$ , and

inserting the definitions (176) into these relations yield the following constraints

$$\sqrt{k_{2,3}^3} ({}^1 N_\alpha) ({}^4 N_\alpha)^5 = -k_4 \sqrt{-2^5 k_1} ({}^{2,3} N_\alpha)^6, \quad \alpha = 1, 2, 3, \quad (179a)$$

$$k_{2,3} ({}^1 N_\alpha) ({}^{5,6} N_\alpha)^3 = \sqrt{-k_1 k_{5,6}} ({}^{2,3} N_\alpha)^4, \quad \alpha = 1, 2, 3, \quad (179b)$$

$$({}^A N_\alpha) ({}^B N_\beta) = ({}^A N_\beta) ({}^B N_\alpha), \quad \alpha \beta = 12, 23, 31; \quad (179c)$$

$$A, B = 1, \{2, 3\}, 4, \{5, 6\}.$$

Only nine of the above constraints above turn out to be independent, e.g., (179a), (179b) and  $({}^1 N_\alpha) ({}^{2,3} N_\beta) = ({}^1 N_\beta) ({}^{2,3} N_\alpha)$ , since the other ones can be written in terms of these nine equations if  $k_1, k_{2,3} = k_2 + 3k_3, k_4, k_{5,6} = 12k_5 - k_6$  are all non-zero. If any of these coefficients are zero, one can choose a different set among the available constraints, but most three of the twelve variables  ${}^A N_\alpha$  are independent.

The HL dynamical system thereby consists of the following evolution equations,

$$\Sigma'_\alpha = \Omega_\lambda \Sigma_\alpha + \mathcal{S}_\alpha, \quad (180a)$$

$${}^1 N'_\alpha = (\Omega_\lambda - 4v - 2\Sigma_\alpha) ({}^1 N_\alpha), \quad (180b)$$

$${}^{2,3} N'_\alpha = \frac{1}{2} (\Omega_\lambda - 2v - 4\Sigma_\alpha) ({}^{2,3} N_\alpha), \quad (180c)$$

$${}^4 N'_\alpha = \frac{2}{5} (\Omega_\lambda - v - 5\Sigma_\alpha) ({}^4 N_\alpha), \quad (180d)$$

$${}^{5,6} N'_\alpha = \frac{1}{3} (\Omega_\lambda - 6\Sigma_\alpha) ({}^{5,6} N_\alpha), \quad (180e)$$

subjected to the constraints

$$0 = \Sigma_1 + \Sigma_2 + \Sigma_3, \quad (180f)$$

$$1 = \Sigma^2 + \Omega_k, \quad \Sigma^2 := (\Sigma_1^2 + \Sigma_2^2 + \Sigma_3^2)/6, \quad (180g)$$

$$\sqrt{k_{2,3}^3} ({}^1 N_\alpha) ({}^4 N_\alpha)^5 = -k_4 \sqrt{-2^5 k_1} ({}^{2,3} N_\alpha)^6, \quad \alpha = 1, 2, 3, \quad (180h)$$

$$k_{2,3} ({}^1 N_\alpha) ({}^{5,6} N_\alpha)^3 = \sqrt{-k_1 k_{5,6}} ({}^{2,3} N_\alpha)^4, \quad \alpha = 1, 2, 3, \quad (180i)$$

$$({}^A N_\alpha) ({}^B N_\beta) = ({}^A N_\beta) ({}^B N_\alpha), \quad \alpha \beta = 12, 23, 31; \quad (180j)$$

$$A, B = 1, \{2, 3\}, 4, \{5, 6\}.$$

where  $\Omega_k$  and  $\Omega_\lambda$  are obtained from (166) and (167);  $\mathcal{S}_\alpha$  is obtained by permuting the indices in  $\mathcal{S}_1$ , which is computed from  $\mathcal{S}_+$  according to (170).

There are in total fifteen variables (three  $\Sigma_\alpha$  and twelve  ${}^A N_\alpha$ ) subjected to eleven constraints (two constraints (180f) and (180g), which also hold for the  $\lambda$ - $R$  models and GR, and nine new independent constraints (180h), (180i) and (180j), relating the variables  ${}^A N_\alpha$ ). This results in a rather formidable constrained dynamical system. However, the system (180) contains several less complicated special invariant sets, which illustrate the above procedure of how to obtain the explicit equations. The special invariant sets are of two types:

- (i) sets obtained by setting some potentials  ${}^A V$  to zero,  $A = 1, \{2, 3\}, 4, \{5, 6\}$ , which corresponds to setting the corresponding variables  ${}^A N_\alpha$  with  $\alpha = 1, 2, 3$  to zero;

- (ii) special Bianchi types obtained by setting one or more constants  $n_\alpha$  to zero, which implies that the corresponding variables  ${}^A N_\alpha$  are zero, for all values of  $A$ .

To illustrate the algorithmic procedure to obtain explicit equations, which require expressing  ${}^A \Omega_k$ ,  ${}^A \Omega_\lambda$  and  ${}^A \mathcal{S}_\alpha$ , based on (165) in the variables  ${}^A N_\alpha$ , let us first consider the case where only  $k_1 \neq 0$  (recall that  $k_1 = -1$  yields the  $\lambda$ - $R$  case). Thus the invariant set defined by  ${}^A N_\alpha = 0$  for all  $A = \{2, 3\}, 4, \{5, 6\}$ ,  $\alpha = 1, 2, 3$  provides an example of an invariant subset of type (i) above, where  $\Omega_k = {}^1 \Omega_k$ ,  $\Omega_\lambda = {}^1 \Omega_\lambda$ ,  $\mathcal{S}_\alpha = {}^1 \mathcal{S}_\alpha$ . Equations (153a) and (154a) yield

$$\begin{aligned} {}^1 V &= 12k_1 e^{8v\beta^\lambda} \bar{R} = -6k_1 e^{8v\beta^\lambda} (\bar{m}_1^2 - 2\bar{m}_1 \bar{m}_+ + \bar{m}_-^2) \\ &= -6k_1 e^{8v\beta^\lambda} (\bar{m}_1^2 + \bar{m}_2^2 + \bar{m}_3^2 - 2\bar{m}_1 \bar{m}_2 - 2\bar{m}_2 \bar{m}_3 - 2\bar{m}_3 \bar{m}_1), \end{aligned} \quad (181)$$

where we have used (151).

Together with (165) and (176a), this leads to

$$\Omega_k = N_1^2 + N_2^2 + N_3^2 - 2N_1 N_2 - 2N_2 N_3 - 2N_3 N_1. \quad (182)$$

Equation (167) yields  $\Omega_\lambda = 4v\Omega_k$ . It remains to determine  $\mathcal{S}_\alpha$ . Equations (181), (169a), (151) and (176a) result in

$$\mathcal{S}_1 = -4 [(N_2 - N_3)^2 - N_1(2N_1 - N_2 - N_3)], \quad (183)$$

where cyclic permutations of (123) yield  $\mathcal{S}_2$  and  $\mathcal{S}_3$ .

A comparison shows that the dynamical system with  $k_1 < 0$  is identical to the system (4), (135), for the  $\lambda$ - $R$  case for which  $k_1 = -1$ . The reason for this is that single curvature terms, associated with the constant  $k_A$ , with  $A = 1, \{2, 3\}, 4$ , admit a scaling symmetry, which correspond to a translation in  $\beta^\lambda$ . This symmetry makes it possible to scale  $k_A$  with an arbitrary positive number, and hence scale the negative coefficient  $k_1$  so that  $k_1 = -1$ .

To illustrate invariant subsets obtained by restricting to a particular Bianchi type (i.e., invariant sets of type (ii) above), we consider Bianchi types I and II. As in the  $\lambda$ - $R$  case, the Bianchi type I subset is just the Kasner circle  $K^\circ$ . In the Bianchi type II<sub>1</sub> case,  $n_2 = n_3 = 0$  implies  ${}^A N_2 = {}^A N_3 = 0$  for all  $A$ . This thereby leaves four variables  ${}^A N_1$  when all constants  $k_1, k_{2,3}, k_4, k_{5,6}$  are non-zero. The constraints (180j) are all identically zero since they involve  ${}^A N_2$  and  ${}^A N_3$ . Similarly the constraints (180h) and (180i) are identically zero for  $\alpha = 2, 3$ . This leaves two constraints (180h) and (180i) for  $\alpha = 1$ , and hence there are two independent variables  ${}^A N_1$ ,  $A = 1, \{2, 3\}, 4, \{5, 6\}$ , in Bianchi type II<sub>1</sub>. Similar statements hold for Bianchi type II<sub>2</sub> and II<sub>3</sub>. The Bianchi type II models break the formal permutation symmetry, e.g., the type II<sub>1</sub> models lead to that  $\bar{m}_2$  and  $\bar{m}_3$ , and thereby  $\bar{m}_\pm$ , are set to zero. In this case, it is convenient to use equation (158) and compute  $\mathcal{S}_- = 0$  from its definition (165), since  $\beta^-$  is a cyclic variable, and then transform the result to obtain  $\mathcal{S}_\alpha$ , which yields the following quantities

$$\Omega_k = ({}^1 N_1)^2 + ({}^{2,3} N_1)^4 + ({}^4 N_1)^5 + ({}^{5,6} N_1)^6, \quad (184a)$$

$$\Omega_\lambda = 4v({}^1 N_1)^2 + 2v({}^{2,3} N_1)^4 + v({}^4 N_1)^5, \quad (184b)$$

$$(\mathcal{S}_1, \mathcal{S}_2, \mathcal{S}_3) = 4 [2({}^1 N_1)^2 + 4({}^{2,3} N_1)^4 + 5({}^4 N_1)^5 + 6({}^{5,6} N_1)^6] T_1, \quad (184c)$$

from which it is straightforward to obtain the type  $\text{II}_1$  dynamical system.

Equation (184) illustrates that  ${}^A\Omega_k$ ,  ${}^A\Omega_\lambda$  and  ${}^A\mathcal{S}_\alpha$  for  $\alpha = 1, 2, 3$  are homogeneous polynomials of  ${}^A\mathcal{N}_\alpha$  of degrees 2, 4, 5, 6 when  $A = 1, \{2, 3\}, 4, \{5, 6\}$ , respectively. In Bianchi type VIII and IX, the number of terms in  ${}^A\Omega_k$ ,  ${}^A\Omega_\lambda$  and  ${}^A\mathcal{S}_\alpha$  increases as the degree of the polynomials become higher due to an increase in the number of cross terms, which leads to a daunting number of terms in  $\Omega_k$ ,  $\Omega_\lambda$  and  $\mathcal{S}_\alpha$ , when  $k_A \neq 0$  for all  $A$ .

## Heuristic HL considerations

Here we will heuristically argue that the heteroclinic network obtained by concatenation of Bianchi type II orbits in the  $\lambda$ - $R$  models given by (134) describes the asymptotics of a broad class of HL models (180).

Equation (162c) shows that the Bianchi type II potential walls for the  ${}^AV$  potential has a speed  ${}^Av$  given by (161a) in the negative  $\beta^+$ -direction, which is obtained in the same way as equation (140) in the  $\lambda$ - $R$  model. Moreover, for the same reason as in the  $\lambda$ - $R$  case, the cross terms for a potential  ${}^AV$  with  $A = 1, \{2, 3\}, 4$  have approximating walls with higher speeds than the Bianchi type II terms, and are not expected to affect generic asymptotic dynamics toward the singularity, as will be discussed below; the case  $A = 5, 6$  is special. Furthermore, a similar argument holds for the type II terms that belongs to different potentials:  ${}^1V_{\text{II}}$  yields slower moving walls than all the other type II potentials, so if any of these are present, the  ${}^1V_{\text{II}}$  contribution to the dynamics is expected to not affect the generic past asymptotic dynamics; similarly  ${}^{2,3}V_{\text{II}}$  is negligible if  ${}^4V$  or  ${}^{5,6}V$  (or both) are non-zero; while if  $k_{5,6} > 0$  all the other terms are expected to be dominated by  ${}^{5,6}V$ .

This leads to a situation where the generic past dynamics is expected to be characterised by a ‘dominant’ Hamiltonian of the form

$$H_{\text{Dom}} = \mathcal{N}(T + V_{\text{Dom}}) = 0, \quad (185)$$

where the kinetic part  $T$  depends on the canonical momenta  $p_\lambda$ ,  $p_\pm$ , according to (120), while the ‘dominant’ potential  $V_{\text{Dom}}$  is the sum of the type  $\text{II}_1$ ,  $\text{II}_2$  and  $\text{II}_3$  terms in the dominant potential  ${}^AV$ ,  $A = \text{Dom}$ , i.e., all potentials with larger  ${}^Bv$  and all the cross terms have been dropped. The dominant potential depends on  $\beta^\lambda$ ,  $\beta^\pm$  as follows:

$$V_{\text{Dom}} = \frac{1}{2}c \left( n_1^a e^{4a(v\beta^\lambda - \beta^+)} + n_2^a e^{2a(2v\beta^\lambda + \beta^+ + \sqrt{3}\beta^-)} + n_3^a e^{2a(2v\beta^\lambda + \beta^+ - \sqrt{3}\beta^-)} \right), \quad (186)$$

where we drop the superscript  $A = \text{Dom}$  on the constants  ${}^A\mathcal{C}$ ,  ${}^Aa$  and  ${}^Av$  for brevity. The value of  $A$  in (186) is determined by the dominant potential, i.e., if all potentials with larger  $A$  are zero. For example,  $A = 1$  corresponds to that  $k_{2,3} = k_4 = k_{5,6} = 0$ , while  $A = 4$  requires  $k_{5,6} = 0$ .

The case  $k_{5,6} > 0$  requires special attention. Although the  ${}^{5,6}V$  potential is expected to suppress all other potentials toward the singularity, note that  ${}^{5,6}V$  only depends on  $\beta^\pm$ . Hence  $\beta^\lambda$  is a cyclic variable in this case (using e.g.  $\mathcal{N} = \text{constant}$  as determining the time variable), which results in that  $p_\lambda$  becomes a conserved quantity. The term

$E = p_\lambda^2/2$  can thus be viewed as an energy for the reduced Hamiltonian problem with potential  ${}^{5,6}V(\beta^\pm)$ . This potential yields a generalized Toda problem in two dimensions, see [13]. Once the existence of  ${}^{5,6}V$  has suppressed the effects of the other potentials, the full remaining Toda problem must be addressed. In the limit,  $E \rightarrow \infty$ , one expects that the dynamics is described by the  $v = 0$  Bianchi type I and II heteroclinic network in the dynamical systems picture, but for small  $E$ , all terms in  ${}^{5,6}V$  comes into play and one can expect a complicated dynamical behaviour, in agreement with the discussions in [6] and [71].

We can adapt dynamical systems variables to the present dominant Hamiltonian system (185). Based on (186), which consists of the three dominant  ${}^A V_{\text{II}\alpha}$ ,  $A = \text{Dom}$ , potentials, we define the following dimensionless variables

$$\tilde{N}_1 := \sqrt{cn_1^a} \left( \frac{e^{2a(v\beta^\lambda - \beta^+)}}{-p_\lambda} \right), \quad (187a)$$

$$\Sigma_\pm := -\frac{p_\pm}{p_\lambda}, \quad \tilde{N}_2 := \sqrt{cn_2^a} \left( \frac{e^{a(2v\beta^\lambda + \beta^+ + \sqrt{3}\beta^-)}}{-p_\lambda} \right), \quad (187b)$$

$$\tilde{N}_3 := \sqrt{cn_3^a} \left( \frac{e^{a(2v\beta^\lambda + \beta^+ - \sqrt{3}\beta^-)}}{-p_\lambda} \right), \quad (187c)$$

where we again drop the superscript  $A=\text{Dom}$  for brevity. In comparison with the variables in (132) for the  $\lambda$ - $R$  models, we keep the same variables  $\Sigma_\pm$ , but the variables  $\tilde{N}_\alpha$  are slightly modified. In particular, there exists an overall factor  ${}^Aa/2$  in the exponent times an expression that is formally the same as in the  $\lambda$ - $R$  case, but with  $v$  replaced with  ${}^A v$ .

The multiplicative factor  ${}^Aa/2$  can be eliminated by a change of the time variable  $\tau_-$  according to  $\tilde{\tau}_- := 2\tau_- / {}^Aa$ . Letting ' denote the new derivative  $d/d\tilde{\tau}_-$  yields the following system of evolution equations

$$\Sigma'_+ = 2 \left( 2v(1 - \Sigma^2)\Sigma_+ + \tilde{N}_2^2 + \tilde{N}_3^2 - 2\tilde{N}_1^2 \right), \quad (188a)$$

$$\Sigma'_- = 2 \left( 2v(1 - \Sigma^2)\Sigma_- + \sqrt{3}\tilde{N}_2^2 - \sqrt{3}\tilde{N}_3^2 \right), \quad (188b)$$

$$\tilde{N}'_1 = -4(v\Sigma^2 - \Sigma_+)\tilde{N}_1, \quad (188c)$$

$$\tilde{N}'_2 = -2(2v\Sigma^2 + \Sigma_+ + \sqrt{3}\Sigma_-)\tilde{N}_2, \quad (188d)$$

$$\tilde{N}'_3 = -2(2v\Sigma^2 + \Sigma_+ - \sqrt{3}\Sigma_-)\tilde{N}_3, \quad (188e)$$

subjected to the constraint

$$1 - \Sigma^2 - \tilde{N}_1^2 - \tilde{N}_2^2 - \tilde{N}_3^2 = 0. \quad (188f)$$

This dynamical system is formally the same as that in (134), but with absent cross terms  $\tilde{N}_1\tilde{N}_2$ ,  $\tilde{N}_2\tilde{N}_3$ ,  $\tilde{N}_3\tilde{N}_1$  and with  $v$  replaced by  ${}^A v$ , where the superscript  $A$  refers the dominant potential  ${}^{A=\text{Dom}}V$ . Thus the two dynamical systems generated by (134) and (188) share the same Bianchi type I and II heteroclinic structure. Since this structure is expected to describe the generic asymptotic dynamics toward the singularity (at least when  $k_{5,6} = 0$ ),

the analysis of the heteroclinic structure in the main part of the paper of the  $\lambda$ - $R$  models is therefore arguably of relevance for the generic singularity of a large class of HL models.

Let us now deduce the ‘dominant’ dynamical system (188) from the general HL dynamical system (180). Recall that the dominant dynamical system was obtained by:

- (i) setting all potentials  ${}^A V$  to zero, except for the potential  ${}^A V$  with  $A = \text{Dom}$ , i.e., the potential with the largest value of  $A \in \{1, \{2, 3\}, 4, \{5, 6\}\}$  with non-zero coefficient  $k_A$ . This corresponds to the invariant subset of (180) for which all variables  ${}^A N_\alpha$  are set to zero, except for  $A = \text{Dom}$ , which leads to three non-zero  ${}^{\text{Dom}} N_\alpha$  variables. Note that the constraints (179) are automatically satisfied for subsets that only involve one of the potentials  ${}^A V$  where  $A = \{1, \{2, 3\}, 4, \{5, 6\}\}$ . We will refer to this invariant subset of (180) as the *invariant dominant subset*;
- (ii) setting all the cross terms in the potential  ${}^A V$  with  $A = \text{Dom}$  to zero, which thereby yields  $V_{\text{Dom}} = {}^A V_{\text{II}_1} + {}^A V_{\text{II}_2} + {}^A V_{\text{II}_3}$  for  $A = \text{Dom}$ . In the dynamical system this is achieved by setting all cross terms involving  ${}^{\text{Dom}} N_1$ ,  ${}^{\text{Dom}} N_2$ ,  ${}^{\text{Dom}} N_3$  in the invariant dominant subset in (180) to zero. This results in a system where  $\Omega_k$ ,  $\Omega_\lambda$  and  $S_\alpha$  are linear in  $({}^{2,3} N_\alpha)^4$ ,  $({}^4 N_\alpha)^5$ ,  $({}^{5,6} N_\alpha)^6$ , if  $A = \text{Dom} = \{2, 3\}, 4, \{5, 6\}$ , respectively. This makes it possible to perform a variable transformation from the dominant variables  ${}^{\text{Dom}} N_\alpha$  to new variables  ${}^{\text{Dom}} \tilde{N}_\alpha$  which yield quadratic polynomials, e.g.,  ${}^{2,3} \tilde{N}_\alpha = ({}^{2,3} N_\alpha)^2$  if  $A = \text{Dom} = \{2, 3\}$ . To finally obtain the system (188) from (180), replace  $v$  with  ${}^A v$ ,  $A = \text{Dom}$ , according to (161a), and replace  ${}^{\text{Dom}} N_\alpha$  with the new variables  $\tilde{N}_\alpha$ . Finally, change the time variable to  $\tilde{\tau}_- := 2\tau_- / {}^A a$ , where  ${}^A a$  is defined in (161b) for  $A = \text{Dom}$ .

The heuristic arguments in this appendix thus suggest that the  $\omega$ -limits (as  $\tau_- \rightarrow \infty$ ) for generic Bianchi type IX solutions (and type VIII, if  $A = \text{Dom} \neq 4$ , as discussed previously) of the evolution equation (180) reside on the union of the Bianchi type I and II subsets on the invariant dominant subset. Replacing  $v$  with  ${}^A v$ ,  $A = \text{Dom}$ , and using the Hamiltonian/Gauss constraint to solve for the single  ${}^{\text{Dom}} N_\alpha$  variable in each of the type  $\text{II}_\alpha$  subsets, leads to the equations in  $(\Sigma_1, \Sigma_2, \Sigma_3)$ -space used in the main text to discuss the heteroclinic network on the union of the type I and II subsets for the  $\lambda$ - $R$  models, if one changes the time variable according to  $\tilde{\tau}_- := 2\tau_- / {}^{\text{Dom}} a$ .<sup>25</sup> The results in the main part of the paper thereby heuristically apply to a broad class of HL models.

## B First principles and the Bianchi hierarchy

In this appendix, we derive monotone functions and conserved quantities at each level of the class A Bianchi hierarchy from the associated scale and automorphism symmetry

---

<sup>25</sup>This is the reason we obtain the results in [27] as special cases of our results for the Bianchi type II  $\lambda$ - $R$  models. Incidentally, we could have introduced the Kasner parameter  $u$ , as in said reference. The Kasner map describing how  $u$  changes follows from (24), (35) and (36). However, the range and domain of  $u$  differ from the critical GR case when  $v \neq 1/2$ . This suggests that one should use an extended Kasner parameter, see [89]. However, since the parameter  $v$  leads to a complicated expression for the Kasner map for  $u$ , we do not pursue this possibility.

hierarchy. These structures are inherited from the first principles of scale and diffeomorphism invariance, as shown for the GR case in [34]. The present models do not change the automorphism group, but they do have different scale symmetries, which yield different results for the  $\lambda$ - $R$  and HL models.

## B.1 $\lambda$ - $R$ models

### Bianchi types VIII and IX

We here derive a monotone function, called  $\Delta$ . The decay of  $\Delta$  in time implies that the type VIII and IX solutions converge to next level in the class A Bianchi hierarchy, the union of the invariant type VI<sub>0</sub> and VII<sub>0</sub> boundary sets, as discussed in Section 6.

The Hamiltonian for Bianchi type VIII and IX is characterized by

$$T + V = \frac{1}{2} (-p_\lambda^2 + p_+^2 + p_-^2) + 6e^{8v\beta^\lambda} \bar{V}(\beta^\pm) = 0. \quad (189)$$

The kinetic part defines the DeWitt metric  $\eta_{AB} = \text{diag}(-1, 1, 1)$  for  $A, B = \lambda, \pm$ , and its inverse  $\eta^{AB} = \text{diag}(-1, 1, 1)$ , since we can write the kinetic part as  $T = \eta^{AB} p_A p_B / 2$ . The diagonal type VIII and IX models admit no (diagonal) automorphisms since all the structure constants,  $n_1, n_2, n_3$ , are non-zero. However, the field equations of all vacuum  $\lambda$ - $R$  models admit a scale symmetry, which thereby leads to a scale symmetry for the potential in (189), obtained by translations in  $\beta^\lambda$ . Moreover, in the potential  $V = 6e^{8v\beta^\lambda} \bar{V}(\beta^\pm)$  the exponent  $8v\beta^\lambda$  is clearly timelike with respect to  $\eta_{AB}$  in  $(\beta^\lambda, \beta^+, \beta^-)$ -space when  $v \in (0, 1)$ . Similarly as in GR, see ch. 10 in [95] and [34], this leads to a monotone function, given by  $e^{8v\beta^\lambda} / p_\lambda^2 \propto (N_1 N_2 N_3)^{2/3}$ . Choosing to scale this with 3 so that  $\Omega_k + \Delta \geq 0$  in Section 6 yields

$$\Delta := 3(N_1 N_2 N_3)^{2/3}, \quad (190a)$$

$$\Delta' = -8v\Sigma^2\Delta, \quad (190b)$$

where we have used the chain rule and (4b).

### Bianchi types VI<sub>0</sub> and VII<sub>0</sub>

We now show that the scale-automorphism group for type VI<sub>0</sub> and VII<sub>0</sub> yields the functions  $(1 + 2v\Sigma_+, Z_{\text{sub}}, Z_{\text{sup}}$  and  $Z_{\text{crit}})$ . These functions have different consequences for the subcritical, supercritical and critical cases, discussed in Section 6. In particular,  $1 + 2v\Sigma_+$  is useful in all cases and is derived first; then we derive  $Z_{\text{sub}}$  ( $Z_{\text{sup}}$ ), which is useful for the subcritical (supercritical) case, where  $Z_{\text{sub}} = Z_{\text{sup}} = Z_{\text{crit}}$  for the critical case.

Let  $n_1 = 0, n_2 = n_3 = 1$  for type VII<sub>0</sub> and  $n_1 = 0, n_2 = -n_3 = 1$  for type VI<sub>0</sub>, without loss of generality. Then, according to equation (157a), the Hamiltonian is described by,

$$T + V = \frac{1}{2} (-p_\lambda^2 + p_+^2 + p_-^2) + 6e^{4(2v\beta^\lambda + \beta^+)} \tilde{m}_-^2 = 0, \quad (191)$$

where we recall that  $\tilde{m}_- = n_2 e^{2\sqrt{3}\beta^-} - n_3 e^{-2\sqrt{3}\beta^-}$ .

There are two special cases characterized by  $\beta^- = p_- = 0$ , discussed in the dynamical systems framework in Section 6. The first is given by the locally rotationally symmetric (LRS) type VII<sub>0</sub> models, which have an extra space-time isometry and thereby a 4-dimensional multiply transitive isometry group. Since  $\beta^- = p_- = 0$  implies  $\tilde{m}_- = 0$  and thus  $V = 0$ , both  $\beta^\lambda$  and  $\beta^+$  become cyclic variables and hence  $p_\lambda$  and  $p_+$  are constants. Moreover, the Hamiltonian constraint yields  $p_+ = \pm p_\lambda$ , which corresponds to the two invariant disjoint lines  $\Sigma_+ = \pm 1$ ,  $\Sigma_- = 0$ ,  $N := N_2 = N_3$ . The second case results in the special type VI<sub>0</sub> models, which exist due to the discrete symmetry  $\beta^- \rightarrow -\beta^-$ , and correspond to a space-time with a discrete isometry, in contrast to the continuous extra isometry in the LRS type VII<sub>0</sub> case. Since  $\beta^- = p_- = 0$  is an invariant set, it follows that so is  $\Sigma_- = 0$ ,  $N_2 = -N_3$ . Moreover, since  $\beta^- = p_- = 0$  implies  $\tilde{m}_-^2 = \text{constant} > 0$ , the Hamiltonian constraint yields  $|\Sigma_+| < 1$ . Below we will treat the special type VI<sub>0</sub> models together with the general ones.

Excluding the special cases with  $\beta^- = p_- = 0$ , the exponent  $4(2v\beta^\lambda + \beta^+)$  and  $\tilde{m}_-$  in the potential in (191) shows that there are only two independent variables in the Hamiltonian,  $2v\beta^\lambda + \beta^+$  and  $\beta^-$ . It hence follows that there is a cyclic variable and an associated conserved quantity. The underlying reason is that the models with  $n_1 = 0$  admit a non-unimodular automorphism in addition to the scale symmetry. Following [34] and [80] and combining the non-unimodular autmorphism and the scale symmetry appropriately yields a variational symmetry and thereby a conserved quantity, given by

$$p_\lambda - 2vp_+ = \text{constant}, \quad (192)$$

as follows from Hamilton's equations.

Since  $p_\lambda$  is monotone, apart from in the LRS type VII<sub>0</sub> case, as follows from Hamilton's equation (133), dividing (192) with  $p_\lambda$  yields a monotone function, except when  $p_\lambda - 2vp_+ = 0$ . This, however, can only happen in the supercritical case  $v \in (1/2, 1)$ , since the Hamiltonian constraint yields  $|p_\lambda| > |p_+|$ . Expressing the quotient  $(p_\lambda - 2vp_+)/p_\lambda$  in the dynamical systems variables results in

$$\frac{p_\lambda - 2vp_+}{p_\lambda} = 1 + 2v\Sigma_+, \quad (193)$$

which evolves according to

$$(1 + 2v\Sigma_+)' = 4v(1 - \Sigma^2)(1 + 2v\Sigma_+). \quad (194)$$

Further insights come from explicitly introducing cyclic variables that respect the kinetic part of the Hamiltonian, which is done next. More specifically, in the subcritical and supercritical cases, we make a Lorentz transformation in the  $(\beta^\lambda, \beta^\pm)$ -space with respect to  $\eta_{AB}$ , where these transformations preserve the form of the kinetic part in (191) by definition, i.e.,  $T = \eta^{AB}p_A p_B/2$ . However, note that with respect to  $\eta_{AB}$ , the exponent  $4(2v\beta^\lambda + \beta^+)$  is spacelike for the subcritical case  $v \in (0, 1/2)$ , null for the critical case  $v = 1/2$ , and timelike for the supercritical case  $v \in (1/2, 1)$ . The different causal characters again reflect that a bifurcation takes place when  $v = 1/2$ .

In the subcritical case,  $v < 1/2$ , a boost with velocity  $-2v$  results in

$$\tilde{\beta}^\lambda = \Gamma(\beta^\lambda + 2v\beta^+), \quad \beta^\lambda = \Gamma(\tilde{\beta}^\lambda - 2v\tilde{\beta}^+), \quad (195a)$$

$$\tilde{\beta}^+ = \Gamma(2v\beta^\lambda + \beta^+), \quad \beta^+ = \Gamma(-2v\tilde{\beta}^\lambda + \tilde{\beta}^+), \quad (195b)$$

where  $\Gamma = (1 - (2v)^2)^{-1/2}$ . Hence (191) is transformed to

$$T + V = \frac{1}{2} (-\tilde{p}_\lambda^2 + \tilde{p}_+^2 + p_-^2) + 6e^{4\tilde{\beta}^+/\Gamma} \tilde{m}_-^2 = 0. \quad (196)$$

The fact that  $\tilde{p}_\lambda$  is conserved leads to a reduced problem for  $\tilde{\beta}^+$  and  $\beta^-$  with energy  $E = \tilde{p}_\lambda^2/2$ . Note that the Hamiltonian thereby takes the same form as when  $v = 0$ , as for the HL models with dominant potential <sup>5,6</sup> $V$ . The reduced problem thereby yields a generalized Toda problem in two dimensions, see [13]. The conserved quantity  $\tilde{p}_\lambda = \Gamma(p_\lambda - 2vp_+)$  results in (193), and consequently (194). Moreover,  $\tilde{p}_\lambda \neq 0$  due to (196), and since we are considering expanding models,  $\tilde{p}_\lambda < 0$ . Since  $\tilde{p}_\lambda$  has the same sign as  $p_\lambda$ , it follows that  $\tilde{p}_\lambda/p_\lambda > 0$ , which implies that  $1 + 2v\Sigma_+ > 0$  in the subcritical case  $v < 1/2$ . As a consequence,  $1 + 2v\Sigma_+$  is a monotone function in the entire state space, as described in (194), apart from when  $\Sigma^2 = 1$ , which only happens for the Bianchi type I and the LRS type VII<sub>0</sub> invariant sets.

When  $p_- \neq 0$ , the Hamiltonian equations for the reduced Toda problem for  $\tilde{\beta}^+$  and  $\beta^-$  implies that a solution originates at  $\tilde{\beta}^+ \rightarrow -\infty$ , and reaches a maximal but finite value of  $\tilde{\beta}^+$ , and then turn back and ends at  $\tilde{\beta}^+ \rightarrow -\infty$ , where the asymptotic origin and end correspond to  $\tau_- \rightarrow \pm\infty$ . To translate these claims into rigorous dynamical results, note that the exponential  $e^{4\tilde{\beta}^+/\Gamma}$  in the potential plays a key role. Dividing the conserved quantity  $\tilde{p}_\lambda^2$  with this exponential yields a dimensionless quantity, which when expressed in the dynamical systems variables results in

$$Z_{\text{sub}} = \frac{(1 + 2v\Sigma_+)^2}{|N_2 N_3|}, \quad (197a)$$

$$Z'_{\text{sub}} = 4(2v + \Sigma_+)Z_{\text{sub}}. \quad (197b)$$

In the supercritical case,  $v > 1/2$ , consider a boost with velocity  $-1/(2v)$ , i.e.,

$$\tilde{\beta}^\lambda = \Gamma \left( \beta^\lambda + \frac{\beta^+}{2v} \right), \quad \beta^\lambda = \Gamma \left( \tilde{\beta}^\lambda - \frac{\tilde{\beta}^+}{2v} \right), \quad (198a)$$

$$\tilde{\beta}^+ = \Gamma \left( \frac{\beta^\lambda}{2v} + \beta^+ \right), \quad \beta^+ = \Gamma \left( -\frac{\tilde{\beta}^\lambda}{2v} + \tilde{\beta}^+ \right), \quad (198b)$$

where  $\Gamma = (1 - (2v)^{-2})^{-1/2}$ . This results in that (191) takes the form

$$T + V = \frac{1}{2} (-\tilde{p}_\lambda^2 + \tilde{p}_+^2 + p_-^2) + 6e^{8v\tilde{\beta}^\lambda/\Gamma} \tilde{m}_-^2 = 0. \quad (199)$$

In this case  $\tilde{p}_+$  is conserved, which implies that  $\tilde{p}_+/p_\lambda = \Gamma(1 + 2v\Sigma_+)$  is monotone when  $\tilde{p}_+ \neq 0$ , since  $p_\lambda$  is monotone. Setting  $\tilde{p}_+ = 0$  yields the invariant set  $1 + 2v\Sigma_+ = 0$ . Invariance under the transformation  $(\beta^+, \tilde{p}_+) \rightarrow -(\beta^+, \tilde{p}_+)$  shows that the models exhibit a discrete symmetry. As a consequence the invariant subset  $1 + 2v\Sigma_+ = 0$  forms a separatrix surface which divides the remaining state space into two disjoint sets. Moreover, the discrete symmetry results in that the flow of (194) is equivariant under a change of sign of the monotone function  $1 + 2v\Sigma_+$ . In addition, the intersection of the special type

VI<sub>0</sub> subset,  $\beta^- = p_- = 0$  (i.e.,  $\Sigma_- = 0$  and  $N_2 = -N_3$ ) and the subset  $1 + 2v\Sigma_+ = 0$  (i.e.,  $\tilde{\beta}^+ = \tilde{p}_+ = 0$ ) yields the fixed point  $\Sigma_+ = -1/(2v)$ ,  $\Sigma_- = 0$ ,  $N_2 = -N_3 = \sqrt{1 - (2v)^{-2}}$ .

In the supercritical case, the above structures are not the only ones that can be extracted from the scale-automorphism group. As in the type VIII and IX models, we have a potential with an exponential with a timelike variable with respect to  $\eta_{AB}$  that multiplies a function that depends on spacelike variables (only  $\beta^-$  in this case), see (199), after the transformation (195). Following ch. 10 in [95], there is a monotone function given by  $6e^{8v\tilde{\beta}^\lambda/\Gamma}/\tilde{p}_\lambda^2$ , except when  $\tilde{\beta}^+ = \tilde{p}_+ = \beta^- = p_- = 0$  in type VI<sub>0</sub>, i.e., at the fixed point in these models. This results in that  $Z_{\text{sup}} \propto \tilde{p}_\lambda^2 e^{-8v\tilde{\beta}^\lambda/\Gamma}$  is monotone, and expressing this function in the state space variables results in

$$Z_{\text{sup}} = \frac{(2v + \Sigma_+)^2}{N_2 N_3}, \quad (200a)$$

$$Z'_{\text{sup}} = 4 \left[ \frac{(1 + 2v\Sigma_+)^2 + (4v^2 - 1)\Sigma_-^2}{2v + \Sigma_+} \right] Z_{\text{sup}}, \quad (200b)$$

where the last equation is obtained from (87). Hence  $Z_{\text{sup}}$  is monotonically increasing, except at the type VI<sub>0</sub> fixed point (90). In type VII<sub>0</sub>, the variables  $\Sigma_+ = -1/(2v)$ ,  $\Sigma_- = 0$  do not correspond to an invariant subset. If an orbit passes through these values, this implies that this only yields an inflection point for the monotonically increasing  $Z_{\text{sup}}$ .

In the critical GR case,  $v = 1/2$ , we introduce the null variables

$$u := \beta^\lambda + \beta^+, \quad w := \beta^\lambda - \beta^+, \quad (201)$$

which results in

$$T + V = -2p_w p_w + \frac{1}{2} p_-^2 + 6e^{2u} \tilde{m}_-^2 = 0. \quad (202)$$

Since  $w$  is a cyclic variable,  $p_w = (p_\lambda - p_+)/2 = \text{constant} \leq 0$ , where the inequality follows from the Hamiltonian constraint and from  $p_\lambda < 0$ , which holds for expanding models. The Hamiltonian constraint implies that the equality only occurs for the LRS type VII<sub>0</sub> models. Apart from this special case,  $1 + \Sigma_+$  is a monotone function in both type VI<sub>0</sub> and VII<sub>0</sub> according to (194) with  $v = 1/2$ .

In the critical GR case,  $v = 1/2$ , the functions  $Z_{\text{sub}} = Z_{\text{sup}} = Z_{\text{crit}}$  in (197) and (200) yields

$$Z_{\text{crit}} = \frac{(1 + \Sigma_+)^2}{N_2 N_3}, \quad (203a)$$

$$Z'_{\text{crit}} = 4(1 + \Sigma_+) Z_{\text{crit}} \quad (203b)$$

Thus  $Z_{\text{sub}} = Z_{\text{sup}} = Z_{\text{crit}}$  is thereby also a monotone function in the critical case, except at the LRS type VII<sub>0</sub> subset  $\Sigma_+ = -1$ ,  $\Sigma_- = 0$ ,  $N_2 = N_3 = N$ .

The underlying reason for the existence of the monotone function  $Z_{\text{sup}} = Z_{\text{crit}}$  in (203) is the scaling property of the potential obtained by a translation in  $u$ , see (202), and the conserved momentum  $p_w$ , which in turn is a consequence of the scale-automorphism group. Apart from the LRS type VII<sub>0</sub> subset where  $p_w = 0$  and thereby  $\Sigma_+ = -1$ , these two features taken together yield the monotone function  $Z_{\text{sup}} = Z_{\text{crit}} \propto p_w^2 e^{-4u} = (p_w e^{-2u})^2$ .

Thus  $Z_{\sup}$  is a monotone function when  $v \in [1/2, 1)$ , but not in the subcritical case  $v \in (0, 1/2)$ . The reason for this is the change in causal character of the exponent  $4(2v\beta^\lambda + \beta^+)$  in the potential and the Hamiltonian constraint (196), which prevents  $\tilde{p}_+^{-2}e^{4\tilde{\beta}^+/\Gamma}$  from being a monotonically changing ‘energy’, as described in the qualitative picture of the dynamics in [92] and ch. 10 in [95] when the exponent is timelike.

Incidentally, the Hamiltonian (199) for type VI<sub>0</sub> is mathematically closely related to the GR Bianchi type II models with a perfect fluid obeying a linear equation of state  $p = w\rho$ ,  $w \in [0, 1)$ , where  $p$  is the pressure and  $\rho$  the energy density, see [88], ch. 10 in [95]. The difference is that due to steeper walls in the heuristic wall description of the Hamiltonian (199) the present models give rise to a heteroclinic cycle, which is not the case for the type II perfect fluid models. Also note that in the subcritical case,  $v \in (0, 1/2)$ , the special type VI<sub>0</sub> models with  $\beta^- = p_- = 0$  yield the same mathematical problem as the type II models discussed next when restricted to the type II LRS case with  $p_- = 0$ , after appropriate translations and rescalings of  $\tilde{\beta}^\lambda$ ,  $\tilde{\beta}^+$  and  $\tau_-$ . Moreover, in the supercritical case, the special type VI<sub>0</sub> models yield the same mathematical problem as the LRS GR Bianchi type I models with a perfect fluid with  $p = w\rho$ .

## Bianchi types II

Next we derive the key building block for the heteroclinic structure from scale-automorphism symmetries, i.e., the straight Bianchi type II trajectories in  $\Sigma_\pm$ -space, and thereby those in  $(\Sigma_1, \Sigma_2, \Sigma_3)$ -space, given by (23).

Without loss of generality, we consider the Bianchi type II<sub>1</sub> case with the Hamiltonian:

$$T + V = \frac{1}{2}(-p_\lambda^2 + p_+^2 + p_-^2) + 6e^{8(v\beta^\lambda - \beta^+)} = 0. \quad (204)$$

Since  $\beta^-$  is a cyclic variable,  $p_-$  is constant. This occurs since the type II models with  $n_2 = n_3 = 0$  admit a unimodular automorphism, which generates a variational symmetry and thereby the conserved momentum  $p_-$ . As in the type VI<sub>0</sub> and VII<sub>0</sub> cases, these models also admit a scale-automorphism symmetry, obtained by combining the scale symmetry with the remaining non-unimodular automorphism, which yields a variational symmetry and an additional cyclic variable. This is made explicit by performing a boost in the  $\beta^+$ -direction in  $(\beta^\lambda, \beta^\pm)$ -space with a velocity  $v$ , i.e.,

$$\tilde{\beta}^\lambda = \Gamma(\beta^\lambda - v\beta^+), \quad \beta^\lambda = \Gamma(\tilde{\beta}^\lambda + v\tilde{\beta}^+), \quad (205a)$$

$$\tilde{\beta}^+ = \Gamma(-v\beta^\lambda + \beta^+), \quad \beta^+ = \Gamma(v\tilde{\beta}^\lambda + \tilde{\beta}^+), \quad (205b)$$

where  $\Gamma = (1 - v^2)^{-1/2}$ . This leads to the following expression,

$$T + V = \frac{1}{2}(-\tilde{p}_\lambda^2 + \tilde{p}_+^2 + p_-^2) + 6e^{-8\tilde{\beta}^+/\Gamma} = 0, \quad (206)$$

which shows that not only  $\beta^-$  but also  $\tilde{\beta}^\lambda$  is a cyclic variable. Thus both  $p_-$  and  $\tilde{p}_\lambda$  are constant.<sup>26</sup>

<sup>26</sup>Note that in the heuristic moving wall description, the wall moves in the *positive*  $\beta^+$ -direction in

Since both  $p_-$  and  $\tilde{p}_\lambda = \Gamma(p_\lambda + vp_+)$  are constants, it follows that dividing the following relation between the constants  $p_- \propto p_\lambda/v + p_+$  with  $-p_\lambda$ , and using that  $\Sigma_\pm = p_\pm/(-p_\lambda)$ , leads to

$$\Sigma_- = \text{constant} \left( \Sigma_+ - \frac{1}{v} \right), \quad (207)$$

where the constant parametrizes the various heteroclinic Bianchi type II orbits. This equation also holds for the initial values  $\Sigma_\pm^i$  of  $\Sigma_\pm$  on  $K^\circlearrowright$  and dividing the above equation with  $\Sigma_-^i = \text{constant} (\Sigma_+^i - v^{-1})$  yields

$$\left( \Sigma_+^i - \frac{1}{v} \right) \Sigma_- = \Sigma_-^i \left( \Sigma_+ - \frac{1}{v} \right). \quad (208)$$

Equation (23) then follows from the definitions  $\Sigma_1 = -2\Sigma_+$  and  $\Sigma_{2,3} = \Sigma_+ \pm \sqrt{3}\Sigma_-$ .

## Bianchi type I

The Kasner circle of fixed points  $K^\circlearrowright$  follows straightforwardly from the scale-automorphism symmetry group. Bianchi type I is obtained by a Lie contraction of Bianchi type II, which results in that all structure constants become zero, which yield an Abelian symmetry group. This leads to one more special automorphism, which, together with the other automorphisms and the (trivial) scale symmetry, implies that all variables  $\beta^\lambda$ ,  $\beta^+$ ,  $\beta^-$  are cyclic, and hence that all momenta  $p_\lambda$ ,  $p_+$ ,  $p_-$  are conserved. Thus  $\Sigma_+$  and  $\Sigma_-$  are constants, and due to the Hamiltonian constraint,  $T + V = (-p_\lambda^2 + p_+^2 + p_-^2)/2 = 0$ , they satisfy  $\Sigma_+^2 + \Sigma_-^2 = 1$ .

## B.2 HL models

Equation (161) and (162) provide a unified picture of the individual  ${}^AV$  potentials for the HL class A Bianchi hierarchy, which we here, for the reader's convenience, repeat:

$${}^AV = e^{4av\beta^\lambda} ({}^A\bar{V}), \quad \text{for types IX and VIII,} \quad (209a)$$

$${}^AV_{VII_0, VI_0} = e^{2a(2v\beta^\lambda + \beta^+)} ({}^A\tilde{V}), \quad \text{for types VII}_0 \text{ and VI}_0, \text{ with } n_1 = 0, \quad (209b)$$

$${}^AV_{II_1} = \frac{c n_1^a}{2} e^{4a(v\beta^\lambda - \beta^+)}, \quad \text{for type II}_1, \quad (209c)$$

where, for notational brevity, we have refrained from writing the superscript  $A$  on  ${}^Aa$ ,  ${}^Av$  and  ${}^Ac$ , where

$${}^1v = v := \frac{1}{\sqrt{2(3\lambda - 1)}}, \quad {}^{2,3}v = \frac{v}{4}, \quad {}^4v = \frac{v}{10}, \quad {}^{5,6}v = 0, \quad (210a)$$

$${}^1a = 2, \quad {}^{2,3}a = 4, \quad {}^4a = 5, \quad {}^{5,6}a = 6, \quad (210b)$$

$${}^1c = -12k_1, \quad {}^{2,3}c = 6k_{2,3}, \quad {}^4c = -24k_4, \quad {}^{5,6}c = 3k_{5,6}. \quad (210c)$$

---

$(\beta^\lambda, \beta^\pm)$ -space with a speed  $v$ , while the wall moves in the negative  $\beta^+$ -direction with time  $\tau_- = -\beta^\lambda$ . The speed of the wall is also the speed of the above boost, which thereby transforms the moving wall to a motionless wall. This yields the bounce law (142) for the moving particle by means of the conserved quantities.

The automorphism group is the same for all models, but the scale-property of the individual potentials is different for different  $A$ . Nevertheless, as seen from (209) there is a close relationship, one simply replace the constants  ${}^1v = v$ ,  ${}^1a = 2$  and  ${}^1c = 12$  in the  $\lambda$ - $R$  case with  ${}^A v$ ,  ${}^A a$  and  ${}^A c$  to take care of this difference. There is thereby a close connection between all single potential term HL models. However, note that for type IX and VIII the exponent  $e^{4av\beta^\lambda}$  is timelike when  $A = 1, \{2, 3\}, 4$  while it is a constant when  $A = 5, 6$  where  $A = 5, 6$  represent a bifurcation since  ${}^{5,6}v = 0$ . Hence, for the same reason as for the  $\lambda$ - $R$  models,  $e^{4av\beta^\lambda}/p_\lambda^2$  yields a monotone function for each HL model with a specific value of  $A \in 1, \{2, 3\}, 4$ . When  $A = 5, 6$ ,  $p_\lambda$  is conserved, which results in that  $({}^{5,6}N_1)({}^{5,6}N_2)({}^{5,6}N_3) = \text{constant}$ .

In type VII<sub>0</sub>, VI<sub>0</sub> and II<sub>1</sub>, one just replaces the boost in the  $\lambda$ - $R$  case with an analogous boost that follows from (209), to obtain similar conserved quantities and monotone functions for each HL model. However, in the dynamical systems description these quantities sometimes take a different form due to the different relations with the associated  $N_\alpha$  variables, see (175) and (176), but e.g.,  $1 + 2v\Sigma_+$  in the  $\lambda$ - $R$  type VII<sub>0</sub> and VI<sub>0</sub> models is just replaced with  $1 + 2^A v\Sigma_+$ . Similarly in type II<sub>1</sub>,  $\Sigma_- = \text{constant}(\Sigma_+ - v^{-1})$  is replaced with  $\Sigma_- = \text{constant}(\Sigma_+ - ({}^A v)^{-1})$ , and thus models with  $A = 1, \{2, 3\}, 4$  have formally the same heteroclinic type II structure as the  $\lambda$ - $R$  models with  $v \in (0, 1)$ , although recall that  ${}^A v$  for those values of  $A$  are differently related to  $\lambda$  than  ${}^1v = v$ , see (210a). There are thus very strong relationships between the dynamics of the  $\lambda$ - $R$  models and the HL models with single curvature terms as potentials.

Then recall the heuristic argument that asymptotically toward the singularity there exists a dominant single potential (the one with the largest value of  $A$ ), and an associated invariant subset in the HL dynamical systems formulation. With the exception that if this is the  ${}^{5,6}V$  potential, which corresponds to a bifurcation since  ${}^{5,6}v = 0$ , the correspondence between conserved quantities and monotone functions between the  $\lambda$ - $R$  models and the remaining HL models suggests that generic dynamics toward the singularity is going to be described by the heteroclinic Bianchi type II and I structure on the dominant invariant subset. This is also suggested by the dominant Hamiltonian and the associated dominant dynamical system. Hence we conjecture that the discrete analysis of the heteroclinic structure in the  $\lambda$ - $R$  case in the main part of the paper is also describing the asymptotic dynamics of HL models for which  ${}^{5,6}V = 0$ . The above also suggests that there are similar dynamical conjectures for these HL models as those in Section 7 for the  $\lambda$ - $R$  case.

## C A unified critical and supercritical treatment

In this Appendix we modify the proof about chaos within the non-generic Cantor set of the supercritical case, given in Section 4.4, to also accommodate the critical GR case, in which chaos is generic. The method pursued in order to achieve chaoticity that suits both the critical and the supercritical cases is the construction of a topological conjugacy to a shift map, in analogy with the use of the encoding map  $h$  in (79). This yields a new proof for chaos in GR and relates the supercritical symbolic dynamics construction to the limiting case of GR, thereby providing a unified treatment of the two cases.

Before we proceed, we mention that there are different ways to incorporate the methods of symbolic dynamics used in the supercritical case to also describe chaos in the critical GR case. We will give a description that is a *continuous* transition from the supercritical case  $v > 1/2$  to the critical case  $v = 1/2$ . This is accomplished by designing a new encoding map  $\tilde{h}$  which is continuous in  $v \in [1/2, 1]$ . This new map behaves in a similar manner as the encoding map  $h$  in (79) for infinite heteroclinic sequences when  $v > 1/2$ , but it also appropriately encodes points that reach the Taub points when  $v = 1/2$ , and thus it remains a well-defined homeomorphism in the limit  $v \rightarrow 1/2$ .

The challenge of a unified treatment lies in the following continuity issue. For all  $v \in [1/2, 1)$ , define the set  $C_v$  of points that never reach the set  $S$ , as in (40). When  $v > 1/2$  decreases, the set  $S$  shrinks and collapses to the Taub points at  $v = 1/2$  (i.e.,  $S = T_1 \cup T_2 \cup T_3$  when  $v = 1/2$ ), where  $C_{1/2}$  thereby consists of points that never reach the Taub points via the Kasner circle map  $\mathcal{K}$ . On the other hand, the heteroclinic chains with period 2, see Figure 14, which are in  $C_v$  (and behaves like its ‘boundary’) when  $v > 1/2$ , converge to the Taub points as  $v \rightarrow 1/2$ , which do not belong to  $C_{1/2}$ . This implies that the set  $C_v$  is not continuous with respect to the parameter  $v$  at  $v = 1/2$ . In other words, the set  $\lim_{v \rightarrow 1/2} C_v$  is different than  $C_{1/2}$ .<sup>27</sup> Thus one should not expect that the encoding map  $h$ , given by (79), is continuous (in  $v$ ) at  $v = 1/2$ . To deal with this discrepancy, and guarantee an accurate continuous transition of non-generic to generic chaos, we also have to encode the Taub points (and their pre-images) in the limit  $v = 1/2$ , which are the limits of the heteroclinic chains with period 2 when  $v > 1/2$ .

Two problems arise when trying to encode the Taub points when  $v = 1/2$ . Consider  $(\alpha\beta\gamma)$  a permutation of  $(123)$ . First, each Taub point lies in two different arcs,  $T_\alpha \in A_\beta \cap A_\gamma$ , and could thereby be described by two different symbols,  $\beta$  or  $\gamma$ , which would make the encoding map ill-defined. Second, it is not clear how to encode each Taub point in order to obtain infinite sequences in  $W_\infty$ , since it is possible to assign different infinite tails to the finite heteroclinic chains that end at the Taub points.

To resolve these problems, recall that each heteroclinic chain with period 2 (where the sequence of points in the set  $K^\circ$  of the heteroclinic chain is encoded by  $\beta\gamma\beta\gamma\dots$  or  $\gamma\beta\gamma\beta\dots$ , in Figure 14) converges to the Taub point  $T_\alpha$  when  $v \rightarrow 1/2$ . In order to guarantee a continuous limit, it is natural that *both* infinite sequences,  $\overline{\beta\gamma} := \beta\gamma\beta\gamma\dots$  and  $\overline{\gamma\beta} := \gamma\beta\gamma\beta\dots$ , encode the Taub point  $T_\alpha$  at  $v = 1/2$ . To ensure that the encoding map is well-defined, each Taub point should be encoded by a single infinite sequence of symbols, and thus the two periodic sequences given by  $\overline{\beta\gamma}$  and  $\overline{\gamma\beta}$  will be considered to be in the same equivalence class in the space of infinite words  $W_\infty$ . This assures that each chain with period 2 is encoded by a single infinite sequence for  $v > 1/2$ , and that each Taub point is encoded by the same sequence when  $v = 1/2$ , which results in continuity in  $v$ .

More precisely, we define an equivalence relation  $\sim$  in  $W_\infty$  as follows. Two sequences

---

<sup>27</sup>Recall that  $C_v$  is a Cantor set (closed, without isolated points and nowhere dense) for  $v \in (1/2, 1)$ . On the one hand, the only common feature the set  $C_{1/2}$  possesses when compared to  $C_v$  with  $v > 1/2$  is that both sets have no isolated points, whereas  $C_{1/2}$  is not closed, nor nowhere dense, since the (countably many) pre-images of Taub points are removed from the Kasner circle. On the other hand, the limiting set  $\lim_{v \rightarrow 1/2} C_v$  is the whole Kasner circle, and is thereby closed, but it has no isolated points and is dense.

$(a_k)_{k \in \mathbb{N}_0}$  and  $(b_k)_{k \in \mathbb{N}_0}$  in  $W_\infty$  are equivalent if, and only if there is an  $n \in \mathbb{N}_0$  such that  $a_k = b_k$  for all  $k = 0, \dots, n-1$  with  $(a_k)_{k \geq n} = \overline{\beta\gamma}$  and  $(b_k)_{k \geq n} = \overline{\gamma\beta}$  for some  $\beta \neq \gamma \in \{1, 2, 3\}$ . We then consider the quotient space endowed with the quotient topology

$$\tilde{W}_\infty := W_\infty / \sim \quad (211)$$

whose elements are the equivalence classes of sequences  $(a_k)_{k \in \mathbb{N}_0}$ , denoted by  $[(a_k)_{k \in \mathbb{N}_0}]$ . An equivalence class thereby contains two or one element(s), if the tail of  $(a_k)_{k \in \mathbb{N}}$  is with period 2 or not, respectively.

The above construction solves the issue of encoding the Taub points, but it introduces a new problem for the heteroclinic chains with period 2: for  $v > 1/2$  the two distinct points of the heteroclinic chain with period 2 given by  $\overline{\beta\gamma}$  and  $\overline{\gamma\beta}$  have the same encoding in  $\tilde{W}_\infty$ , since  $[\overline{\beta\gamma}] = [\overline{\gamma\beta}]$ . To guarantee injectivity of the encoding map, we must relate these two points by means of another equivalence relation. When  $v > 1/2$  we consider the quotient space

$$\tilde{C}_v := C_v / \sim, \quad (212)$$

where two points  $p, q \in \tilde{C}_v$  are equivalent if, and only if, they are contained in the same heteroclinic chain with period 2 of the Kasner circle map  $\mathcal{K}$ . To summarize: elements of  $\tilde{C}_v$  are the equivalence classes of points  $p$ , denoted by  $[p]$ , where an equivalence class contains two or one element(s) if  $p$  has period 2 or not, respectively.

The *encoding map* is now defined as

$$\begin{aligned} \tilde{h} : D(\tilde{h}) &\rightarrow \tilde{W}_\infty \\ [p] &\mapsto \tilde{h}([p]) := [(a_k)_{k \in \mathbb{N}}], \end{aligned} \quad (213)$$

where the domain is the set

$$D(\tilde{h}) = \begin{cases} \tilde{C}_v & \text{if } v > 1/2, \\ \lim_{v \rightarrow 1/2} \tilde{C}_v & \text{if } v = 1/2, \end{cases} \quad (214)$$

and where the sequence  $(a_k)_{k \in \mathbb{N}_0}$  is built as follows:

1. If  $\mathcal{K}^k(p) \neq T_\alpha$  for all  $k \in \mathbb{N}_0$ , then the symbol  $a_k$  is uniquely defined for all  $k \in \mathbb{N}_0$  as the index of the open arc where  $\mathcal{K}^k(p)$  lies, i.e.  $\mathcal{K}^k(p) \in \text{int}(A_{a_k})$ .
2. If  $\mathcal{K}^n(p) = T_\alpha$  for some  $n \in \mathbb{N}_0$ , where  $n$  is the minimum of such values, let

$$h([p]) := [a_0 \dots a_{n-1} \overline{\beta\gamma}], \quad (215)$$

where  $(\alpha\beta\gamma)$  is a permutation of (123).

For  $v > 1/2$  the domain is the previously constructed Cantor set  $C_v = C$ , which does not contain the Taub points, and thus case 2 above never happens. Moreover, the encoding  $\tilde{h}$  coincides with  $h$  in (79), except for the heteroclinic chains with period 2: they consist of two distinct points in  $C_v$  which are identified in  $\tilde{C}_v$  by the equivalence relation in (212), and their two encodings in  $W_\infty$  are identified in  $\tilde{W}_\infty$  by the equivalence relation in (211)

(for example  $[\beta\gamma] = [\gamma\beta]$ ). Furthermore, it is only for  $v = 1/2$  that the Taub points can be reached, so that case 2 above occurs, where a period 2 tail has been added in order to obtain a continuous limit.

Hence,  $\tilde{h}$  is a well-defined homeomorphism in the following commuting diagram,

$$\begin{array}{ccc} D(\tilde{h}) & \xrightarrow{\mathcal{K}} & D(\tilde{h}) \\ \tilde{h} \downarrow & & \downarrow \tilde{h} \\ \tilde{W}_\infty & \xrightarrow{\sigma} & \tilde{W}_\infty \end{array}$$

where  $\sigma$  is the shift to the right of sequences, which thereby establishes that the map  $\mathcal{K}$  is chaotic.

## Acknowledgements

JH was supported by the DFG collaborative research center SFB647 Space, Time, Matter. PL was supported by FAPESP, 17/07882-0, 18/18703-1, in addition to the encouraging, enduring and enlightening discussions with Bernold Fiedler and Hauke Sprink. CU would like to thank the Institut für Mathematik at Freie Universität in Berlin for kind hospitality.

## References

- [1] A. Alho, J. Hell and C. Uggla. Global dynamics and asymptotics for monomial scalar field potentials and perfect fluids. *Class. Quant. Grav.* **32**, (14:145005), (2015).
- [2] L. Andersson, H. van Elst, W. C. Lim and C. Uggla. Asymptotic Silence of Generic Singularities. *Phys. Rev. Lett.* **94**, 051101, (2005).
- [3] H. Anzai. Ergodic Skew Product Transformations on the Torus. *Osaka Math. J.* **3**, 1, (1951).
- [4] A. Arbieto, A. Junqueira and B. Santiago. On Weakly Hyperbolic Iterated Function Systems. *Bull. Braz. Math. Soc.* **48**, 111-140, (2017).
- [5] A. Ashtekar and J. Samuel. Bianchi cosmologies: the role of spatial topology. *Class. Quant. Grav.* **8**, 2191-2215, (1991).
- [6] I. Bakas, F. Bourliot, D. Lust and M. Petropoulos. Mixmaster universe in Hořava-Lifshitz gravity. *Class. Quant. Grav.* **27**, 045013, (2010).
- [7] I. Bakas, F. Bourliot, D. Lust, and M. Petropoulos. Geometric flows in Hořava-Lifshitz gravity. *J. High Energ. Phys.* **131**, (2010).
- [8] V. A. Belinskiĭ, I. M. Khalatnikov, and E. M. Lifshitz. Oscillatory approach to a singular point in the relativistic cosmology. *Adv. Phys.* **19**, 525, (1970).
- [9] V. A. Belinskiĭ, I. M. Khalatnikov, and E. M. Lifshitz. A general solution of the Einstein equations with a time singularity. *Adv. Phys.* **31**, 639, (1982).

- [10] F. Béguin. Aperiodic oscillatory asymptotic behavior for some Bianchi spacetimes. *Class. Quant. Grav.* **27**, 185005, (2010).
- [11] J. Bellorin and A. Restuccia. On the consistency of the Hořava theory. *Int. J. Mod. Phys. D* **21**, 1250029, (2012).
- [12] C. Bonatti, L.J. Diaz and M. Viana. *Dynamics Beyond Uniform Hyperbolicity*. Springer-Verlag, (2005).
- [13] O.I. Bogoyavlensky. *Methods in the qualitative Theory of Dynamical Systems in Astrophysics and Gas Dynamics*. Springer-Verlag, (1985).
- [14] B. Brehm. Bianchi VIII and IX vacuum cosmologies: Almost every solution forms particle horizons and converges to the Mixmaster attractor. [arXiv:1606.08058](https://arxiv.org/abs/1606.08058), (2016).
- [15] G. Calcagni. Cosmology of the Lifshitz universe. *J. High Energy Physics* **2009**, 112, (2009).
- [16] S. Carloni, M. Chaichian, S. Nojiri, S. D. Odintsov, M. Oksanen and A. Tureanu. Modified first-order Hořava-Lifshitz gravity: Hamiltonian analysis of the general theory and accelerating FRW cosmology in power-law F(R) model. *Phys. Rev. D* **82**, 065020, (2010).
- [17] D. M. Chitré. *Ph.D. Thesis*. University of Maryland, (1972).
- [18] T. Damour, M. Henneaux, and H. Nicolai. Cosmological billiards. *Class. Quant. Grav.* **20**, R145, (2003).
- [19] T. Damour, M. Henneaux, A. D. Rendall, and M. Weaver. Kasner like behavior for supercritical Einstein matter systems. *Ann. Henri Poincaré* **3**, 1049, (2002).
- [20] T. Damour, O. M. Lecian. Statistical Properties of Cosmological Billiards. *Phys. Rev. D* **83**, 044038, (2011).
- [21] R. Devaney. *An introduction to chaotic dynamical systems*. Westview press, Second Edition, (2003).
- [22] T. Dutilleul. Chaotic dynamics of spatially homogeneous spacetimes. PhD Thesis, Université Paris 13 - Sorbonne Paris Cité, (2019). [Link](#).
- [23] H. van Elst and C. Uggla. General relativistic 1+3 orthonormal frame approach revisited *Class. Quant. Grav.* **14**, 2673, (1997).
- [24] K. Falconer. *Fractal Geometry: Mathematical Foundations and Applications*. John Wiley and Sons, Second Edition, (2013).
- [25] S. Foster. *Scalar Field Cosmological Models With Hard Potential Walls*. [arXiv:gr-qc/9806113](https://arxiv.org/abs/gr-qc/9806113), (1998).
- [26] D. Garfinkle. Numerical simulations of generic singularities. *Phys. Rev. Lett.* **93**, 161101, (2004).

- [27] L. Giani and A. Y. Kamenshchik. Hořava–Lifshitz gravity inspired Bianchi-II cosmology and the mixmaster universe. *Class. Quant. Grav.* **34**, 085007, (2017).
- [28] D. Giulini and C. Kiefer. Wheeler-DeWitt metric and the attractivity of gravity. *Phys. Lett. A* **193**, 21, (1994).
- [29] C. Grebogi, E. Ott, S. Pelikan and J. Yorke. Crises, sudden changes in chaotic attractors, and transient chaos. *Physica D* **7**, 181-200, (1983).
- [30] C. Grebogi, E. Ott and J. Yorke. Chaotic Attractors in Crisis. *Phys. Rev. Lett.* **48**, 1507, (1982).
- [31] J. M. Heinzle and C. Uggla. A new proof of the Bianchi type IX attractor theorem. *Class. Quant. Grav.* **26**, 075015, (2009).
- [32] J. M. Heinzle and C. Uggla. Mixmaster: Fact and Belief. *Class. Quant. Grav.* **26**, 075016, (2009).
- [33] J. M. Heinzle and C. Uggla. Dynamics of the spatially homogeneous Bianchi type I Einstein-Vlasov equations. *Class. Quant. Grav.* **23**, 3463, (2009).
- [34] J. M. Heinzle and C. Uggla. Monotonic functions in Bianchi models: why they exist and how to find them. *Class. Quant. Grav.* **27**, 015009, (2010).
- [35] J. M. Heinzle and C. Uggla. Spike statistics. *Gen. Rel. Grav.* **45**, 939, (2013).
- [36] J. M. Heinzle, C. Uggla and W. C. Lim. Spike oscillations. *Phys. Rev. D* **86**, 104049, (2012).
- [37] J. M. Heinzle, C. Uggla, and N. Röhr. The cosmological billiard attractor. *Adv. Theor. Math. Phys.* **13**, 293-407, (2009).
- [38] M. Henneaux, A. Kleinschmidt and G. L. Gómez. A dynamical inconsistency of Horava gravity. *Phys. Rev. D* **81**, 064002, (2010).
- [39] P. Hořava. Membranes at Quantum Criticality. *J. High Energy Phys.* **0903**, 020, (2009).
- [40] P. Hořava. Quantum Gravity at a Lifshitz Point. *Phys. Rev. D* **79**, 084008, (2009).
- [41] J. Hutchinson. Fractals and Self Similarity. *Indiana Univ. Math. J.* **30**, 713-747, (1981).
- [42] R.T. Jantzen. The dynamical degrees of freedom in spatially homogeneous cosmology. *Commun. Math. Phys.* **64**, 211–232, (1979).
- [43] R.T. Jantzen. *Spatially Homogeneous Dynamics: A Unified Picture*. in *Proc. Int. Sch. Phys. “E. Fermi” Course LXXXVI on “Gamov Cosmology”*, R. Ruffini, F. Melchiorri, Eds. North Holland, Amsterdam, (1987) and in *Cosmology of the Early Universe*, R. Ruffini, L.Z. Fang, Eds., World Scientific, Singapore, (1984).

[44] I. M. Khalatnikov, E. M. Lifshitz, K. M. Khanin, L. N. Shur, and Y. G. Sinai. On the stochasticity in relativistic cosmology. *J. Stat. Phys.* **38**, 97, (1985).

[45] A. Katok and L. Mendoza. Dynamical Systems with Non-Uniformly Hyperbolic Behavior. *Supplement to "Introduction to the Modern Theory of Dynamical Systems", Encyclopedia of Mathematics and its Applications* **54**, Cambridge University Press, Cambridge, (1995).

[46] E. Kiritsis and G. Kofinas. Hořava-Lifshitz cosmology. *Nuclear Physics B* **821**, 467, (2009)

[47] H. Lee and E. Nungesser. Self-Similarity Breaking of Cosmological Solutions with Collisionless Matter. *Ann. Henri Poincaré* **19**, 2137–2155, (2018).

[48] H. Lee, E. Nungesser, and P. Tod. On the future of solutions to the massless Einstein–Vlasov system in a Bianchi I cosmology. *Gen. Rel. Grav.* **52**, 48, (2020).

[49] G. Leon and A. Paliathanasis. Extended phase-space analysis of the Hořava-Lifshitz cosmology. *Eur. Phys. J. C* **79** 746 (2019).

[50] Y.T. Li and J.A. Yorke. Period 3 Implies Chaos. *American Math. Month.* **82**, 985-992, (1975).

[51] S. Liebscher, J. Härterich, K. Webster, and M. Georgi. Ancient Dynamics in Bianchi Models: Approach to Periodic Cycles. *Commun. Math. Phys.* **305**, 59, (2011).

[52] S. Liebscher, A. D. Rendall, and S. B. Tchapnda. Oscillatory singularities in Bianchi models with magnetic fields. *Ann. Henri Poincaré* **14**, 1043–1075, (2013)

[53] E. M. Lifshitz and I. M. Khalatnikov. Investigations in relativistic cosmology. *Adv. Phys.* **12**, 185, (1963).

[54] Y. Lima. Symbolic dynamics for nonuniformly hyperbolic systems. *To appear in Ergodic Theory Dyn. Sys.* (2020).

[55] W. C. Lim, C. Uggla and J. Wainwright. Asymptotic Silence-breaking Singularities. *Class. Quant. Grav.* **23**, 2607, (2006).

[56] W. C. Lim. New explicit spike solution – non-local component of the generalized Mixmaster attractor. *Class. Quant. Grav.* **25**, 045014, (2008).

[57] W. C. Lim. Non-orthogonally transitive G2 spike solution. *Class. Quant. Grav.* **32** 16, 162001, (2015).

[58] R. Loll and L. Pires. Role of the extra coupling in the kinetic term in Hořava-Lifshitz gravity. *Phys. Rev. D* **90**, 124050, (2014).

[59] P. V. Loocke. The Art of Iterated Function Systems with Expanding Functions. In *Proceedings of Bridges 2009: Mathematics, Music, Art, Architecture, Culture*, eds. C. Kaplan and R. Sarhangi. Tarquin Publications, 55–62, (2009).

[60] P. K.-H. Ma. A Dynamical Systems Approach to the Oscillatory Singularity in Cosmology. M. Math. thesis, University of Waterloo, unpublished (1988).

[61] P. K.-H. Ma and J. Wainwright. A dynamical systems approach to the oscillatory singularity in Bianchi cosmologies. In *Relativity Today*, ed. Z. Perjes. Nova Science Publishers, (1992).

[62] M. A. H. MacCallum. *Cosmological models from a geometric point of view*. In *Cargèse Lectures in Physics*, Vol. 6 (1973) ed. E. Schatzman. Gordon & Breach.

[63] E. Matias and L.J. Diaz. Non-hyperbolic Iterated Function Systems: semifractals and the chaos game. *Fund. Math.* **250**, 21-39, (2020).

[64] J. Milnor. On the Concept of Attractor. *Commun. Math. Phys.* **99**, 177-195, (1985).

[65] C. W. Misner. Mixmaster universe. *Phys. Rev. Lett.* **22**, 1071, (1969).

[66] C. W. Misner. Quantum cosmology I. *Phys. Rev.* **186**, 1319, (1969).

[67] C. W. Misner, K .S. Thorne, and J. A. Wheeler. *Gravitation*. W. H. Freeman and Company, San Francisco, (1973).

[68] Y. Misonoh, K. Maeda, and T. Kobayashi. Oscillating Bianchi IX universe in Hořava-Lifshitz gravity. *Phys. Rev. D* **84**, 064030, (2011).

[69] G. Montani, M. V. Battisti, R. Benini, and G. Imponente. Classical and Quantum Features of the Mixmaster Singularity. *Int. J. Mod. Phys. A* **23**, 2353, (2008).

[70] S. Mukohyama. Hořava-Lifshitz Cosmology: A Review. *Class. Quant. Grav.* **27** 223101 (2010).

[71] Y. S. Myung, Y-W Kim, W-S Son and Y-J. Park. Universe in the  $z=3$  deformed Hořava-Lifshitz gravity. *J. High Energ. Phys.* **1003** 085 (2010).

[72] Y. S. Myung, Y-W Kim, W-S Son and Y-J. Park. Chaotic universe in the  $z = 2$  Hořava-Lifshitz gravity. *Phys. Rev. D* **82** 043506 (2010).

[73] Y. Pesin and H. Weiss. On the Dimension of Deterministic and Random Cantor-like Sets, Symbolic Dynamics, and the Eckmann-Ruelle Conjecture. *Commun. Math. Phys.* **182**, pp. 105-153, (1996).

[74] P. Prusinkiewicz and G. Sandness. Attractors and repellers of Koch curves. In *Proceedings of Graphics Interface '88*, pp. 217–228, (1988).

[75] M. Reiterer and E. Trubowitz. The BKL Conjectures for Spatially Homogeneous Spacetimes. [arXiv:1005.4908v2](https://arxiv.org/abs/1005.4908v2) (2010).

[76] A. D. Rendall. Global dynamics of the mixmaster model. *Class. Quantum Grav.* **14** 2341 (1997).

[77] A. D. Rendall. Late-time oscillatory behaviour for self-gravitating scalar fields. *Class. Quant. Grav.* **24**, 667-677, (2007).

- [78] H. Ringström. Curvature blow up in Bianchi VIII and IX vacuum spacetimes. *Class. Quant. Grav.* **17** 713 (2000).
- [79] H. Ringström. The Bianchi IX attractor. *Ann. Henri Poincaré* **2** 405 (2001).
- [80] K. Rosquist, C. Uggla, and R.T. Jantzen. Extended dynamics and symmetries in vacuum Bianchi cosmologies. *Class. Quant. Grav.* **7** 611 (1990).
- [81] K. Rosquist, C. Uggla, and R.T. Jantzen. Extended dynamics and symmetries in perfect fluid Bianchi cosmologies. *Class. Quant. Grav.* **7** 625 (1990).
- [82] N. Röhr and C. Uggla. Conformal regularization of Einstein's field equations. *Class. Quant. Grav.* **22** 3775 (2005).
- [83] S. E. Rugh. Chaos in the Einstein equations – characterization and importance. In *Deterministic Chaos in General Relativity*, eds. D. Hobill, A. Burd and A. Coley. Plenum Press, (1994).
- [84] A. Sharkovskii. Co-existence of cycles of a continuous mapping of the line into itself. *Ukrainian Math. J.* **16**, 61-71, (1964).
- [85] T. P. Sotiriou. Hořava-Lifshitz gravity: a status report. *J. of Physics: Conference Series* **283** 012034 (2011).
- [86] F. Takens. Heteroclinic attractors: Time averages and moduli of topological conjugacy. *Bull. Br. Math. Soc.* **25**, 107-120, (1994).
- [87] A. H. Taub. Empty Space-Times Admitting a Three Parameter Group of Motions. *Ann. Math.* **53**, 472-490, (1951).
- [88] C. Uggla. Asymptotic cosmological solutions: Orthogonal Bianchi Type II models. *Class. Quant. Grav.* **6**, 383-396, (1989).
- [89] C. Uggla. Recent developments concerning generic spacelike singularities. *Gen. Rel. Grav.* **45**, 1669, (2013).
- [90] C. Uggla. Spacetime Singularities: Recent Developments. *Int. J. Mod. Phys. D* **22**, 1330002, (2013).
- [91] C. Uggla, H. van Elst, J. Wainwright and G.F.R. Ellis. The past attractor in inhomogeneous cosmology. *Phys. Rev. D* **68**, 103502, (2003).
- [92] C. Uggla R. T. Jantzen, K. Rosquist and K. H. Zur-Mühlen. Remarks about late stage homogeneous cosmological dynamics. *Gen. Rel. Grav.* **23**, 947, (1991).
- [93] J. Wainwright, M. J. Hancock and C. Uggla. Asymptotic self-similarity breaking at late times in cosmology. *Class. Quant. Grav.* **16**, 2577-2598, (1999).
- [94] J. Wainwright and L. Hsu. A dynamical systems approach to Bianchi cosmologies: orthogonal models of class A. *Class. Quant. Grav.* **6**, 1409-1431, (1989).
- [95] J. Wainwright and G.F.R. Ellis. *Dynamical systems in cosmology*. Cambridge University Press, Cambridge, (1997).